Drug development and novel combination strategies with phytochemicals for precision medicine in cancer

A THESIS
SUBMITTED TO THE FACULTY OF
UNIVERSITY OF MINNESOTA
BY

SEUNG HO SHIN

IN PARTIAL FULFILLMENT OF THE REQUIREMENTS
FOR THE DEGREE OF
DOCTOR OF PHILOSOPHY

ADVISOR: ZIGANG DONG

AUGUST 2017

Acknowledgements

I thank my advisor Professor Zigang Dong for being a great supervisor, mentor, and scientific father to me and providing an atmosphere for conducting interdisciplinary research. He has been very supportive and given me excellent advice throughout my Ph.D. I admire his smile, patience, and communication skills and ability to adapt cutting-edge technologies quickly. Under his guidance I was able to study precision oncology.

My life as a graduate student in the U.S. would have been much harder without help of Professor Ann M. Bode. She always answers my questions with a smile and supports me to solve all problems. Her positive attitude motivates me to “think big, start small and move fast.” I also would like to thank my committee members, Professors Yuk Sham and Carlos Sosa, for graciously serving on my thesis committee and for their constructive comments towards my graduate education.

I have been fortunate to have met a lot of scientists at The Hormel Institute and they have made my scientific life interesting and fun. I always learn something from lab meetings. I thank Drs. Do Young Lim, Margarita Malakhova, Kanamata Reddy, Naomi Oi, Weiya Ma, Kun Yeong Lee, Joohyun Ryu, Ki Beom Bae, Eunmiri Roh, Hanyong Chen, Ke Yao, Tatyana Zykova, Hiroyuki Yamamoto, Mi-Sung Kim, Chengjuan Zhang, Feng Zhu, Haitao Li, Cong Peng, Jong Eun Kim, Hyosun Kim, Tianshun Zhang, Qiushi Wang, Sung Keun Jung, Tara adams, Tae-Gyu Lim, Sung-Young Lee, Yang Fu, Ge Yang, Wei Li, Yi Zhang, Chengcheng Shi, Soouk Kang, Ting Wang, Keke Wang, Yaping Han, Donghoon

Yu, Hongxun Wang, Ruihua Bai, Guoguo Jin, Yuqiao Sheng, Zhenjiang Zhao, Zhiping Guo, Yan Li and Alyssa Langfald. I especially thank Todd Schuster for helping me through numerous cell cycle and apoptosis experiments.

I am grateful for Professors Mee-Hyun Lee, Kangdong Liu and Hong-Gyum Kim at The China-US (Henan) Cancer Institute in Zhengzhou, Henan, China. I thank Fangfang Liu, Ting Wang, Mengqiu Song and Bingbing Lu for their time and efforts on PDX projects.

Back in South Korea, Professors Hyong Joo Lee and Ki Won Lee provided me an opportunity to study abroad and pursue my dream. Professor Sanguine Byun has been a great mentor, senior scientist, and role model. I feel like he is my older brother.

I give special thanks to my family for being supportive throughout Ph.D. course. I also thank my parents in law, Byung In Roh and Hyun Soon Yang who encouraged me to pursue scientific carrier, my cousin, Professor Eunha Kim who supported my science and piano, and also other relatives who always wished big things for me.

Dedication

This dissertation is dedicated to my parents, Dr. Hyun Jong Shin and Mi Ran Lee, and my sister, Soo Kyung Shin.

I also dedicate this dissertation to my wife, Eunmi Roh.

Abstract

Precision medicine refers to matching the most accurate and effective treatment to each individual, and has the potential to manage diseases. In cancer, however, developing drug candidates and finding effective combination strategies are in great demand. Here, we present a framework covering drug development against a specific oncoprotein, effective combinations of drug and natural compounds, and a physiologically-achievable chemoprevention strategy. First, HI-B1 is synthesized and identified as a direct β-catenin inhibitor. A colon cancer patient-derived xenograft (PDX) model with a high level of β-catenin is sensitive to HI-B1. Second, a combination of aspirin with a ginger extract shows synergistic effect. Combining a ginger extract with aspirin treatment can significantly reduce the effective dose of aspirin while retaining its therapeutic effects in PDX mouse models. Third, multiple phytochemicals at low doses accumulatively inhibit one key protein to exert their chemopreventive and therapeutic effects. Natural ERK2 inhibitors are discovered using chemoinformatics, crystallography, cell biology and biochemistry. Each outcome could be used in a precision oncology workflow to help prevent and treat cancer efficiently.

Table of Contents

Chapter 3: The synergistic effect of aspirin and ginger extract against colon cancer

List of Tables

Chapter 1

Chapter 3

Chapter 4

List of Figures

Chapter 2

Chapter 3

Chapter 4

Chapter 1:

Addressing the challenges of applying precision oncology

1.1 Summary

Precision oncology is described as the matching of the most accurate and effective treatments with the individual cancer patient. Identification of important gene mutations, such as *BRCA1/2* that drive carcinogenesis, helped pave the way for precision diagnosis in cancer. Oncoproteins and their signaling pathways have been extensively studied, leading to the development of target-based precision therapies against several types of cancers. Although many challenges exist that could hinder the success of precision oncology, cutting-edge tools for precision diagnosis and precision therapy will assist in overcoming many of these difficulties. Based on the continued rapid progression of genomic analysis, drug development, and clinical trial design, precision oncology will ultimately become the standard of care in cancer therapeutics.

1.2 Introduction

Improving efficacy, minimizing the adverse side effects of drugs, and overcoming acquired resistance to drug treatment have been major goals and emphases in cancer therapy. In order to attain the objectives of precision oncology, basic and clinical researchers have identified and clarified differences derived from genetic features between individuals. The existence of specific genetic differences between individuals is exemplified by the finding in 1932 that phenylthiocarbamide (PTC) exhibits the unusual property of either tasting very bitter or having no taste at all based on the individual's genetics. Notably, this trait is inherited to the next generation (1-2). The "one-size-fits-all

strategy" is no longer relevant to cancer treatment. The tailoring of distinct treatments to each specific individual became known as "personalized medicine" (3) and later the name was changed to "precision medicine" (4). Many countries have now launched government-driven projects focusing on precision medicine, including the Precision Medicine Initiative (National Institutes of Health, USA) (4), Cancer Moonshot program (5) (National Cancer Institute, USA) and HORIZON 2020 Work Programme for 2016 to 2017 (EU) (6).

The accelerating momentum of precision medicine, and especially precision oncology, has stemmed from the increasing amount of "-omics" information acquired from patients and, importantly, the successful integration of the fields of basic and clinical cancer research (see a detailed discussion in Appendix). Next generation sequencing instrumentation is capable of sequencing several genomes a day at a cost of about $1,000 each, making this technology an essential and straightforward part of translational cancer research (7). Driver-gene mutations identified from comprehensive genome analyses are now frequently detected in many cancer patients; and the aberrant gene products are currently being targeted by specific antagonists or monoclonal antibodies (8). Oncologists are now able to stratify subsets of cancer and make informed therapeutic decisions. Consequently, targeted therapy has gained credibility in reinforcing and/or replacing conventional cytotoxic chemotherapy. Several targeted agents are presently approved by the FDA and are being used clinically against several types of cancer.

Here, we categorize the work flow of precision oncology into two segments, precision diagnosis and precision therapy, and provide milestones and important aspects characterizing each segment. By reviewing targeted therapies clinically approved against breast cancer, lung cancer and melanoma, we reveal the current status and expose possible challenges in precision oncology. Two of the most effective state-of-the-art tools for the success of precision oncology are also described.

1.3 Precision oncology for patients–from precision diagnosis to precision therapy

In order to better understand and utilize precision oncology (i.e., precision medicine as it applies to cancer), analyzing the procedures step by step is crucial. Precision oncology comprises precision diagnosis and precision therapy. Precision diagnosis begins with an accurate diagnosis of each individual cancer patient and ideally classifies subjects into cancer patients and individuals at high risk for specific cancers (9). By detecting biomarkers that are associated with specific cancer types such as *BRCA1/2* mutations in breast cancer (10-11), we can diagnose the current or potential risks of each individual. Accumulating evidence shows that multiple biomarkers (so called "signature") can help in creating more precise and evidence-based therapeutic strategies to modulate cancer (12-13). Establishing molecular subtypes and categorizing tumors into one of the subtypes enhances the accuracy of therapeutic options (14). The information derived from precision diagnosis reveals the precise medical measures,

including surgery, radiation, chemotherapy, adjuvant therapy, supplements, and/or vaccines, that are needed for each individual.

Precision therapy matches the most effective treatment to the individual cancer patient based on the genetic profile of the specific cancer, and can be divided into two categories that include precision chemotherapy and precise therapeutic procedures. Precision chemotherapy is the use of the correct drugs prescribed that assures maximum benefit with minimum risk or toxicity for the patient. Therapeutic measures could include surgery and radiation therapy tailored to the patient's needs.

1.4 Precision diagnosis

Information-based diagnosis can assist clinicians, not only in identifying tumor type and stage, but in revealing important genetic mutations that drive carcinogenesis. Advances in technology have clearly resulted in more effective therapeutic decisions. Final goals include optimization of clinical outcomes, avoidance of unnecessary therapies, minimized side effects, and overcoming or avoiding drug resistance.

1.4.1 *BRCA1/2* are a milestone for precision diagnosis

The discovery of the breast cancer susceptibility genes, *BRCA1/2*, was traced from a family with a history of breast cancer, and indicated the association between genetic features and the early onset of the disease (10-11). In addition to other breast cancer susceptibility genes, the *BRCA1/2* mutation test is one of the most well-established

models in precision oncology. It has become a guideline that aids clinicians in creating prevention strategies and targeted therapies. More than one million individuals have been tested for *BRCA1/2* mutations worldwide (15).

The landscape of mutations in the *BRCA1/2* genes has been extensively studied and the relationship between the mutations and breast cancer risk is also well-defined. More than 1,800 different variants (i.e., intronic changes, insertions, deletions and missense mutations) have been observed in *BRCA1* and 2,000 different variants have been reported to occur in *BRCA2* (15). *BRCA1*/2 mutations are currently the most significant gene variations in breast cancer surpassing tumor protein p53 (*TP53*), phosphatase and tensin homolog (*PTEN*), liver kinase B1 (*LKB1*) and cadherin1 (*CDH1*) mutations (15-17). *BRCA1/2* mutations are estimated to account for approximately 15% of the relative familial risk of breast cancer (15). Mutations in *BRCA1* and *BRCA2* reportedly contribute equally to early-onset breast cancer (18).

1.4.2 Development and improvement of genetic tests

Recent progress in immunohistochemistry (IHC) has helped clinicians to identify the presence of specific biomarkers and to categorize patients in pathology (19). Detection of HER2 (20) in breast cancer and PD-L1 (21) in lung cancer based on IHC aided the prescription of suitable drugs for the patients. However, many other techniques are currently available to quantify changes in gene expression, and include RT-PCR (22), DNA arrays (23), NanoString technology (24), comparative genomic hybridization arrays, and single nucleotide polymorphism analysis (25). Genetic tests have been

developed for diagnostic, predictive and prognostic purposes and some have been approved by the FDA, whereas others are still under development for breast cancer (26-34), lung cancer (35-41) and melanoma (42-46) (Table 1.1). Although the most significant genes, such as *BRCA1*/2, can only predict or explain a portion of disease susceptibility, the number of genes examined in a single test has continually increased to improve accuracy (13). Of particular note (Table 1.1), the 70-gene signature test for breast cancer (MammaPrint by Agendia) (26) showed the most efficacy in a clinical trial (47). The study in 6,693 women with early-stage breast cancer was conducted to examine whether the gene signature test could reduce the use of chemotherapy. For patients who had high clinical risk and low genomic risk for recurrence, the difference in the 5-year survival rates between chemotherapy (98.8%) and no-chemotherapy (97.3%) was only 1.5% (47). The result shows that approximately 46% of women with breast cancer who are at high clinical risk might not require chemotherapy and that the 70-gene signature could aid in treatment decisions (47). The Oncotype Dx test by Genomic Health also helps clinicians in selecting proper treatment options for patients with invasive breast cancer (31, 48). The Oncotype Dx test generates a recurrence score (0-100) by analyzing the expression of 21 genes (49-50). Survival rates of patients with high recurrence scores (31 and higher) have been improved by adjuvant chemotherapy, whereas patients with low recurrence scores (less than 17) are unlikely to get benefits from the chemotherapy (48).

Table 1.1 Genetic tests for breast cancer, lung cancer and melanoma

Type	Test name	Institution	FDA approval	No. of genes	Ref.
Breast cancer	MammaPrint	Agendia	Yes	70	(26)
	Prosigna	NanoString Tech.		50	(30)
	GeneSearch BLN test	Veridex		2	(27)
	INFORM HER2 Dual ISH	Ventana		1	(29)
	HER2 CISH pharmDx Kit	Dako		1	(28)
	Oncotype Dx	Genomic Health	No	21	(31)
	EndoPredict	Sividon Diagnostics		11	(32)
	Breast Cancer Index test	BioTheranostics		7	(33)
	FEMTELLE	Sekisui Diagnostics		2	(34)
Lung cancer	Therascreen EGFR RGQ PCR kit	QIAGEN	Yes	1	(37)
	cobas EGFR Mutation Test	Roche		1	(35)
	VENTANA ALK (D5F3) CDx Assay	Ventana Medical Systems		1	(38)
	Vysis ALK Break Apart FISH Probe Kit	Abbott Molecular		1	(36)
	Lung Cancer Mutation Panel	Quest Diagnostics	No	34	(39)
	Lung Cancer Comprehensive Mutation and Translocation Panel	ARUP Laboratories		11	(40)
	SnaPshot Multiplex System	Thermo Fisher		11	(41)
Melanoma	cobas 4800 BRAF V600	Roche	Yes	1	(42)
	THxID-BRAF	bioMerieux		1	(43)
	53-Immune Gene Network Panel	Icahn School of Medicine Mount Sinai	No	53	(44)
	myPATH	Myriad		23	(45)
	Sentosa SQ Melanoma Panel	Vela Diagnostics		10	(46)

1.5 Precision therapy

Precision therapies have been applied in breast cancer, lung cancer and melanoma, but many challenges still need to be addressed.

1.5.1 Breast cancer and targeted therapy

The most well-known target-based treatment against breast cancer is directed at the estrogen receptor (ER) and the human epidermal growth factor receptor 2 (HER2; Table 1.2) (51). The discovery of these two protein receptors opened a new avenue for targeted therapy that showed improved efficacy compared to aromatase inhibitors, which suppress plasma estrogen levels in postmenopausal women (52). Tamoxifen, a pro-drug targeting the ER, is metabolized in the liver into active metabolites that have a higher affinity for the ER compared to the parental tamoxifen (53). Trastuzumab is a monoclonal antibody targeting HER2 and is used in patients with breast cancers overexpressing this receptor (Table 1.2) (54-55). Trastuzumab inhibits the activity of HER2, which forms heterodimers with other tyrosine kinase receptors (i.e., EGFR, HER3 and HER4) and promotes tumorigenesis (56). From a clinical trial of 469 women with metastatic breast cancer overexpressing HER2, combinational treatment with trastuzumab and standard chemotherapy attenuated disease progression compared to standard chemoptherapy alone (i.e., median, 4.6 vs. 7.4 months) (57). The objective response rate (i.e., 32 vs. 50%) and survival time (i.e., median, 20.3 vs. 25.1 months) were also improved by the addition of trastuzumab to the chemotherapy (57). A combination of pertuzumab, trastuzumab, and chemotherapy (i.e., docetaxel) improved

the median overall survival time (i.e., 40.8 vs. 56.5 months) compared to trastuzumab-only plus chemotherapy (58). A conjugate drug of a HER2 monoclonal antibody and a cytotoxic drug, ado-trastuzumab emtansine, prolonged progression-free survival and overall survival with lower adverse effects compared with a combination of lapatinib and chemotherapy (Table 1.2) (59).

Table 1.2 Targeted therapies in breast cancer

Target gene	Alteration	Drug type	Examples
HER2/ERBB2	Amplification/mutation	HER2 inhibitor	Trastuzumab, Ado-trastuzumab emtansine, Pertuzumab, Lapatinib
ER	-	ER inhibitor	Tamoxifen
	Amplification	ER downregulator	Fulvestrant
EGFR	Amplification/mutation	EGFR inhibitor	Gefitinib, Erlotinib, Afatinib, Osimertinib, Olmutinib, Cetuximab
PI3-K	Amplification/mutation	mTOR inhibitor	Rapamycin, Everolimus
AKT1/2/3	Amplification		
PTEN	Mutation/deletion		
mTOR	Amplification		
KRAS	Amplification/mutation	BRAF, MEK inhibitor	Vemurafenib, Trametinib
BRAF	Amplification/mutation		
NF1	Mutation		
CDKN1B	Alteration	CDK4 inhibitor	Palbociclib
CCND1	Amplification		
BRCA1/2	Mutation/deletion	PARP inhibitor	Olaparib
ATM	Mutation		
ATR	Mutation		

1.5.2 Challenges of targeted breast cancer therapies

The identification of driver genes in breast cancer increases the likelihood of matching the correct, most effective drug to the right patient. Only a few genes, however, have been validated to act as driver genes. *BRCA1/2, estrogen receptor alpha (ESR1), HER2, PI3-K/Akt/mTOR, Egfr, cyclin dependent kinase 4 (CDK4)/Rb, Ras/Raf/mitogen-activated protein kinase kinase (MEK)* are known to be critical in breast cancer therapy (Table 1.2) (60-61). For instance, somatic mutations of *PI3-K* occur in more than 10% of all breast cancers (61) and *Akt1* and *Akt3* mutations and *PTEN* deletion contribute to the activation of the PI3-K pathway (25, 62). Nevertheless, approximately 50% of the familial relative risk (the ratio of the risk of disease for a relative of an affected individual to that for the general population) of breast cancer is still unexplained (15). Couch *et al.* estimated that contributions of genes including *BRCA1/2, TP53, PTEN, LKB1, CDH1,* and known/predicted single nucleotide polymorphisms in breast cancer, and the current knowledge of genetic variations, only covered half of the breast cancer risk (15).

Variants of uncertain significance (VUS) add another layer of complication in breast cancer treatment. VUS refers to changes in a normal gene sequence for which the clinical association with disease is unclear (63). Although many efforts have been made to evaluate and classify genetic variants, including missense, intronic, and small in-frame insertions and deletions (64-66), the rarity of the individual VUS makes interpretation difficult because of insufficient statistical power.

Furthermore, some breast cancer patients lack good target proteins for therapy. Triple-negative breast cancer (TNBC), for example, is negative for ER and progesterone

receptor (PgR) and lacks HER2 amplification and therefore cannot be treated with classic endocrine therapy or HER2-targeted therapy (67-68). The loss of HER2 expression in metastatic tumors compared with HER2-amplified primary breast cancers is frequently observed, and ER-positive/PgR-positive/HER2-amplified tumors become TNBC after chemotherapy (51, 69-70). Although alternative molecular targets, such as EGFR, which is frequently amplified and is related to poor prognosis (71-72), are being elucidated (Table 1.2), TNBC has only a small number of therapeutic options, and remains a difficult type of cancer in the field of breast cancer therapy (73).

1.5.3 Lung cancer and targeted therapies

FDA approval of gefitinib, an epidermal growth factor receptor (EGFR) inhibitor (74), accelerated target-based therapy in lung cancer patients replacing cytotoxic chemotherapy for first-line therapy (75-76). For patients with EGFR-activating mutations (exon19del or L858R), erlotinib (77-78) also performed better than conventional chemotherapies, such as cisplatin. EGFR-targeted therapy was combined with cytotoxic drugs as a combination therapy that showed improved progression-free survival (79-80). However, almost all patients treated with the EGFR inhibitors acquired resistance to the drugs due to secondary EGFR mutations such as T790M (81-82). Second-generation EGFR inhibitors (e.g., afatinib (83-84)) were designed to target mutant EGFR better than the wild-type receptor. Third-generation EGFR inhibitors, including osimertinib and olmutinib, irreversibly bind to EGFR T790M and have been approved for use in the U.S and South Korea, respectively (Table 1.3) (85-87).

Crizotinib is an FDA-approved inhibitor of anaplastic lymphoma kinase (ALK), Ros proto-oncogene 1 (ROS1), and Met proto-oncogene (MET; Table 1.3). ALK is a cell surface protein that stimulates signaling pathways, such as the Ras/Raf/MEK, PI3-K/mTOR, and Janus kinase (JAK)/signal transducer and activator of transcription (STAT) pathways (88), and is activated by gene translocation and fusion with other genes (89-94). ROS1 is an orphan receptor tyrosine kinse (RTK) activated by chromosomal rearrangement and fusion with other genes (95). MET, another type of RTK, is overexpressed/amplified or exhibits an exon 14 skip-mutation in non-small cell lung cancer (NSCLC) patients (96). Crizotinib has shown its superiority over standard chemotherapy in ALK-positive lung cancer patients (97-98) and ROS1-rearranged NSCLC patients (99). Lung adenocarcinoma patients harboring the MET exon 14 splice site mutation also responded to crizotinib (100). However, ALK mutations, such as R1174L, L1196M and R1275Q, conferred resistance to crizotinib and led to the development of second-generation ALK inhibitors. FDA has approved the use of ceritinib (101), which targets the L1196M gatekeeper mutation, and alectinib (102), which targets the R1174L, L1196M and R1275Q mutations.

BRAF is a signaling protein activated by various RTKs. In NSCLC, 2-4% of patients possess BRAF V600 mutations (96). Although BRAF inhibitors (vemurafenib and dabrafenib) were originally developed for the treatment of melanoma, recent clinical trials with the inhibitors showed potential in BRAF V600 mutant NSCLC patients (Table 1.3). Vemurafenib resulted in tumor regression in the majority (14 of 19) of NSCLC patients, and the objective response rate was 42% (103). In a phase 2 trial, dabrafenib

treatment with trametinib, a MEK inhibitor, reached 63% overall response in BRAF V600E-mutant NSCLC patients, who had documented tumor progression after previous platinum-based chemotherapy (104).

Immunotherapy has received substantial attention recently as a cancer therapy. Unlike other therapies, the goal of immunotherapy is to boost or restore the ability of immune cells to kill tumor cells (105). Tumor cells suppress and evade the immune system through interactions between the programmed cell death protein 1 (PD-1) of T-cells and the PD ligand 1 (PD-L1) of tumor cells (106). Two monoclonal antibodies against PD-1 (Table 1.3), including nivolumab (107-110) and pembrolizumab (111-112), have received FDA approval for second-line treatment against NSCLC that express PD-L1.

Table 1.3 Targeted therapies in lung cancer

Target gene	Alteration	Drug type	Candidate
EGFR	Amplification	EGFR inhibitor	Gefitinib, Erlotinib, Afatinib, Osimertinib, Olmutinib
ALK	Translocation/mutation	ALK inhibitor	Crizotinib, Alectinib, Ceritinib
MET	Amplification	MET/ROS1 inhibitor	Crizotinib, Cabozantinib
RET	Amplification/mutation		
ROS1	Fusion		
PD-L1	-	PD-1 inhibitor	Nivolumab, Pembrolizumab
HER2	Amplification	HER2 inhibitor	Trastuzumab, Afatinib, Dacomitinib
BRAF	Amplification/mutation	BRAF inhibitor	Vemurafenib, Dabrafenib

1.5.4 Challenges of targeted lung cancer therapies

The war against drug resistance is probably the most difficult challenge in lung cancer treatment. Clonal evolution, the accumulation of genetic and epigenetic changes over time in individual cells (113-114), is now believed to be the root of drug resistance (115-116). Biopsies that were taken after the failure of rociletinib targeting EGFR mutant (T790M)-expressing lung cancer (117) showed that at least a portion of the resistant tumor still expressed the T790-wild-type protein (116). The wild-type clones existed before treatment with rociletinib. Piotrowska *et al.* concluded that combination treatment using rociletinib targeting mutant EGFR T790M clones and other drugs targeting wild-type EGFR T790 are required to further improve the drug response rate and final outcomes (116). However, when first-generation EGFR inhibitors (gefitinib and erlotinib) and third-generation EGFR inhibitors (rociletinib/CO-1686, osimertinib/AZD9291, olmutinib/HM61713 and WZ4002) were used in combination, a new mutation of C797S emerged and complicated the therapeutic options (118). Studies showed that if the C797S mutation was on a different allele of T790M, combination treatment with gefitinib and WZ4002 inhibited EGFR signaling. In contrast, if C797S and T790M were on the same EGFR allele, the combination of gefitinib and WZ4002 was not effective (118). Monitoring changes in cancer cells at the molecular level will be helpful in preventing and resolving drug resistance in lung cancer.

1.5.5 Melanoma and targeted therapies

BRAF in the mitogen-activated protein kinase (MAPK) pathway (Ras-Raf-MEK-ERK) is constitutively activated by mutations in 40% of melanomas (119). The most common mutations are V600E and V600K, representing 73% and 19%, respectively (120). The growth of BRAF V600E-expressing melanoma can be inhibited directly by vemurafenib (121) or dabrafenib (Table 1.4) (122). Drug resistance, also called "bypass tracks", is increasingly relevant as targeted therapy emerges (123). Patients with BRAF mutations acquired resistance due to increased expression and phosphorylation of platelet-derived growth factor receptor beta (PDGFβ) and N-Ras (124). The MEK inhibitor, trametinib, also suppresses BRAF V600E- or V600K-expressing melanomas by targeting the BRAF downstream MAPK pathway (Table 1.4) (125). Because drug monotherapies commonly result in resistance (124, 126), combination treatment with a BRAF inhibitor and a MEK inhibitor has been prescribed to increase the patient's response rate and also lengthen their survival time (127). Especially, combination therapy as a first-line approach increased overall survival rates in a clinical trial (128). In patients with BRAF V600 mutations, a combination of cobimetinib (MEK inhibitor) and vemurafenib treatment showed median overall survival of 22.3 months, compared with 17.4 months by placebo and vemurafenib treatment (128).

Melanoma cells express the CTLA-4 and PD-1 immune receptor proteins that are normally expressed in T-cells. Because each of these two proteins can inhibit activation of T-cells and down-regulate the immune response, the abnormal expression of CTLA-4 and PD-1 in tumor cells is suggested as a molecular mechanism of immune evasion in

tumors (129). Ipilimumab, a CTLA-4 monoclonal antibody, was approved by the FDA for treatment of patients with metastatic melanoma (Table 1.4) (130-131). The PD-1 monoclonal antibodies, nivolumab (132-134) and pembrolizumab (135), were also effective against metastatic melanoma (Table 1.4). Ipilimumab and nivolumab are also used in combination to treat melanoma (136).

1.5.6 Challenges of targeted melanoma therapies

Similar to other types of cancer, one of the greatest challenges in melanoma treatment is the relapse and development of resistant disease after therapy. Recently, even patients who have undergone immunotherapy were shown to acquire resistance to PD-1 blockade in melanoma (137). Zaretsky *et al*. reported a delayed relapse of patients who had had initial tumor regression induced by continuous pembrolizumab treatment. The analyses of biopsies showed that JAK1/2 truncating mutations resulted in loss of PD-L1 expression and changed the molecular profile of the melanoma (137-138). Overall, although immunotherapy has become a promising and unique strategy for cancer treatment, an integrative strategy should be prepared to prevent drug resistance.

Table 1.4 Targeted therapies in melanoma

Target gene	Alteration	Drug type	Candidate
BRAF	Amplification/mutation	BRAF inhibitor	Vemurafenib, Dabrafenib
MEK	Amplification/mutation	MEK inhibitor	Trametinib, Cobimetinib
CTLA-4	Amplification	CTLA-4 inhibitor	Ipilimumab
PD-1	-	PD-1 inhibitor	Nivolumab, Pembrolizumab

1.6 Tools for precision oncology

The demand for new diagnostic and treatment tools has been driven by precision oncology. In particular, the use of liquid biopsies and patient-derived xenograft (PDX) models has received considerable attention from researchers and clinicians. For precision diagnosis, having new diagnostic platforms like liquid biopsies is crucial because this type of assay can gather information from patients in a manner that is minimally-invasive. For precision therapy, testing drugs in a paradigm like the PDX model is beneficial because this model can be used to represent tumors of patients before drugs are subscribed.

1.6.1 Liquid biopsies

A biopsy is an examination of tissue obtained from a living body to discover the presence, cause, or extent of a disease. Although biopsies have become more important as the field of precision oncology continues to expand, sampling some types of tumors is still difficult and can result in diagnostic errors. To address this problem, biofluid samples, including serum, plasma, saliva, urine and cerebrospinal fluid, are now being used to screen for tumors, characterize molecular features, and analyze tumor types (139-142). Liquid biopsies can provide clear information regarding the genetic makeup of each tumor. Because liquid biopsies are relatively non-invasive, clinicians can repeat sampling and monitor disease progression over time without performing solid-tissue biopsies. Circulating tumor cells (CTCs) and cell-free DNA (cfDNA) are promising components of liquid biopsies.

CTCs are cancer cells that are shed into the vascular system from the primary tumor and are circulating around the body in the blood (143). CTCs have been detected in patients with metastatic tumors at an average concentration of 1-10 cells/ml, but are extremely rare in individuals without tumors or with non-malignant tumors (139, 144-145). Circulating non-tumor epithelial cells in the blood of patients undergoing surgery and the difficulty in identifying markers of CTCs pose challenges to this technology. However, because dynamic changes occur in surface markers of CTCs, analysis of DNA/RNA from CTCs can enable clinicians to predict tumor progression and drug susceptibility of the patient (142, 146). A clinical trial with CTCs showed its promise as a prognostic marker and limitation as an indicator of changing chemotherapy (147). The trial divided patients with metastatic breast cancer into four groups. Patients whose CTC number was not increased at baseline remained on initial therapy (arm A), and patients whose CTC numbers had been increased, but later decreased after 21 days of therapy, also remained on the initial therapy (arm B). Patients whose CTC numbers were consistently increased were randomly assigned to maintain initial therapy (arm C1) or changed to an alternative therapy (arm C2). Overall survival rates between arms A, B, and C (sum of C1 and C2) showed significant differences between groups (i.e., 35 vs. 23 vs. 13 months, respectively). However, no difference was observed between overall survival of arm C1 and C2. This result indicates that CTC is a strong prognostic marker of overall survival in patients with metastatic breast cancer, although changing chemotherapy option based on CTC does not prolong the overall survival rate (147). In

summary, monitoring the efficacy of adjuvant therapies is feasible with CTC-based liquid biopsies, and analyses of CTCs will be one of the key players in precision diagnosis.

cfDNA refers to tumor DNA released from primary cancers into the biofluids of cancer patients (142). The majority of cfDNA is derived from cells that have undergone apoptosis or necrosis and then release fragments of DNA of approximately 150-180 bp in length (140, 142). Similar to acquiring CTC, tumor cell-derived cfDNA is difficult to obtain because of the extensive amount of cfDNA that is also released from non-malignant cells (148). Nevertheless, cfDNA could provide a better diagnostic tool than CTCs from the same patient to detect mutations (149). Because cfDNA could be used to monitor clonal evolution and emergence of drug resistance (150), this type of analysis might assist clinicians in making tailored therapeutic decisions for cancer patients in the future.

1.6.2 Patient-derived xenograft (PDX) models

The PDX model uses actual patient tumor fragments that have been sectioned from the cancer patient and implanted into immunodeficient mice (151). By treating mice harboring the PDX tumor fragment, the efficacy of a drug can be predicted before being subscribed to the actual patient. Thus PDX is a platform that provides evidence-based guidelines in choosing the correct and most effective drug to prescribe to a patient. For preclinical drug development, the PDX model overcomes the important limitation of using conventional cancer cell lines, which have developed characteristics that do not accurately reflect the actual cancer patient tumor. Conventional cell line-based xenografts

lack the broad diversity and heterogeneity of cancer (152). In contrast, the PDX model preserves the heterogeneity and microenvironment of the original tumor after being passaged in mice (151-152). In 1985 the PDX model was confirmed to have good predictive value in showing that drug responses from PDX models corresponded very well with the response from patients (153). The tumor heterogeneity of the PDX was shown to be well preserved in patient-derived tumor cells (PDTC) (154). These results support the potential of the PDTC-PDX pipeline for drug development. Although the lack of functional immune reactions in this model is a limitation, humanized mice that mimic the human immune system and resultant microenvironment allow researchers to better understand translational oncology (155). Overall, this clinically relevant mouse model should be beneficial in drug development and precision therapy for cancer patients.

Establishing PDX models worldwide reflects the high expectations of translating preclinical research to the clinic. Novartis, a large pharmaceutical company (Switzerland), has established about 1,000 PDX models expressing a diverse pool of driver mutations in cancer (156). EurOPDX, a European consortium for PDX, has established more than 1,500 subcutaneous and orthotopic PDX models (157) and the Jackson Laboratory (ME, USA) has created about 550 PDX models (157). The US-China (Henan) Hormel Cancer Institute (Zhengzhou, China) has established unique PDX models that include Wilms' tumor and esophageal cancer models. Dana-Farber Cancer Institute (MA, USA) established a Public Repository of Xenografts (PRoXe), which includes PDXs of leukemia and lymphoma (158). Of particular note, EurOPDX launched

cBioPortal where information on models and their molecular annotation have been opened to the public to provide a platform of PDX studies (159).

1.7 Limitations and prospects of precision oncology

Despite the growing enthusiasm and enormous investment in precision oncology, empirical evidence and verification is still critically needed showing that precision therapy is significantly better than conventional treatments (160-161). Results from one of the first clinical trials based on precision oncology were not promising (162). In this trial, the genomic information of patients was analyzed and patients who had targetable driver mutations were subjected to precision therapy. Unfortunately, the use of molecular-targeted drugs did not result in improved progression-free survival compared to treatments based on the clinicians' choice (i.e., randomized trial). Another study that enrolled patients with different types of tumors, including colon, thyroid and ovarian cancer expressing the BRAF V600 mutation, showed similar results (103). In this study, vemurafenib, an FDA-approved drug against melanoma, was only effective on some of the non-melanoma patients. These results suggest that prescription of drugs against a certain type of cancer does not guarantee success in treatment of other types of cancers although they harbor the same mutation/alteration on the target protein.

Several factors could have led to the lack of success of the current precision oncology-based trials (163). One factor could be the lack of specific molecular-targeted drugs. Drugs are not yet available for many drivers in carcinogenesis at least partly due to

the tremendous cost in money and time. Furthermore, many drugs are so toxic that clinicians are forced to reduce the dose, which results in only a partial inhibition of the targeted pathway giving the tumor the opportunity to develop resistance to the drugs. Other factors include tumor heterogeneity and constant evolution (115, 164). In addition, the genomic signature from one part of the tumor measured at a certain time point likely does not represent other parts or different time points of tumor development. These features pose a huge hurdle to precision oncology.

To address tumor heterogeneity and evolution, the National Cancer Institute recently revealed a new trial design of genomically-informed precision therapy referred to as the NCI-MATCH (Molecular Analysis for Therapy Choice) Trial (165-166). NCI-MATCH aims to identify 'actionable mutations' and test whether a drug or drug combinations are active against specific molecular abnormalities (166). The multi-arm phase 2 trial initially aimed to screen 3,000 patients and enroll 1,000 adults with advanced solid tumors for which standard therapy has not yet been developed. The initial trial with 10 treatment arms has completed accrual and patient recruitment was closed in November 2015 for planned interim analysis. Based on the low number of actionable mutations and the enrollment number exceeding expectations from the interim analysis, the trial reopened on May 31, 2016, extending treatment arms to 24 and aiming to screen 6,000 patients (167). Genetic variants of the patients will be analyzed for 143 genes and the patients assigned to one of several different treatment groups (165). The hope is that this new design will increase the flexibility of clinical decisions and improve the overall outcome of the patients.

One of the most promising and successful examples of precision oncology is the treatment of chronic myeloid leukemia (CML) with imatinib (168). The high proportion of the clonal BCR–ABL translocation in CML enabled almost all CML patients to benefit from imatinib (169). Likewise, finding concurrent driver mutations or clonal markers will benefit a large group of people. The hope is that predicting/monitoring changes in cells and dividing patients with subgroups before or at the point of cancer relapse will improve clinical outcomes.

Pan-cancer precision diagnosis and therapy are emerging. For instance, pembrolizumab, a PD-1 inhibitor, is approved by the FDA for treatment of metastatic melanoma (170), metastatic NSCLC (171), Hodgkin's lymphoma (172), and metastatic head and neck squamous cell carcinomas (173). Although the proportion of patients who are eligible for the treatment is lower than that of imatinib-CML cases, this target-based approach provided a better treatment option compared to adjuvant chemotherapy. Furthermore, RTK inhibitors also aim to cover patients across various cancer types. One of the newest approaches is a fibroblast growth factor receptor (FGFR) inhibitor that directly targets its genetic alterations. BGJ398, a FGFR1-3 inhibitor, was tested in patients with advanced solid tumors including lung, breast, bladder, colon and liver (174). The phase 1 trial showed that BGJ398 exhibits anti-tumor activity against FGFR1-amplified NSCLC and FGFR3-mutant bladder cancer (174). For precision diagnosis, eligible patients for targeted therapies will be screened and for precision therapy, the targeted drug(s) will be administered at a correct dose to benefit each individual.

The advances in lipidomics, proteomics and metabolomics will aid in the implementation of precision oncology. In the field of lipidomics, arachidonic acid is a signaling precursor that has attracted interest for anti-cancer therapy (175-176). A recent study of lipidomic profiling showed that lung tumors possess higher levels of arachidonic acid-containing phospholipids and phosphatidylinositols compared to normal tissue (176). Myc inactivation caused a significant decrease in arachidonic acid and its lipid metabolites (176). These results suggest that arachinonic acid and its metabolites can serve as biomarkers in precision diagnosis. In the field of proteomics, cryo-electron microscopy (cryo-EM) has received considerable attention as a tool for "visual proteomics" (168, 177). For example, the structure of the ATP-binding cassette subfamily G2 (ABCG2), a human multidrug transporter, revealed that two cholesterol molecules are bound to a hydrophobic pocket between the transmembrane domains (178). The cryo-EM structure provides structural insights of cholesterol recognition and pharmacokinetics of ABCG2 in precision therapy. In the field of metabolomics, gut microbiota possess a large repertoire of metabolizing xenobiotics, small molecules that are foreign to the human body (179). For example, irinotecan becomes SN-38, an active topoisomerase inhibitor in the body (180). SN-38 is glucuronidated by host liver enzymes and loses its activity (SN-38G). However, bacterial β-glucuronidase hydrolyzes and reactivates SN-38G in the large intestine causing intestinal damage and diarrhea (180). Accumulative knowledge of microbiota in each patient could enhance the efficacy of precision therapy and lower adverse side effects.

To summarize, precision oncology has emerged to improve efficacy, minimize side effects of drugs and avoid drug resistance in cancer therapy. Precision oncology is categorized into two segments, precision diagnosis and precision therapy. In precision diagnosis, mutations of important genes such as *BRCA1/2* have led clinicians to tailor treatment options to individuals. Improvement on genetic tests facilitated molecular target-based precision therapy. In breast, lung and melanoma, drugs that inhibit important target proteins prolonged progression-free survival and overall survival of the patients compared to genotoxic chemotherapy. Although difficulties due to clonal evolution and cancer heterogeneity still exist, state-of-the-art tools such as liquid biopsies and PDX models will enhance the efficacy of precision diagnosis and precision therapy, respectively. Supported by government-driven projects worldwide, precision oncology will be the standard pipeline of cancer therapy.

Chapter 2:

A small molecule inhibitor of the β-catenin-TCF4 interaction suppresses colorectal cancer growth *in vitro* and *in vivo*

2.1 Summary

Colorectal cancer is associated with aberrant activation of the Wnt pathway. β-Catenin plays essential roles in the Wnt pathway by interacting with T-cell factor 4 (TCF4) to transcribe oncogenes. We synthesized a small molecule, referred to as HI-B1, and evaluated signaling changes and biological consequences induced by the compound. HI-B1 inhibited β-catenin/TCF4 luciferase activity and preferentially caused apoptosis of cancer cells in which the survival is dependent on β-catenin. The formation of the β-catenin/TCF4 complex was disrupted by HI-B1 due to the direct interaction of HI-B1 with β-catenin. Colon cancer patient-derived xenograft (PDX) studies showed that a tumor with higher levels of β-catenin expression was more sensitive to HI-B1 treatment compared to a tumor with lower expression levels of β-catenin. The different sensitivities of PDX tumors to HI-B1 were dependent on the β-catenin expression level and potentially could be further exploited for biomarker development and therapeutic applications against colon cancer.

2.2 Introduction

Colon cancer is the third most common cancer diagnosed in both men and women in the United State (181). Although the incidence rate of colon cancer is decreasing due to introduction of colonoscopy and removal of precancerous lesions, incidence and death rates are still increasing among people younger than 50 years old (181). Chemotherapy of colon cancer has been heavily dependent on 5-fluorouracil (5-FU), a genotoxic drug that

blocks DNA synthesis and replication. Since target-based intervention was introduced in cancer therapy, epidermal growth factor receptor (EGFR) inhibitors combined with 5-FU-based treatment have increased the overall survival rate of colorectal cancer patients with *K-ras* wild-type gene expression (182-183). However, the elucidation of additional important targets and the development of specific inhibitors are still challenging goals.

β-catenin is a central component of the Wnt signaling pathway, and aberrant expression or prolonged activation of β-catenin is frequently associated with various diseases, including cancer (184-186). The role of β-catenin and Wnt signaling in carcinogenesis has been studied extensively in cancer, especially in colorectal cancer. The expression level and the activity of β-catenin is tightly regulated by its upstream regulator, the destruction complex, which includes the tumor suppressor adenomatous polyposis coli (APC), glycogen synthase kinase 3β (GSK3β), casein kinase 1α (CK1α) and the scaffold protein AXIN (187). When translocated from the cytosol to the nucleus, β-catenin binds with T-cell factor 4 (TCF4) to transcribe target genes such as *axin2* (188), *cyclin D1* (189) and *c-myc* (190).

The importance of the Wnt pathway in tumorigenesis has made it a promising target for drug development (186). Over the past decade, the down-regulation of Wnt signaling in cancer cells was achieved by small molecules (191). Compounds that target upstream of β-catenin include tankyrase inhibitors IWR-1 (192) and XAV939 (193) and casein kinase 1α activator pyrvinium (194). These inhibitors facilitate β-catenin degradation by enhancing the activity of the β-catenin destruction complex. Direct inhibition of β-catenin by PKF115-584 (195) and CGP049090 (196) reduces target gene

expression without affecting the protein expression level of β-catenin. Methyl 3-([(4-methylphenyl)sulfonyl]amino)benzoate (MSAB) was recently reported to target β-catenin and induce ubiquitination (197). MSAB selectively killed Wnt-dependent cancer cells (197). Despite these efforts, the effectiveness of Wnt/β-catenin inhibitors in clinical trials is yet to be proven, and strategies to identify patients who will respond to the inhibitors are still largely elusive (186).

The patient-derived xenograft (PDX) model comprises a surgically dissected clinical tumor sample that is implanted into immuno-deficient mice (159). Unlike established cell lines that are cultured *in vitro* for many passages, the PDX tumor is believed to recapitulate tumor heterogeneity and, thus, better reflects the features of the original human cancer (151-152). In particular, the PDX model has become a valuable tool to test small molecules with anti-cancer activities in drug discovery and biomarker development (152, 198). Although the PDX model can be perceived as time-consuming to establish and might be highly variable, drug responses obtained from PDX mice are highly consistent with responses observed in human patients (159). For example, the overall response rates of EGFR antibodies in PDX colorectal cancer studies were similar to those found in the clinic (199-200). A comparative analysis of EGFR antibody sensitivities in PDX models (201) and patient (202) populations in different studies revealed that the response rate in PDX can reflect the clinical outcome (159).

Herein, we synthesized a small molecule, referred to as HI-B1, and report that the small molecule shows an inhibitory effect against β-catenin/TCF4 luciferase activity in colon cancer cells. HI-B1 preferentially causes apoptosis of cancer cells in which the

survival is dependent on β-catenin. The inhibition of the β-catenin/TCF4 pathway by HI-B1 resulted in apoptosis and binding assays show that β-catenin is a direct target protein of HI-B1. HI-B1 disrupts the interaction between β-catenin and TCF4 *in vitro* and *ex vivo*. A PDX colon cancer study showed that HI-B1 inhibits the growth of tumors with a high expression level of β-catenin, but was not effective against tumors with a low level of β-catenin. We anticipate that these preclinical results will provide the groundwork for translational research of β-catenin inhibitors and development of biomarkers to match patients with inhibitors in era of precision oncology.

2.3 Results

2.3.1 HI-B1 preferentially attenuates growth and induces apoptosis of cancer cells in which β-catenin is essential for survival.

HI-B1 was synthesized (Figure 2.1a), and subjected to a β-catenin/TCF4 luciferase assay to test its efficacy against the Wnt/β-catenin signaling pathway. HI-B1 inhibited β-catenin/TCF4 luciferase activity in a dose-dependent manner in two different colon cancer cell lines (Figure 2.1b). Because the inhibition of Wnt/β-catenin activity can reportedly kill cancer cells (192, 195-196, 203-207), the effect of HI-B1 on cell growth and apoptosis was investigated. HI-B1 treatment suppressed growth of several types of colon cancer cells (DLD1, CACO2 and HCT116), but did not affect the H838 lung cancer cell line (Figure 2.1c). Because H838 was reported as a cell line that expresses little or no β-catenin (208), the specificity of HI-B1 on the β-catenin pathway

was further examined. By using short hairpin RNA that target β-catenin, we were able to find cell lines in which the survival is dependent on β-catenin. Knockdown of β-catenin resulted in apoptosis in DLD1, CACO2 and HCT116 cells, whereas H838 and CCD-18Co cells were only marginally affected by the knockdown (Figure 2.1d). HI-B1 treatment also preferentially resulted in more apoptosis in DLD1, CACO2 and HCT116 compared to H838 and CCD-18Co cells (Figure 2.1e).

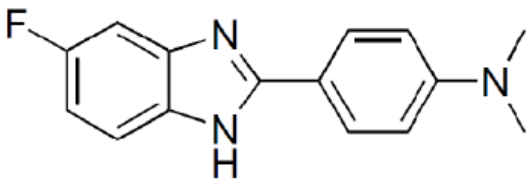

HI-B1

Figure 2.1a Chemical structure of HI-B1.

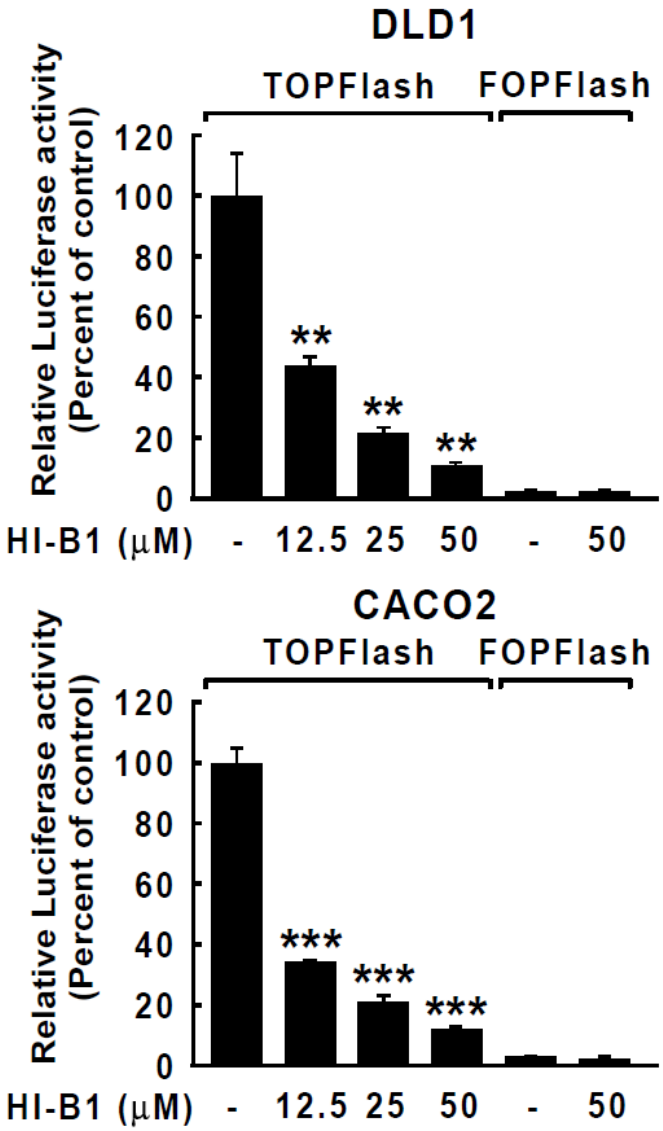

Figure 2.1b The effect of HI-B1 on β-catenin/TCF4 luciferase activity. DLD1 *(upper panel)* and CACO2 *(lower panel)* cells were transfected with TOPFlash, which contains TCF4 binding sequences, or FOPFlash (as a negative control) and then treated with different doses of HI-B1 for 24 hr. Firefly luciferase activity was normalized with Renilla luciferase activity.

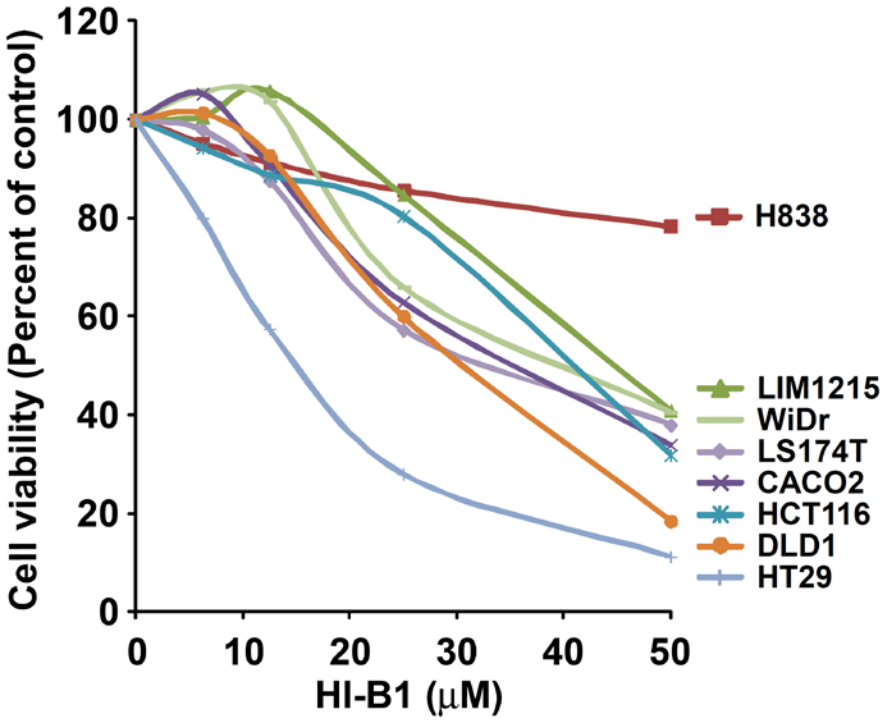

Figure 2.1c The effect of HI-B1 on cell viability. Cells were treated with HI-B1 at different doses for 48hr and then viability was assessed by MTS assay.

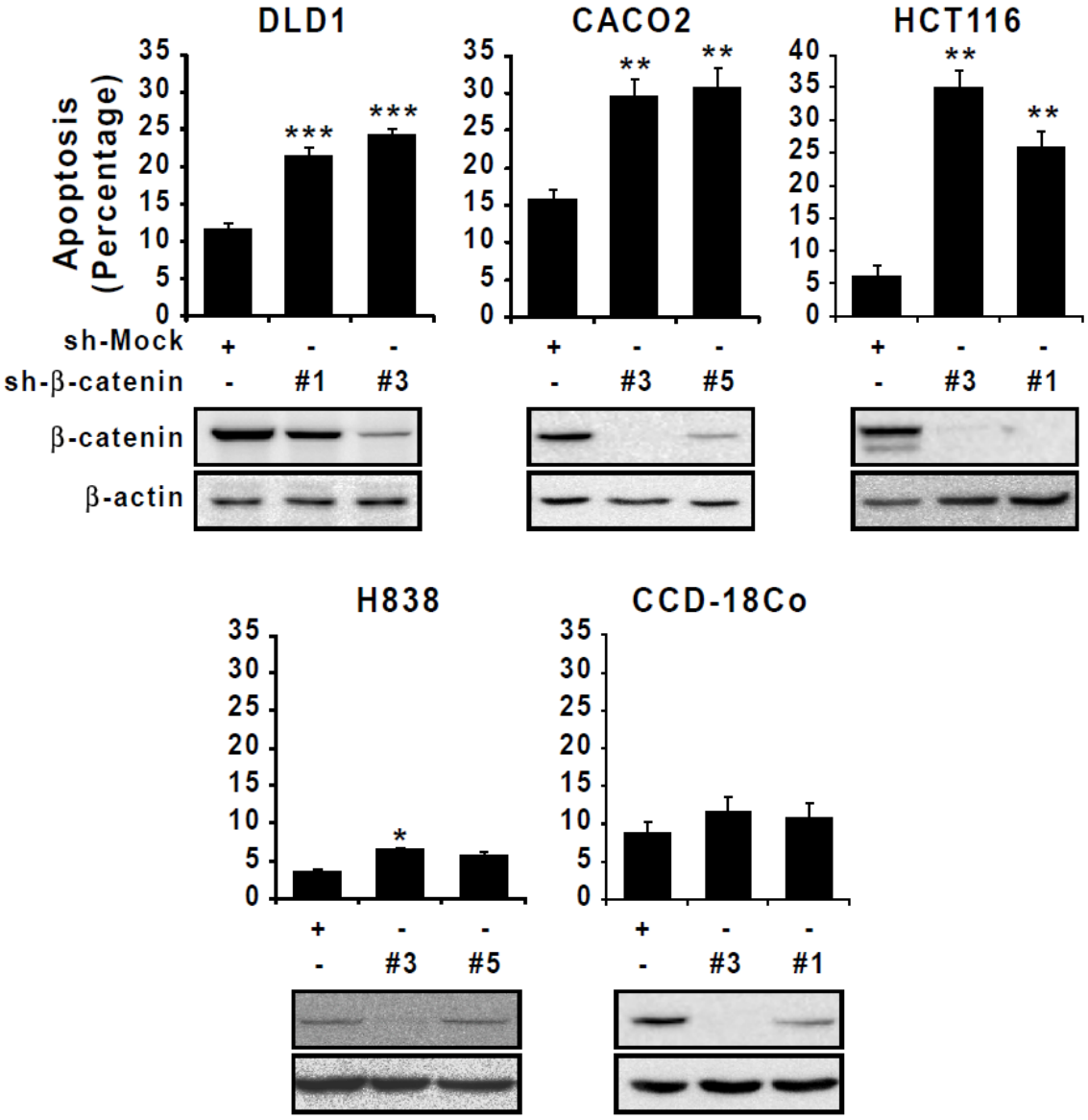

Figure 2.1d The effect of β-catenin knock-down on apoptosis in DLD1, CACO2, HCT116, H838 and CCD-18Co cell lines. Cells were incubated for 48 hr after the shRNA infection and antibiotic selection. Apoptosis was measured by annexin V/propidium iodide staining and flow cytometry.

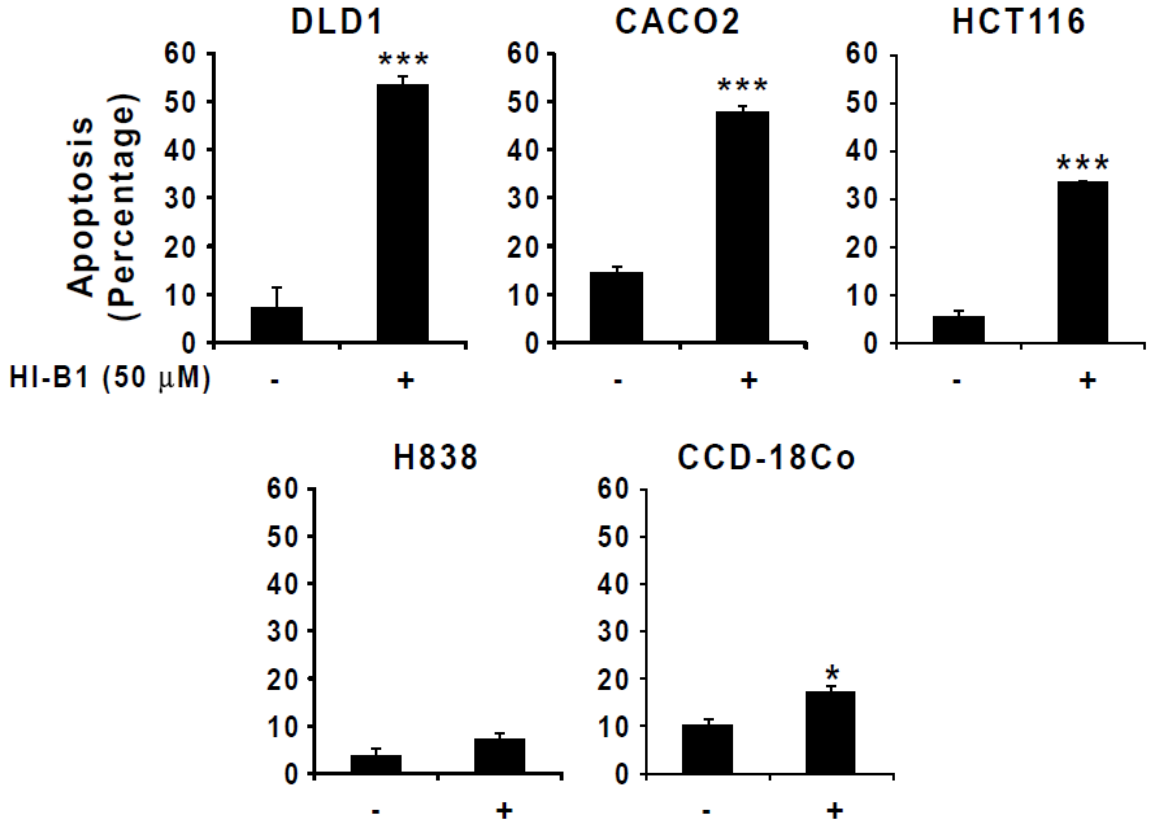

Figure 2.1e The effect of HI-B1 on apoptosis in DLD1, CACO2, HCT116, H838 and CCD-18Co cell lines. Cells with β-catenin-dependent growth (DLD1, CACO2 and HCT116) and β-catenin independent growth (H838 and CCD-18Co) were treated with HI-B1. Apoptosis was measured after 48 hr of treatment with flow cytometry. All values of graphs present mean ± standard deviation (SD) (in triplicate). Significant differences were calculated by one-way ANOVA compared with DMSO-treated group or sh-mock group (*P < 0.05, **P < 0.01, ***P < 0.001).

2.3.2 HI-B1 inhibits anchorage-independent growth of colon cancer cells by reducing β-catenin target gene expression.

Because β-catenin is a primary driver in colon cell transformation (209), the effect of HI-B1 was examined using soft agar, a laboratory measurement of cell transformation and anchorage-independent growth of cancer cells. Results indicated that HI-B1 treatment significantly inhibited anchorage-independent growth of DLD1 and HT-29 colon cancer cells (Figure 2.2a). The growth of CACO2, another colon cancer cell line, was also suppressed by HI-B1 in a 7-day proliferation assay (Figure 2.2b). To further confirm the effect of HI-B1 on the β-catenin pathway, an H-ras/β-catenin-induced foci formation assay was conducted. According to previous studies (210-211), constitutively active Ras facilitates nuclear translocation of β-catenin to induce cell transformation. In agreement with these results (211), foci formation of NIH3T3 cells was substantially induced by co-transfection of H-ras and β-catenin, but not by single gene transfection (Figure 2.2c). Notably, HI-B1 attenuated H-ras/β-catenin-induced foci formation. These results reveal that HI-B1 inhibits anchorage-independent growth and foci formation where β-catenin plays an important role.

We next focused on the details of the Wnt/β-catenin signaling pathway affected by HI-B1. Quantitative real-time PCR results showed that HI-B1 treatment decreased mRNA expression of *cyclin D1* and *axin2* in DLD1 and CACO2 cell lines (Figure 2.2d). HI-B1 also down-regulated cyclin D1 and c-Myc protein levels (Figure 2.2e). Of particular note, the β-catenin protein level was not changed by HI-B1 either at the protein or mRNA level. This suggests that HI-B1 could inhibit the nuclear translocation of β-

catenin (212) or directly bind to β-catenin and suppress its activity (186). Cytosolic and nuclear fractions were treated or not treated with HI-B1 and results showed that nuclear translocation of β-catenin was not altered by the compound, which suggested a direct-binding mechanism of action (Figure 2.2f).

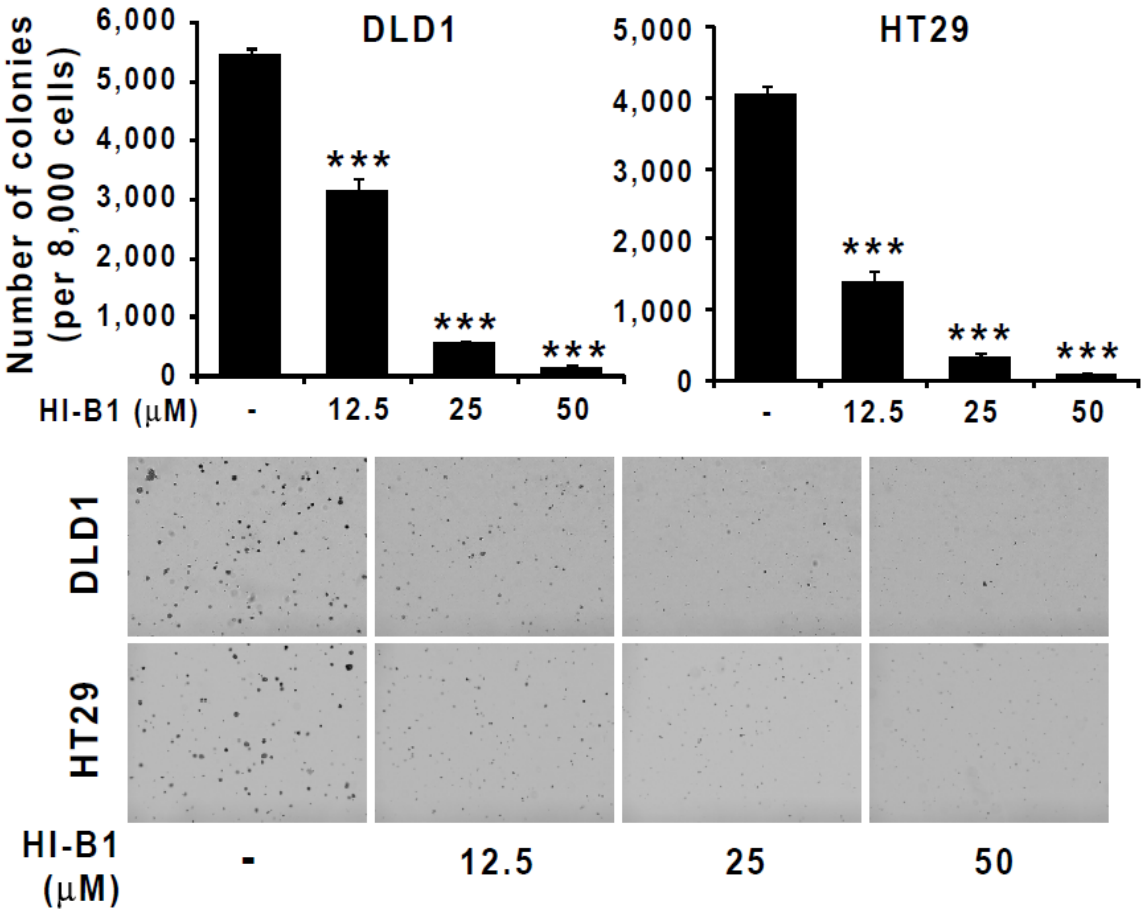

Figure 2.2a The effect of HI-B1 on anchorage-independent growth of DLD1 and HT29 colon cancer cell lines. Cells were seeded into 0.3%-agar-containing medium with various concentrations of HI-B1 and the numbers of colonies was counted at Day 7.

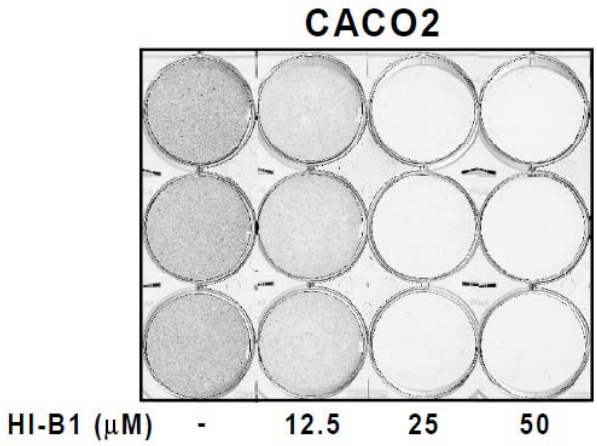

Figure 2.2b The inhibitory effect of HI-B1 on CACO2 cell growth. Cells were seeded on 6-well plates with various concentrations of HI-B1 and then stained with crystal violet solution at Day 7.

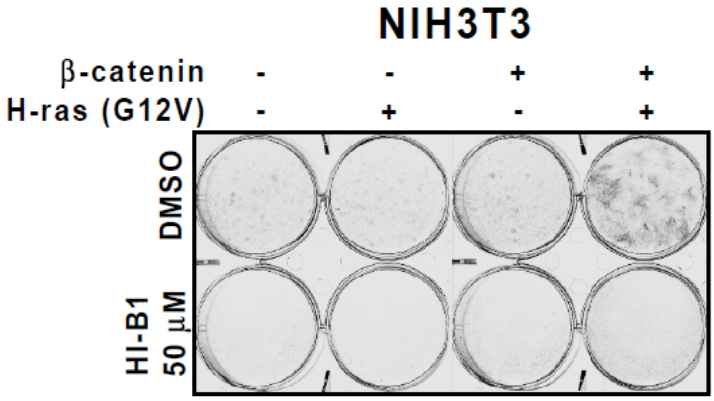

Figure 2.2c The inhibitory effect of HI-B1 on β-catenin/H-ras-induced cell transformation of NIH-3T3. Foci formation was induced by co-transfection of β-catenin and H-ras (H12V) in NIH3T3. After transfection, cells were treated with HI-B1 and stained with crystal violet solution (Day 14). The medium was changed every other day.

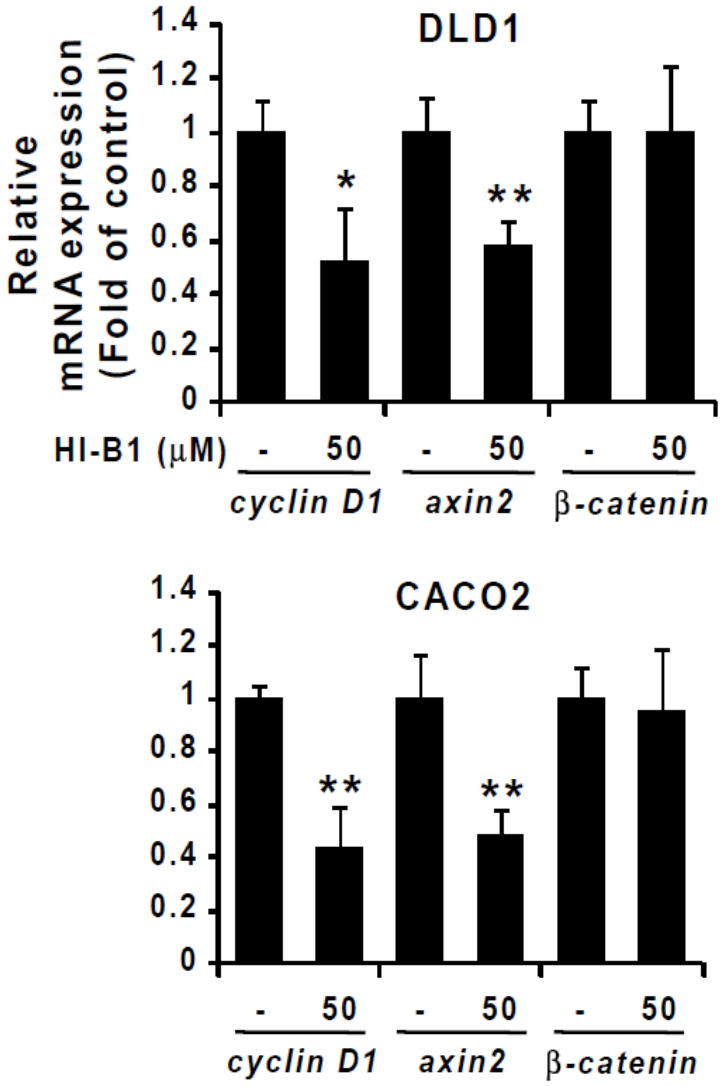

Figure 2.2d The effect of HI-B1 on mRNA expression of β-catenin target genes in DLD1 and CACO2 cells. After 24 hr of HI-B1 treatment, mRNA was harvested from the cells and relative amount was measured by qRT-PCR. All values of graphs present mean ± SD (in triplicate). Significant differences were calculated by one-way ANOVA compared with DMSO-treated group (*P < 0.05, **P < 0.01, ***P < 0.001).

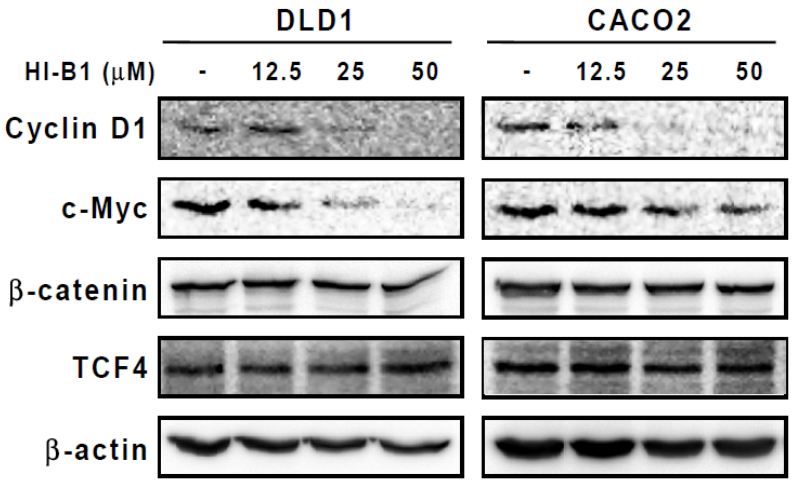

Figure 2.2e The effect of HI-B1 on cyclin D1 and c-Myc protein expression. After 24 hr of HI-B1 treatment, protein was harvested from the cells and relative amount was measured by western blotting.

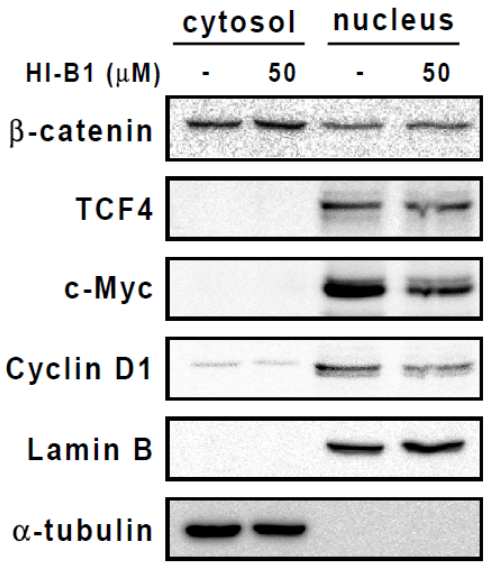

Figure 2.2f The effect of HI-B1 on β-catenin translocation in DLD1 cell. The cytosol and the nucleus portions of the cells were fractionated at 24hr of HI-B1 treatment. Lamin B and α-tubulin were used as a cytosol and a nucleus marker, respectively.

2.3.3 HI-B1 directly binds with β-catenin, but not TCF4, to disrupt the β-catenin/TCF4 interaction.

To determine whether HI-B1 binds to β-catenin, HI-B1 was conjugated to Sepharose 4B-beads and incubated with cell lysates. β-Catenin was detected by Western blot and results showed that HI-B1 directly binds with β-catenin (Figure 2.3a). Notably, TCF4, which is a binding partner of β-catenin, with which it forms a complex and induces gene transcription, was not bound to HI-B1. The interaction between β-catenin and TCF4 has been implicated as a core element of the Wnt pathway in colorectal cancer cell growth (213). The binding of HI-B1 with β-catenin disrupted the interaction between β-catenin and TCF4 *in vitro* (Figure 2.3b). His-tagged β-catenin and GST-tagged TCF4 were incubated with or without HI-B1 and His-β-catenin was pulled down with nickel beads. The amount of TCF4 co-immunoprecipitated with β-catenin was decreased in HI-B1 treated groups. The effect of HI-B1 against β-catenin/TCF4 complex formation was also confirmed in DLD1 and CACO2 cell lines (Figure 2.3c). These results demonstrate that HI-B1 directly binds with β-catenin and disrupts the β-catenin/TCF4 interaction.

We next conducted *in silico* docking, to predict the important binding residues of HI-B1. A nitrogen atom was found to be responsible for a hydrogen bond with β-catenin (Figure 2.3d). HI-B1-NC, a derivative of HI-B1 in which the nitrogen atom (N) is substituted with a carbon atom (C), was synthesized and its biological activities were compared with HI-B1. The N to C substitution completely attenuated the effect of HI-B1 against DLD1 colon cancer cell growth (Figure 2.3e). The inhibitory effect on β-catenin/TCF4 luciferase activity was also eliminated by the substitution (Figure 2.3f).

Overall, the nitrogen atom of HI-B1was found to be important for its direct binding with β-catenin.

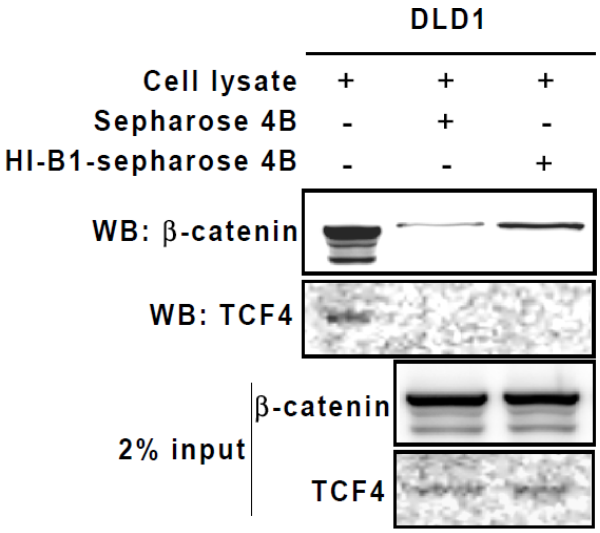

Figure 2.3a Binding assay of HI-B1 on β-catenin *ex vivo*. HI-B1 was conjugated with Sepharose 4B beads and incubated with cell lysates. Protein co-immunoprecipitated with the beads was analyzed by western blotting.

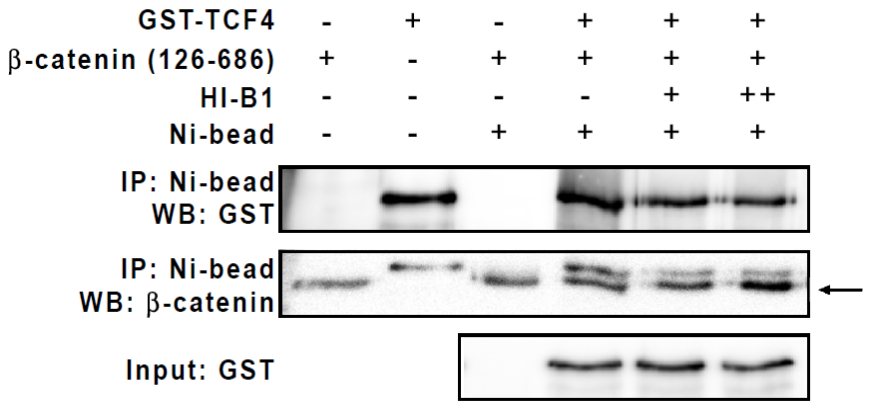

Figure 2.3b The effect of HI-B1 on β-catenin/TCF4 interaction *in vitro*. HI-B1 disrupts the formation of the β-catenin/TCF4 complex *in vitro*. His-tagged β-catenin (126-686) was immunoprecipitated with nickel beads and the amount of TCF4 was detected by western blotting.

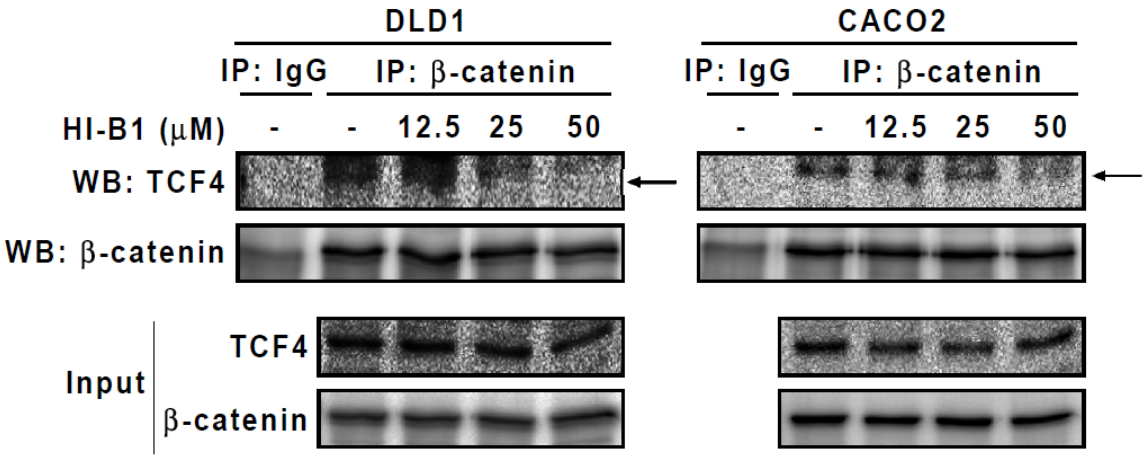

Figure 2.3c The effect of HI-B1 on β-catenin/TCF4 interaction in DLD1 and CACO2 cell lines. Cell lysates were harvested after 24hr of HI-B1 treatment. β-Catenin was immunoprecipitated and binding proteins was detected by western blotting.

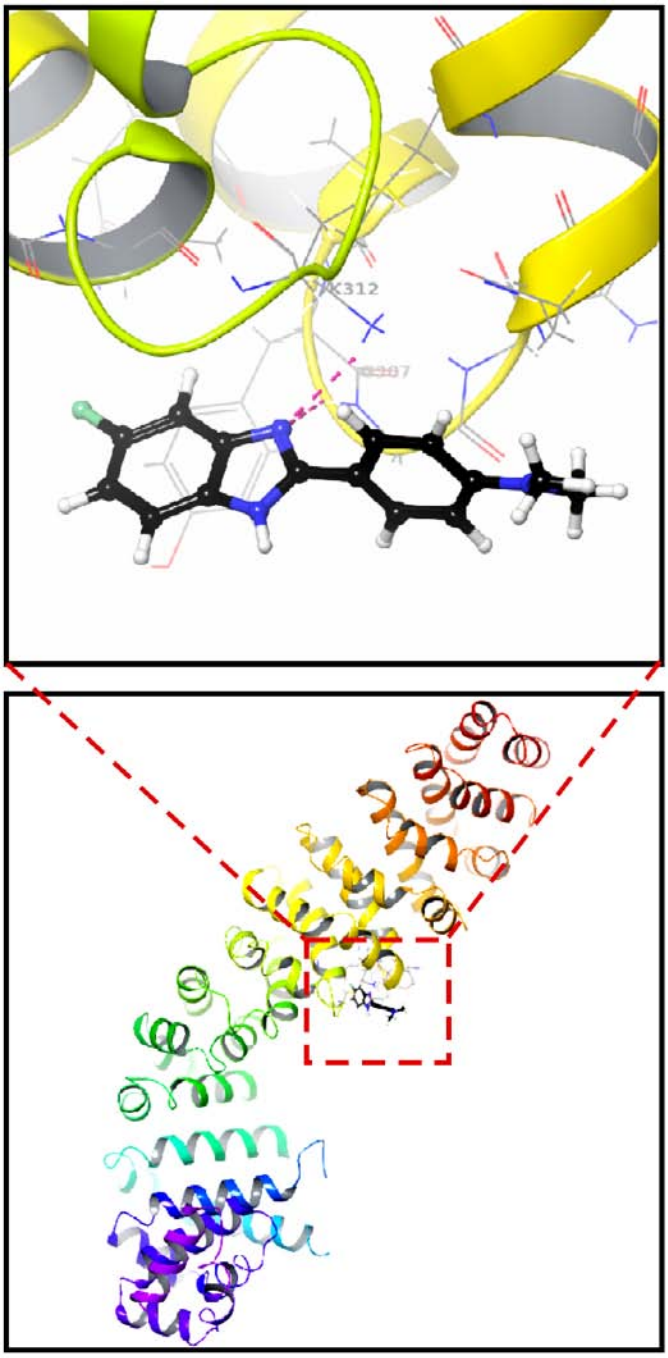

Figure 2.3d Molecular docking predicts the interaction of HI-B1 and β-catenin. A nitrogen atom of HI-B1 forms a hydrogen bond with β-catenin (upper panel) from Extra precision (XP) docking *in silico* (lower panel).

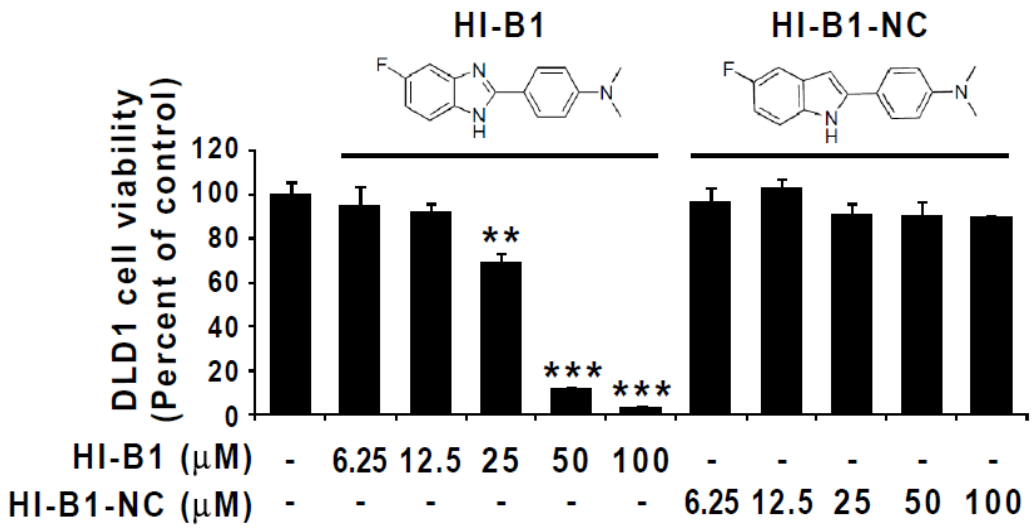

Figure 2.3e The effect of HI-B1 and HI-B1-NC on cell viability. HI-B1 and HI-B1-NC (a nitrogen atom was substituted with a carbon) were treated to DLD1 cells (n=3). Proliferation was measured by MTS assay at 48 hr.

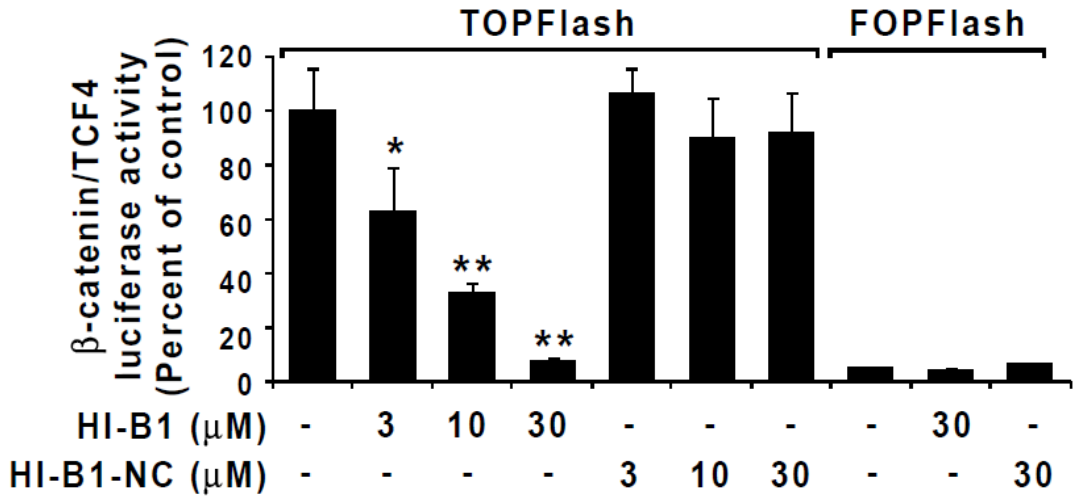

Figure 2.3f The effect of HI-B1 and HI-B1-NC on luciferase activity. β-catenin/TCF4 luciferase activity was measured by luminometer at 24 hr. Significant difference with DMSO-treated group by One-way ANOVA (*P < 0.05, **P < 0.01, ***P < 0.001).

2.3.4 HI-B1 suppresses polyp formations in APC^{min} model and decreases the growth of patient-derived xenograft (PDX) tumors with a high expression level of β-catenin.

To verify the efficacy of HI-B1 *in vivo*, a PDX colon cancer model was utilized. Tumor fragments were from two different patients (JG5 and JG14) and immunohistochemistry analysis of the two PDX tumors indicated a difference in β-catenin expression. JG5 had a high level of β-catenin expression compared to JG14 (Figure 2.4a). The effect of HI-B1 was examined on each of the two colon cancer PDX models to determine whether the expression level of β-catenin could be a predictive marker for sensitivity to a β-catenin inhibitor. Interestingly, HI-B1 treatment reduced the weight and volume of the JG5 PDX tumor, but had no effect on the JG14 PDX tumor (Figure 2.4b and c). Although the efficacy of HI-B1 against only two PDX tumors with differential levels of β-catenin expression, this suggests that tumors with higher levels of β-catenin might be more sensitive to β-catenin inhibitor treatment. The decrease in c-myc expression by HI-B1 was confirmed by immunohistochemistry (Figure 2.4d). Further studies testing HI-B1 in more PDX tumors will be needed.

To further confirm the *in vivo* efficacy of HI-B1, the APC^{Min} mouse model was utilized. This mouse model exhibits aberrant activation of β-catenin, and HI-B1 treatment reduced the number of polyps (Figure 2.4e). In addition, the mRNA expression levels of *c-myc* and *cyclin D1* (Figure 2.4f and g) were also decreased. Overall, these results indicate that HI-B1 inhibits β-catenin-driven tumorigenesis *in vivo*.

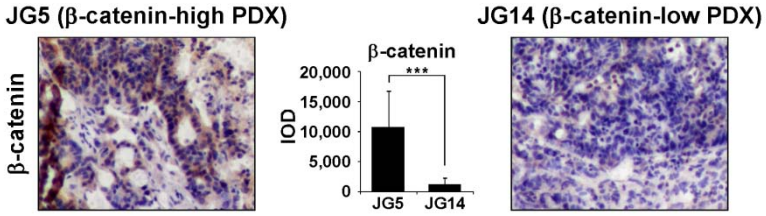

Figure 2.4a β-Catenin expression levels in colon cancer PDX. Integrated optical density (IOD) of immunohistochemistry was quantified using Image-Pro Plus software.

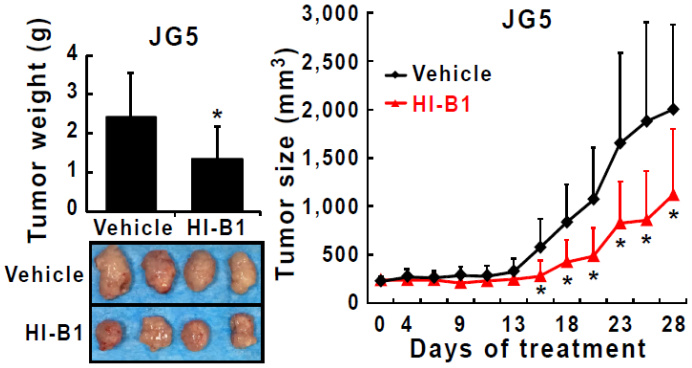

Figure 2.4b HI-B1 inhibits JG5 tumor growth. HI-B1 was administered per os (p.o) (orally) three times a week at a dose of 50 mg/kg (n = 8/group). Tumor size was measured three times a week and the weight was measured at the end of experiments.

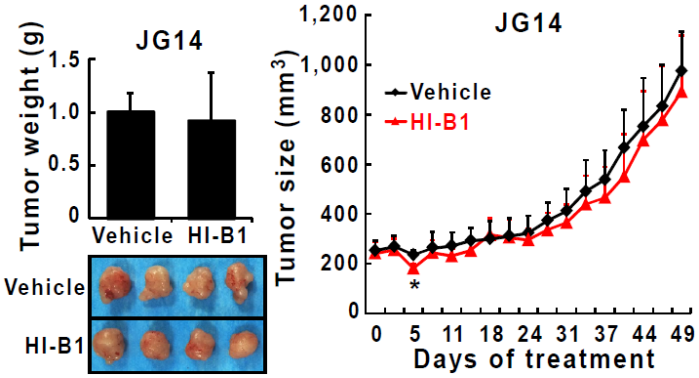

Figure 2.4c HI-B1does not affect JG14 tumor growth.

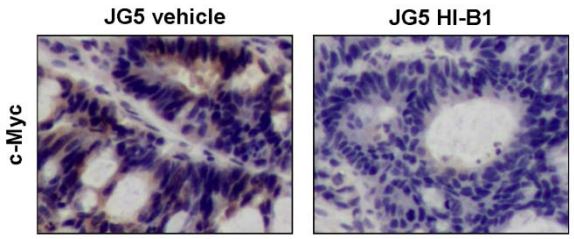

Figure 2.4d The effect of HI-B1 on c-Myc expression of JG5 PDX tumor. In the JG5 PDX tumor, c-Myc Expression level change by HI-B1 treatment was measured by IHC.

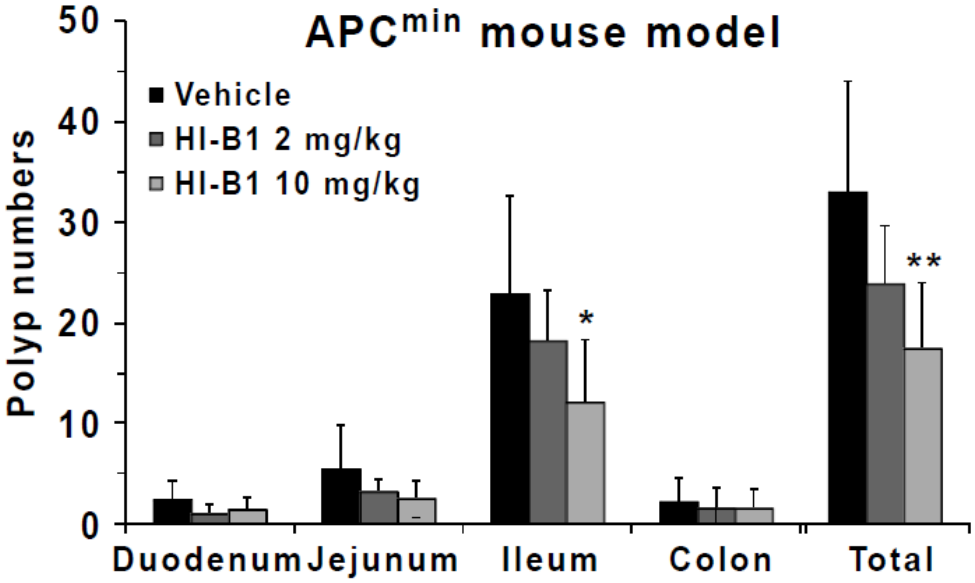

Figure 2.4e HI-B1 reduced polyp formation driven by aberrant activation of β-catenin in APC^{min} mouse model. The indicated doses of HI-B1 were administered p.o. for 10 weeks, and mice were sacrificed for analysis of intestinal carcinogenesis (n = 6/group).

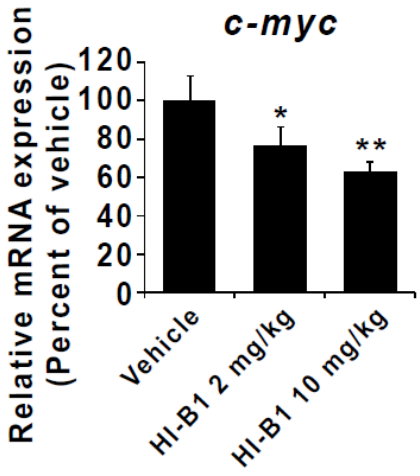

Figure 2.4f The effect of HI-B1 on *c-myc* mRNA expression in APC^{min} mouse model. Small intestine tissue was prepared from the same position of ileum from mice, and then mRNA expression levels of *c-myc* was quantified by qRT-PCR.

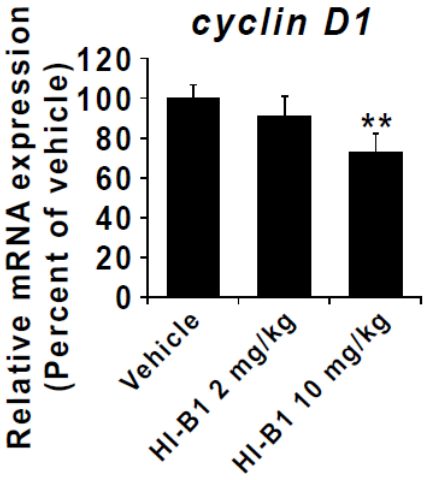

Figure 2.4g The effect of HI-B1 on *cyclin D1* mRNA expression in APC^{min} mouse model. Small intestine tissue was prepared from the same position of ileum from mice, and then mRNA expression levels of *cyclin D1* was quantified by qRT-PCR. (One-way ANOVA; *P < 0.05, **P < 0.01, significant difference compared to the vehicle group.)

2.4 Discussion

Most cases of sporadic colon cancer are caused by genetic mutations of several Wnt pathway proteins, including APC, axin and β-catenin, resulting in stabilization of β-catenin and the formation of the β-catenin/TCF4 complex (185, 214). Although a number of inhibitors against the Wnt pathway and β-catenin have already been identified, the development of β-catenin inhibitors with specificity on the β-catenin pathway still has value. In this study, the identification of HI-B1 as an inhibitor of β-catenin/TCF4 luciferase activity (Figure 2.1b) provided an opportunity to develop a drug candidate against the β-catenin pathway. The molecular mechanism of HI-B1 was investigated and revealed its direct binding to β-catenin and disruption of the β-catenin/TCF4 interaction (Figure 2.3b and c). Based on the promising *in vitro* experimental results, we sought to establish its efficacy *in vivo*. A PDX tumor expressing high levels of β-catenin was more sensitive to β-catenin inhibitor treatment compared to another tumor expressing lower levels of β-catenin (Figure 2.4b and c). Notably, we showed that a β-catenin inhibitor could attenuate the growth of a colon cancer patient-derived tumor, and that sensitivity to the inhibitor might be dependent on the expression level of β-catenin.

Our study provides a rationale for detecting β-catenin levels when Wnt/β-catenin inhibitors are tested to colon cancer patients. The significant difference between β-catenin expression levels of colon cancer patients (Figure 2.4a) was rather unexpected, regarding the well-known importance of β-catenin in colorectal cancer (186). As HER2 (human epidermal growth factor receptor 2)-targeted drugs, such as lapatinib and trastuzumab, are recommended only to HER2-positive breast cancer patients (215), HI-B1 was only

effective in PDX where β-catenin is highly expressed (Figure 2.4b and c). These results suggest that β-catenin expression level might be correlated with the efficacy of Wnt/β-catenin inhibitors against colon cancer. Such information could be further exploited for biomarker development and therapeutic applications against colon cancer, especially in ongoing clinical trial of Wnt pathway inhibitors.

2.5 Materials and Methods

2.5.1 Reagents

All antibodies were commercially available, including β-catenin, β-actin, cyclin D1, α-tubulin and GST from Santa Cruz Biotechnology (Santa Cruz, CA), c-Myc and TCF4 from Cell Signaling Technology (Beverly, MA), lamin B from Calbiochem (San Diego, CA). The luciferase assay substrate and the Cell Titer 96 Aqueous One Solution Reagent [3-(4,5-dimethylthiazol-2-yl)-5-(3-carboxymethoxyphenyl)-2-(4-sulfophenyl)-2H-tetrazolium, inner salt (MTS)] kit were from Promega (Madison, WI).

2.5.2 Synthesis of 4-(5-fluoro-1H-benzo[d]imidazol-2-yl)-N,N-dimethylaniline (HI-B1)

To a solution of 4-(Dimethylamino)benzaldehyde (2.98 g, 20 mmol) in ethanol (40 mL), Sodium dithionite (3.48 g, 20 mmol) in water (20 mL) was added. The resulting mixture was stirred at room temperature for 20 min and then 4-Fluoro-1,2-phenylenediamine (2.52 g, 20 mmol) was added portion wise. The resulting reaction

mixture was refluxed for about 14 h. The solution was then diluted with water. The obtained brown precipitate was filtered and purified by recrystallization from ethanol to give 2.5 g of 4-(5-fluoro-1H-benzo[d]imidazol-2-yl)-N,N-dimethylaniline. Nuclear magnetic resonance (NMR) spectra were determined in acetone-d_6 using a Varian instrument (^{1}H, 400 MHz). ^{1}H NMR (400 MHz, DMSO-d_6) δ 7.97 (d, J = 8.8 Hz, 2H), 7.50 (dd, J = 8.4, 4.8 Hz, 1H), 7.32 (dd, J = 9.1, 2.4 Hz, 1H), 7.02 (td, J = 8.6, 2.4 Hz, 1H), 6.85 (d, J = 8.8 Hz, 2H), 3.01 (s, 6H). Electrospray ionisation mass spectrometry (ESI-MS) calculated $(M+H)^+$ 256.1172, found 256.1294.

2.5.3 Cell culture

All cell lines were purchased from American Type Culture Collection (ATCC, Manassas, VA) except for LIM1215 from Sigma-Aldrich (St. Louis, MO). Cells were comprehensively authenticated by PCR using human-specific primers and morphology checks through microscopes before being frozen as recommended (216), and free of mycoplasma from Hoechest 33258 staining (217-218). Each vial of frozen cells was thawed and used in experiments for a maximum of 8 wk. Cells were cultured in RPMI 1640 (DLD1, LIM1215, H838) or MEM (CACO2, LS174T, WiDr, CCD-18Co) or McCoy's 5A (HCT116, HT29) or DMEM (293T) containing penicillin (100 units/mL), streptomycin (100 µg/mL), and 10% fetal bovine serum (FBS; Gemini Bio-Products, Calabasas, CA). The NIH3T3 cell line was cultured in DMEM with 10% calf serum (CS; Gemini Bio-Products). All cells were incubated at 37°C with 5% CO_2.

2.5.4 Luciferase assay

Transient transfection was performed using jetPEI (Promega). Assays to detect firefly luciferase and Renilla activities were performed according to the manufacturer's manual (Promega). Briefly, cells were seeded onto 10-cm plates and co-transfected with 400 ng of the *Renilla luciferase* internal control gene and 4 μg of the *TOPFlash* luciferase reporter construct containing three tandem Tcf consensus binding sites upstream of luciferase cDNA, or the *FOPFlash* luciferase reporter construct, a plasmid with mutated Tcf binding sites. After 16 h of transfection, cells were trypsinized and seeded onto 48-well plates, and then treated with respective compounds for 24 hr. Luciferase and Renilla activities were measured using their respective substrates.

2.5.5 MTS assay

Cells were seeded (1×10^3 cells/well) in 96-well plates, incubated overnight and then treated with different doses of HI-B1. After incubation for 2 days, 20 μL of CellTiter96 Aqueous One Solution (Promega) were added and then cells were incubated for 1 hr at 37°C in a 5% CO_2 incubator. Absorbance was measured at 492 nm.

2.5.6 Lentivirus production and infection

The shRNA of β-catenin clones (sh-ctnnb1 #1: TRCN0000003843, AGGTGCTATCTGTCTGCTCTA; #3: TRCN0000003845, GCTTGGAATGAGACTGCTGAT; #5: TRCN0000010824, CCATTGTTTGTGCAGCTGCTT) were purchased from University of Minnesota

Genomics Center (Minneapolis, MN). The lentiviruses were generated from 293T packaging cells. The cell culture supernatant fraction containing lentivirus was harvested from 293T cells at 24 or 48 hr after transfection. The cells were infected with the lentiviruses in the presence of 10 μg/ml of polybrene (Sigma Aldrich, St. Louis, MO). After 24 hr of infection, the cells were treated with puromycin for selection, and then pooled for subsequent analysis.

2.5.7 Flow cytometry for analysis of apoptosis

For analysis of apoptosis, cells (1.5×10^5 cells per well) were seeded into six-well plates and cultured overnight, then exposed to 50 μM HI-B1 for 48 h. Cells were trypsinized, washed twice with cold PBS. They were then resuspended with PBS and incubated for 5 min at room temperature with annexin V-FITC plus propidium iodide. Cells were analyzed using a FACSCalibur flow cytometer (BD Biosciences, San Jose, CA).

2.5.8 Anchorage-independent cell transformation assay

Cells (8×10^3/well) suspended in 10% Basal Medium Eagle (Sigma Aldrich) were added to 0.3% agar with different doses of HI-B1 in a top layer over a base layer of 0.5% agar with the same concentration of HI-B1. The cultures were maintained at 37°C in a 5% CO_2 incubator for 1 wk and then colonies were counted under a microscope using the Image-Pro Plus software (v.6.1) program (Media Cybernetics, Rockville, MD).

2.5.9 7-day proliferation assay

CACO2 cells were seeded into 6-well plates (2×10^5 cells/well) and cultured with or without different doses of HI-B1. After 7 days of incubation, cells were fixed with 4% paraformaldehyde (in PBS), and then stained with 0.5% crystal violet (in water) (219).

2.5.10 Foci formation assay

Transformation of NIH3T3 cells was performing following standard protocols. Cells were transiently transfected with combinations of pcDNA3-H-RasG12V (100 ng), pcDNA3-β-catenin (1 μg) and pcDNA3-mock (as compensation to achieve equal amounts of DNA) plasmids and incubated overnight. Then the cells were cultured in 5% CS-DMEM with or without HI-B1 for 2 wk. The media were changed every other day. Foci were fixed and stained with 0.5% crystal violet (220).

2.5.11 Western blot analysis

Cells were disrupted on ice for 30 min in cell lysis buffer (20 mM Tris pH 7.5, 150 mM NaCl, 1 mM Na_2EDTA, 1 mM EGTA, 1% Triton X-100, 2.5 mM sodium pyrophosphate, 1 mM β-glycerophosphate, 1 mM sodium vanadate, and 1 mM PMSF [phenylmethylsulfonyl fluoride]) with protease inhibitor cocktail (Roche, Switzerland). The supernatant fraction was harvested after centrifugation at 13,000 rpm for 10 min. Protein concentrations were determined with the Bio-Rad protein assay reagent (Richmond, CA). For nuclear and cytosol fractions, NE-PER Nuclear and Cytoplasmic Extraction Reagents (Thermo Scientific, Waltham, MA) were used according to the

manufacturer's protocol. The protein lysates were separated by SDS-PAGE and transferred to polyvinylidene fluoride membranes in 20 mM Tris-HCl (pH 8.0), containing 150 mM glycine and 15% (v/v) methanol. Membranes were blocked with 5% non-fat dry milk in 1 x TBS containing 0.05% Tween 20 (TBS-T) and incubated with primary antibodies at 4°C overnight. Protein bands were visualized by the LAS4000 Biomolecular Imager (GE Healthcare, United Kingdom) and Western Lightning Plus ECL (Perkin Elmer, Waltham, MA) after incubation with appropriate secondary antibodies.

2.5.12 Quantitative PCR (qRT-PCR)

Total RNA from cells was extracted using RNeasy Plus Mini Kit (Qiagen, Valencia, CA) following the manufacturer's instructions. The reverse transcription reaction was performed with the amfiRivert cDNA Synthesis Platinum Master Mix (GenDepot, Barker, TX). Expression of the indicated genes was assessed with a 7500 real time PCR system (Applied Biosystems, Carlsbad, CA) using the Power SYBR Green Master Mix (Life Technology, Grand Island, NY). Reaction plates were incubated in a 96-well thermal cycling plate at 95°C for 10 min and then underwent 40 cycles of 15 s at 95°C and 1 min at 59°C. All reactions were performed in triplicate. Relative quantitation (RQ) was calculated using the $2^{-\Delta Ct}$ method, where ΔCt symbolizes the change in Ct between the sample and reference mRNA. The following primers were used to detect expression: GAPDH, 5'-AGCCACATCGCTCAGACAC-3' (forward), 5'-GCCCAATACGACCAAATCC-3' (reverse); cyclin D1, 5'-

AGCTCCTGTGCTGCGAAGTGGAAAC -3’ (forward), 5’-AGTGTTCAATGAAATCGTGCGGGGT -3’ (reverse); AXIN2, 5’-CTGGCTCCAGAAGATCACAAAG-3′ (forward) and 5′-ATCTCCTCAAACACCGCTCCA-3′ (reverse); β-catenin, 5’-ACCTTTCCCATCATCGTGAG-3′ (forward), 5’-AATCCACTGGTGAACCAAGC-3’ (reverse).

2.5.13 Protein purification

A construct comprising residues 126-686 of human β-catenin (AB451264) was subcloned into pET-46 Ek/LIC vector (EMD Millipore). The recombinant His-fusion β-catenin was expressed in *E.coli* BL21 (DE3) and purified by affinity chromatography using nickel-nitrilotriacetic acid-agarose. (HisPur™ Ni-NTA, Thermo Scientific).The protein was eluted from the resin with 250 mM imidazole, 150 mM NaCl, 20 mM tris, pH 8.0, and purified further on a gel-filtration HiLoad 16/60 Superdex-200 column (GE Healthcare) equilibrated with buffer (150 mM NaCl, 20 mM CAPS, pH 10.5).

2.5.14 *Ex vivo* pull-down assays

Cell lysates (500 μg) were incubated with HI-B1-Sepharose 4B (or Sepharose 4B only as a control) beads (50 μL 50% slurry) in reaction buffer (50 mM Tris, pH 7.5, 5 mM EDTA, 150 mM NaCl, 1 mM DTT, 0.01% NP-40, and 2 mg/mL bovine serum albumin). After incubation with gentle rocking overnight at 4°C, the beads were washed

3 times with buffer (50 mM Tris, pH 7.5, 5 mM EDTA, 150 mM NaCl, 1 mM DTT, and 0.01% NP-40) and the binding proteins were visualized by Western blotting.

2.5.15 Co-immunoprecipitation assay

Cells were treated with the indicated concentrations of HI-B1 for 24 hr and then disrupted with lysis buffer. Immunoprecipitation was performed by incubating overnight with anti-β-catenin. Protein G Agarose beads (50 μl) (GenDepot, Barker, TX) were added and the solution was incubated for 6 hr at 4°C. The beads were washed 3 times with lysis buffer. Bound proteins were harvested and visualized by Western blotting.

2.5.16 *In silico* molecular docking

The Glide module from Schrödinger Suite 2011 was used for prediction of a small molecule-protein binding mode. A crystal structure of a human β-catenin structure (PDB ID:1JPW) was downloaded from Protein Data Bank. The binding pocket was selected around the K312 and K435 residues, which are reported to be important in the β-catenin/TCF4 binding mode. The XP (extra precision) docking was repeated more than 30 times, and the most frequent outcomes of β-catenin in chemical-protein interaction were selected as possible binding residues.

2.5.17 Animal Experiment protocols

All animal experiments were reviewed and approved by the Institutional Animal Care and Use Committees of the University of Minnesota (Minneapolis, MN) and Zhengzhou University (Zhengzhou, Henan, China).

2.5.18 Patient-derived xenografts (PDX)

Fresh tumor tissue fragments were collected from colon cancer patients and transferred at 4°C in FBS-free RPMI 1640 medium with antibiotics. Tumor tissues were trimmed into 3–5 mm sizes within 2 hr after surgical resection, and implanted subcutaneously in 6 to 8 week-old female SCID mice (Vital River Laboratories Co., Ltd., Beijing, China). Once mass formation reached 1500 mm^3, mice of this first generation of xenografts (named P1) were sacrificed and the tumors were passaged and expanded for 3 more generations (P2 and P3). When P4 tumors reached an average volume of 50 mm^3, mice were divided into different groups (n = 8/group) and treated with vehicle or HI-B1 50 mg/kg, respectively, 3 times a week by oral gavage. HI-B1 was dissolved in 5% DMSO and 5% PEG containing PBS. Mice were sacrificed at the end of the experiment and tumors extracted. Tumor volume was calculated using the following formula: tumor volume (mm^3) = (length × width ×height × 0.5). These studies were approved by the Ethics Committee of Zhengzhou University. Patients whose tumors were used in these studies were completely informed and provided consent.

2.5.19 APC^{min} mouse model

C57BL/6J-$Apc^{Min/+}$ mice (APC^{min} mice, RRID:IMSR_JAX:002020) were purchased from the Jackson Laboratory (Bar Harbor, ME), bred and genotyped according to the manufacturer's protocol. Male 6-week-old mice were treated with vehicle or 2 or 10 mg/kg/day of HI-B1 by oral gavage for 10 weeks (n = 6/group). At the end of the experimental period, the intestine and colon were removed, opened longitudinally, and fixed flat between filter paper sheets in 10% buffered formalin overnight. These sections were stained with a 0.2% methylene blue (Sigma-Aldrich) solution, and the mucosal surfaces were assessed for counting polyps with a stereoscopic microscope. One cm-long sections were prepared from the same position of ileum across the groups, and mRNA was extracted for further real-time PCR analysis.

2.5.20 Immunohistochemistry

Colon cancer patients-derived xenograft samples were fixed in 10% formalin overnight, embedded in paraffin, and sectioned at 5 μm of thickness. The sections were stained with haematoxylin and eosin (H&E) according to standard protocols.
Immunohistochemistry
staining for β-catenin and c-Myc was performed using an ABC complex kit (PK-6100, Vector Laboratories, Burlingame, CA). Harris's haematoxylin was used for counter staining. The staining intensity was quantified by calculating the integrated optical density (IOD) using the Image Pro-Plus 6.1 software program (Media Cybernetics) (221).

Chapter 3:

The synergistic effect of aspirin and ginger extract against colon cancer

3.1 Summary

Colon cancer is the third most diagnosed cancer type in the U.S. Aspirin has received a considerable attention due to its anti-cancer effects on colon cancer patients with *PIK3CA* mutations. Ginger extract (GE) has protective effect against aspirin-induced hemorrhagic ulcer, and active components of GE possess anti-colon cancer effects. This led us to investigate on the effects and mechanisms of aspirin and GE combination. Co-treatment of aspirin and GE resulted in synergistic cytotoxicity in HCT116, DLD1 and HCT15 colon cancer cell lines. The combination treatment caused apoptosis by enhancing p53 and p21 protein expressions. 6-Shogaol was identified as an active component of GE showing inhibition of anchorage-independent growth and direct binding with Akt1/2. In colon cancer patient-derived xenograft (PDX) models, co-treatment of aspirin 100 mg/kg plus GE 5 mg/kg significantly suppressed tumor growth. Of note, tumor-suppressive effects were similar between the combination group and aspirin 400 mg/kg group, but weight loss was shown only in aspirin-only group. The combination of aspirin and GE could be further exploited for therapeutic applications against colon cancer.

3.2 Introduction

Aspirin (acetylsalicylic acid) is one of the most frequently used drugs against multiple purposes including pain, fever and inflammatory conditions (222). In past decade, the effect of aspirin has been investigated in colon cancer which is the third most

common cancer type diagnosed in the United State (223-226). Several lines of studies on colon cancer showed that aspirin causes apoptosis and inhibits tumor growth (227-229). Especially, aspirin prescription showed a hazard ratio of 0.53 in mortality of colon cancer patients who did not use aspirin before the diagnosis (224). However, aspirin has adverse effects including hazard ratio of 2.07 in gastrointestinal bleeding even at low doses (230). Therefore the dosage reduction which aims the reduction of toxicity while maintaining the therapeutic efficacy is important for patients who use aspirin (231). Finding another small molecules or drug-like medications will benefit patients who take aspirin for colon cancer treatment.

Phosphoinositide 3-kinase (PI3-K)/Akt/mammalian target of rapamycin (mTOR) pathway is a central component of colon cancer progression, and the proteins are overexpressed in colon cancer (232). Activated PI3-K/Akt/mTOR signaling results in down-regulation of p53, a tumor suppressor (233-234). In colon cancer patients with activating mutations on *PIK3CA*, regular aspirin usage after diagnosis was associated with improved colon cancer-specific survival and overall survival (hazard ratio: 0.18, and 0.54), respectively (235). However, aspirin usage did not improve survival rates in *PIK3CA*-wild type patients (235). This result showed that aspirin exerts its effect against colon cancer in which PI3-K/Akt/mTOR pathway is activated. Small molecules that inhibit the signaling, such as 6-gingerol targeting Akt1/2 (236), might help aspirin in suppressing *PIK3CA*-mutant tumor growth.

Ginger (*Zingiber officinale* Roscoe, Zingiberaceae) is one of the most widely used dietary ingredients worldwide in the forms of condiment, tea or extracts (237-238).

Ginger is reported to be effective not only for ulcerative colitis and inflammation, but for treatment against cancer (237). Ginger powder reduced aspirin-induced hemorrhagic ulcer in stomach of rats (239). Ginger extracts (GE) and its active constituents, 6-gingerol and 6-shogaol, showed inhibitory effects against colon cancer (240-242). 6-Gingerol inhibited the tumor growth of HCT116 colon cancer cell xenograft by directly binding with leukotriene A4 (241). 6-Shogaol suppressed HT-29 colon cancer cell growth by activating peroxisome proliferator-activated receptor γ (242). The anti-ulcer and anti-cancer effects of ginger showed the possibility that ginger might reduce the toxicity of aspirin while maintaining the efficacy of aspirin. However, the combination of ginger extracts (GE) and aspirin and their molecular mechanism against colon cancer are still remained unclear.

Herein, we tested the combination of GE and aspirin against colon cancer cells *in vitro* and *in vivo*. Treatment of GE or aspirin inhibits proliferation and anchorage-independent growth of HCT116, DLD1 and HCT15 colon cancer cell lines. When treated in combination, GE and aspirin exerts synergistic effects against the colon cancer cell growth. Co-treatment of GE and aspirin significantly increases apoptosis and increased protein expression levels of p53 and p21. High-performance liquid chromatography (HPLC) analysis reveals that 6-gingerol, 6-shogaol, 8-gingerol and 10-gingerol are major components of GE. Among the four compounds, 6-shogaol shows the strongest inhibitory effects against colon cancer. GE and 6-shogaol directly binds to Akt1/2. Colon cancer patient-derived xenograft (PDX) results show that co-treatment of aspirin 100 mg/kg and GE 5 mg/kg has similar therapeutic effects compared to aspirin 400 mg/kg treatment.

3.3 Results

3.3.1 Ginger extract and aspirin inhibit anchorage-independent growth and cell proliferation of HCT116, DLD1 and HCT15 colon cancer cell lines.

Based on the selective effect of aspirin on *PIK3CA*-mutant colon cancer patients (235), we chose HCT116, DLD1 and HCT15 colon cancer cell lines in where *PIK3CA* mutations are present (243-244). Aspirin and GE were tested on anchorage-independent growth and cell proliferation to confirm their effects (245-246) and calculate IC50 values that are needed for combination analysis (231). IC50 of aspirin on inhibiting anchorage-independent cell growth were 1.7, 1.9 and 2.2 mM in HCT116, DLD1 and HCT15 cell lines, respectively (Figure 3.1a). GE also inhibited anchorage-independent growth of the three colon cancer cells showing IC50 values of 2.3, 5.2 and 6.8 μg/ml, respectively (Figure 3.1b). In cell proliferation assay that cells are grown in anchorage-dependent condition, aspirin also inhibited the proliferation of HCT116, DLD1 and HCT15 cell lines (IC50: 2,4, 3.0 and 2.5 mM; Figure 3.1c). GE showed its inhibitory effects on cell proliferation showing higher IC50 values compared to the soft agar assay (IC50: 24, 38 and 31 μg/ml; Figure 3.1d). These result showed that aspirin and GE can suppress colon cancer growth when treated individually.

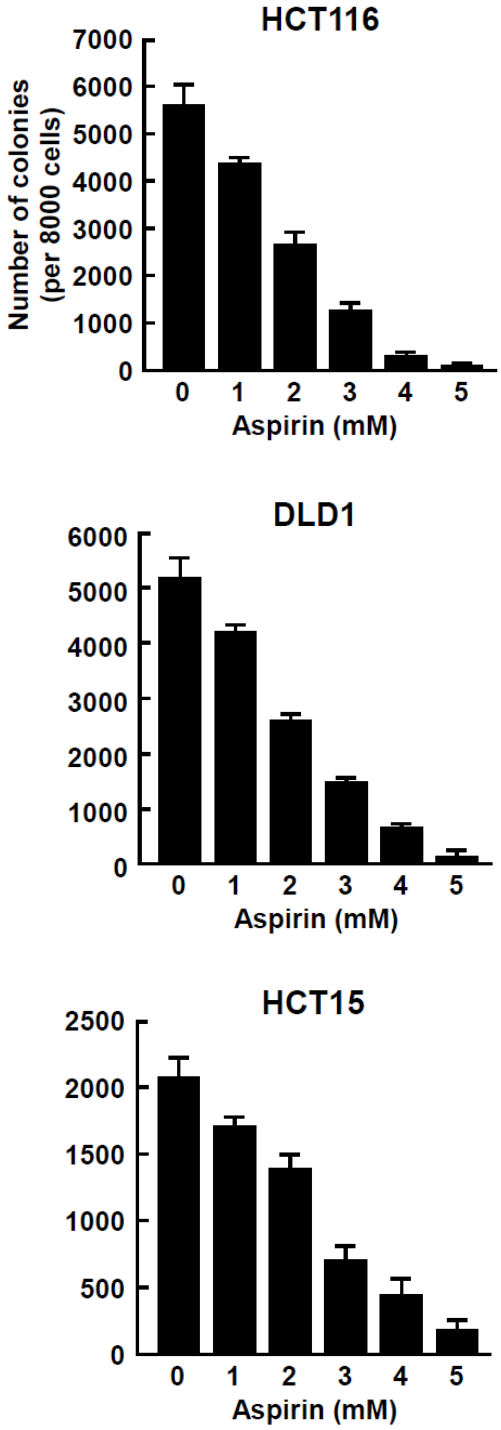

Figure 3.1a The effect of aspirin on anchorage-independent growth of HCT116, HT29 and DLD1 cell lines. The numbers of colonies were counted after 5-10 days.

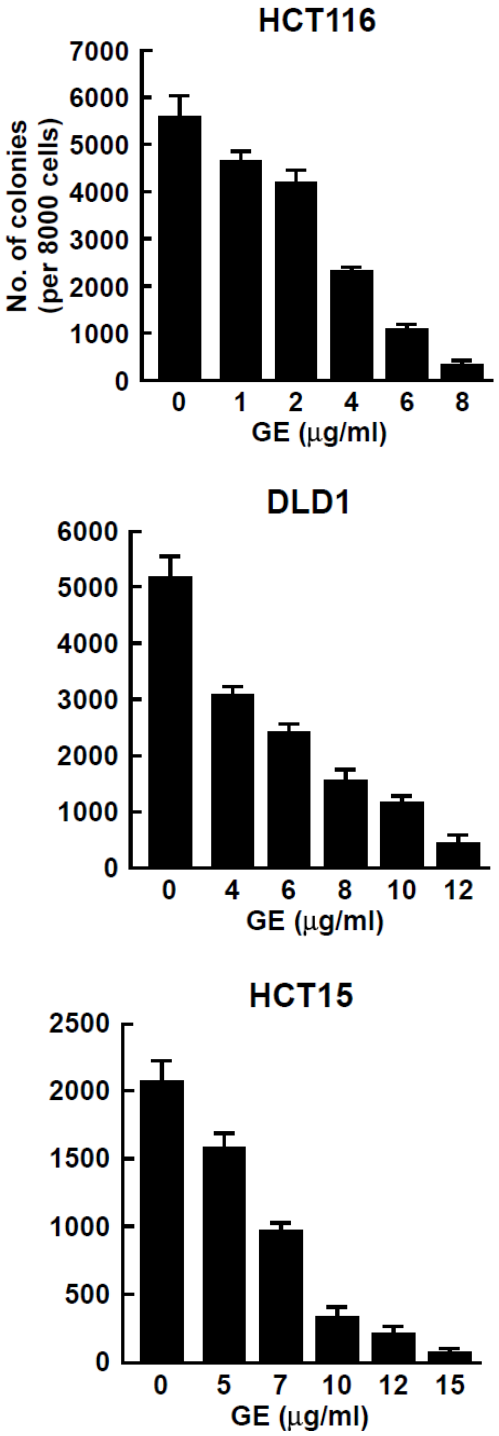

Figure 3.1b The effect of ginger extract (GE) on anchorage-independent growth of HCT116, HT29 and DLD1 cell lines. The colonies were counted after 5-10 days.

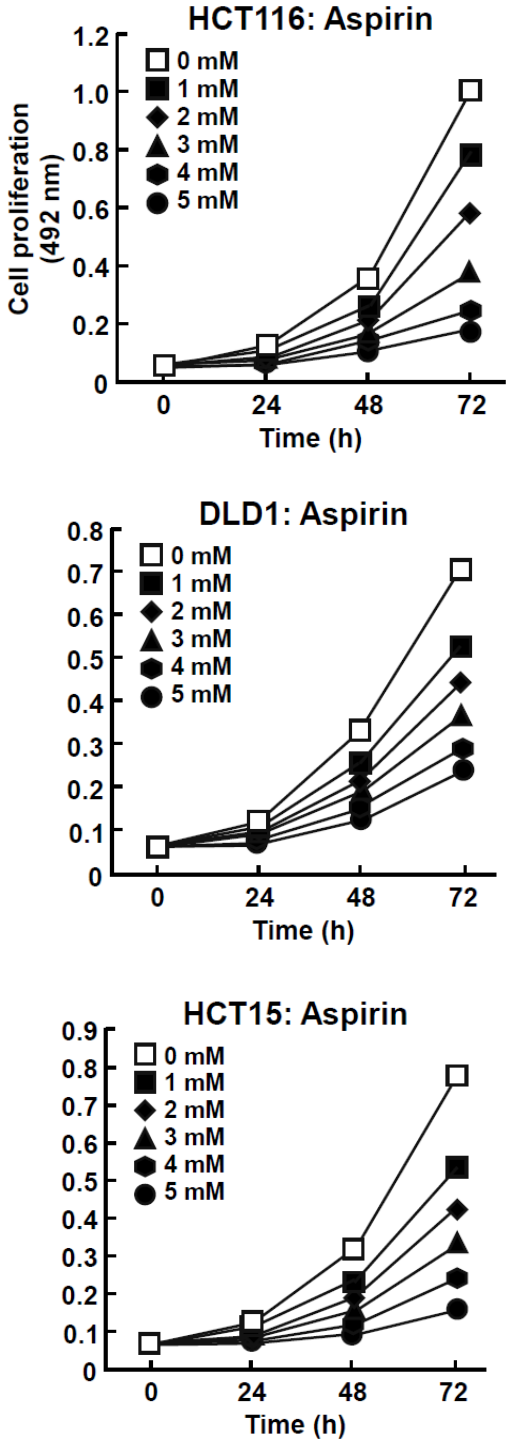

Figure 3.1c The effect of aspirin on cell proliferation. Cells were treated with aspirin (0-5 mM) and proliferation was determined at the indicated time points by MTS assay.

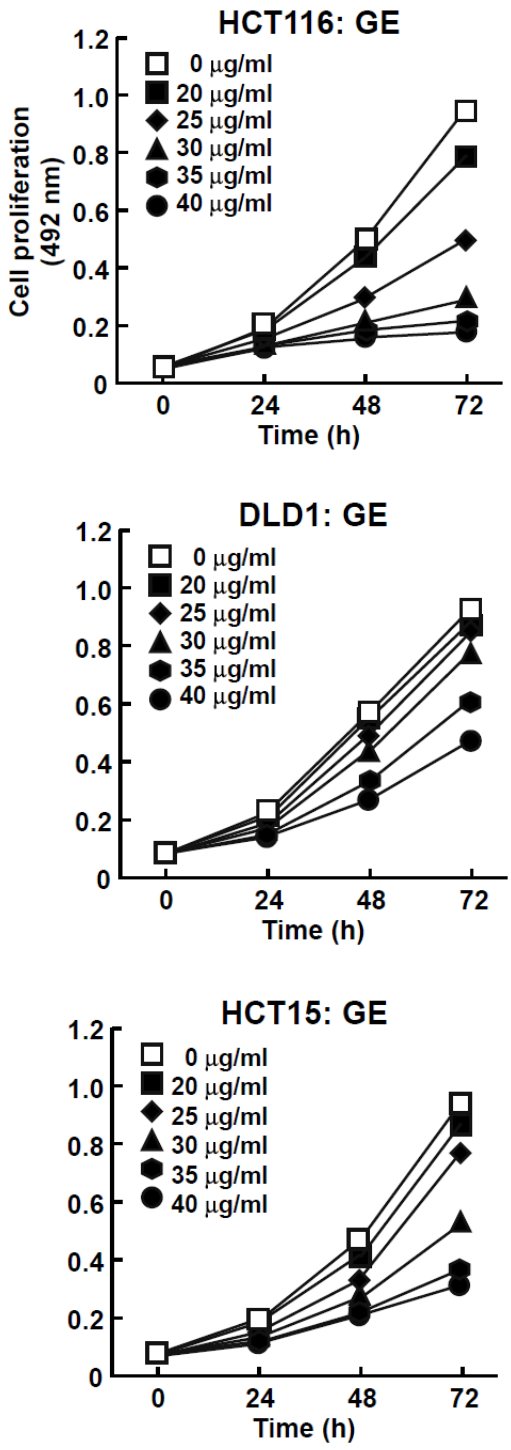

Figure 3.1d The effect of GE on cell proliferation. Cells were treated with GE (0-40 µg/ml) and proliferation was determined at the indicated time points by MTS assay.

3.3.2 Ginger extract and aspirin show synergistic effects when co-treated to colon cancer cells.

We next focused on the combinational effects of aspirin and GE. Different doses of GE were co-treated with aspirin and their efficacy was tested in anchorage-independent colon cancer cell growth. The percentage of the inhibition (Fraction affected: Fa) was then calculated to measure combination index (CI) which determines antagonism, additive effect and synergism between combinational treatments (231). Based on IC50 values of ginger extract and aspirin mentioned above, CI of co-treatment groups were determined. CI result showed that ginger extract and aspirin are synergistic when treated together against anchorage-independent cell growth of cancer cells (Figure 3.2a). Of particular note, the two treatments were more synergistic together at higher dosages resulting in CI of 0.1 to 0.3 which indicates very strong synergism. Formazan production assay also showed that 20 μg/ml of GE treatment can reduce IC50 value of aspirin from 2.28 to 0.66 mM (Figure 3.2b). We sought to find if the combination treatment triggers apoptosis, a programmed cell death. When treated individually, aspirin 5 mM treatment increased apoptosis by 4% and GE 15 μg/ml increased apoptosis by 9% in HCT116 cell line (Figure 3.2c). The combination treatment of aspirin and GE showed 26% increase of apoptosis. Protein expression of p53 and p21, tumor suppressors, were increased in aspirin and GE combination group (Figure 3.2d). This result supports the synergistic effect of aspirin and GE against colon cancer cell growth.

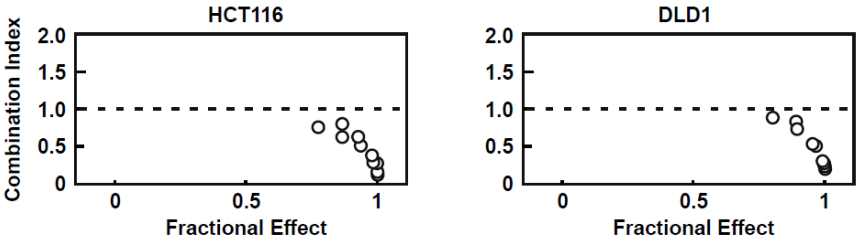

	Aspirin (mM)	GE (μg/ml)	Fa	CI
1	2	1	0.774	0.763
2	2	2	0.866	0.638
3	2	4	0.934	0.518
4	2	6	0.982	0.289
5	2	8	0.997	0.122
6	3	1	0.864	0.810
7	3	2	0.927	0.633
8	3	4	0.978	0.387
9	3	6	0.990	0.283
10	3	8	0.997	0.164

	Aspirin (mM)	GE (μg/ml)	Fa	CI
1	2	4	0.800	0.896
2	2	6	0.894	0.738
3	2	8	0.954	0.541
4	2	10	0.994	0.212
5	2	12	0.996	0.190
6	3	4	0.888	0.837
7	3	6	0.966	0.512
8	3	8	0.995	0.219
9	3	10	0.992	0.302
10	3	12	0.995	0.259

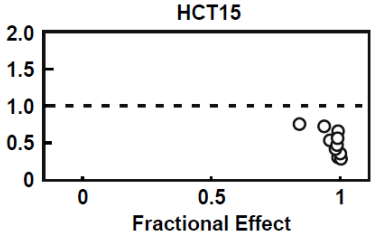

	Aspirin (mM)	GE (μg/ml)	Fa	CI
1	2	5	0.840	0.774
2	2	7	0.937	0.632
3	2	10	0.973	0.593
4	2	12	0.989	0.299
5	2	15	0.984	0.237
6	3	5	0.931	0.687
7	3	7	0.958	0.637
8	3	10	0.987	0.499
9	3	12	0.991	0.301
10	3	15	0.996	0.251

Figure 3.2a Aspirin and ginger extract (GE) combination shows strong synergistic effect. HCT116, DLD1, HCT15 cells were treated with different combinations of aspirin and GE for 5-10 days and then colonies were counted. The number of colonies was converted into affected fraction (Fa) among total cell population. Combination index (CI) was calculated according to Materials and Methods. CI values less than 0.85 indicate synergistic effect.

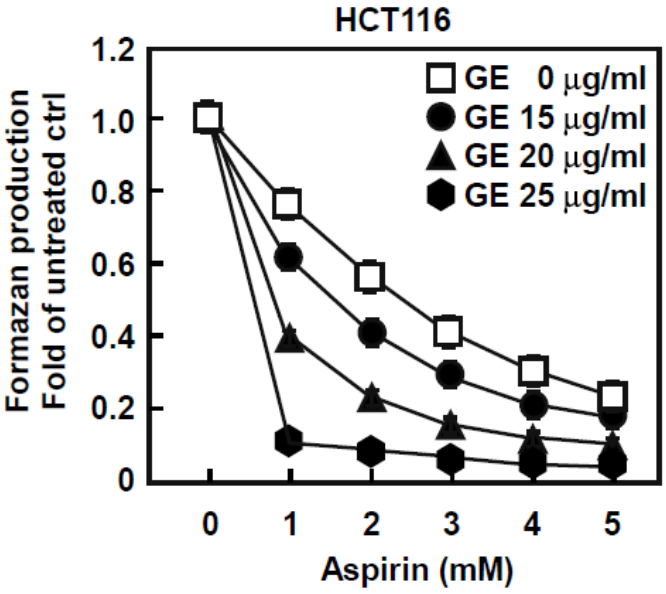

GE (μg/ml)	Aspirin IC50 (mM)
0	2.28
15	1.45
20	0.66
25	0.07

Figure 3.2b The effect of GE on IC50 values of aspirin. Aspirin and GE were co-treated to HCT116 cells for 72h at different concentrations, and IC50 values of aspirin at presence of GE were calculated.

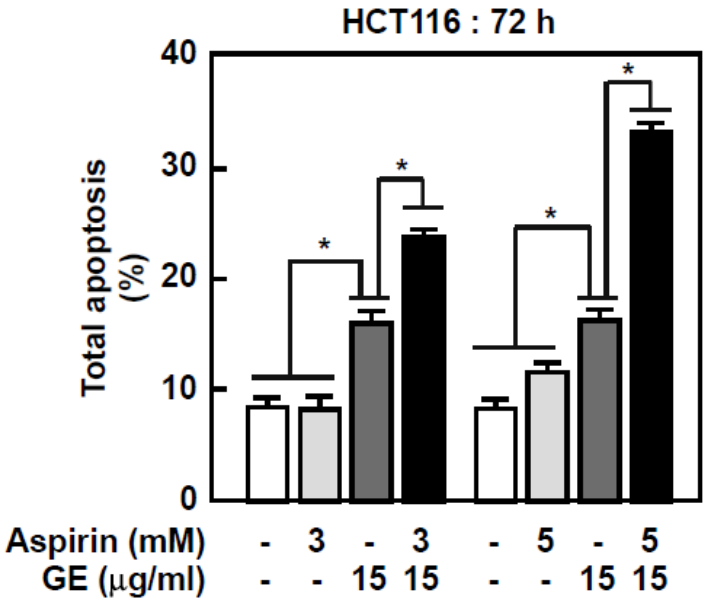

Figure 3.2c The effects of aspirin and GE on apoptosis. Aspirin and/or GE were treated for 72h. Apoptosis was measured with flow cytometry. The asterisk (*) indicates a significant decrease compared with untreated control ($p < 0.05$).

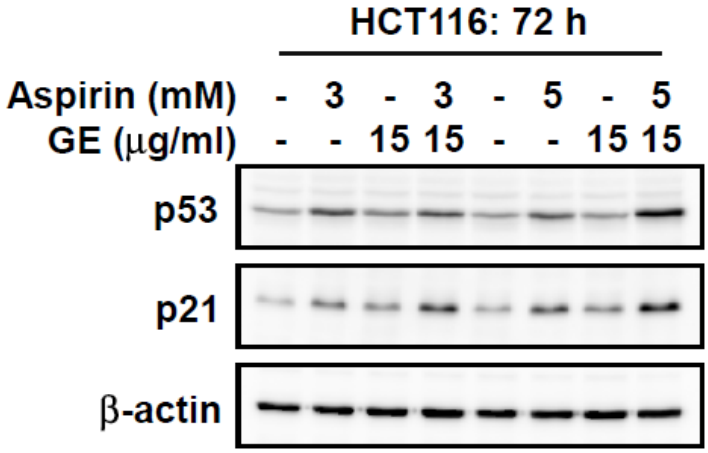

Figure 3.2d The effects of aspirin and GE on p53 and p21 expression levels. Aspirin and/or GE were treated for 72h and protein lysates were analyzed by western blots.

3.3.3 6-Shogaol, a major component of the GE, shows inhibitory effect against anchorage-independent growth of HCT116.

To elucidate details of the anti-cancer effect of GE, we sought to find the major ingredients of the extract. High-performance liquid chromatography (HPLC) result showed that 6-gingerol, 6-shogaol, 8-gingerol and 10-gingerol are four major components of the GE (Figure 3.3a and b). 6-Gingerol was the most abundant small molecule among the components, followed by 6-shogaol, 8-gingerol and 10-gingerol (Table 3.1). Based on the HPLC result, GE was reconstituted with the relative concentrations of the four major ingredients and tested in anchorage-independent growth and cell proliferation of HCT116 DLD1 (Figure 3.3c and d). Reconstituted ginger extract was similar to the original ginger extract. Among the four components, 6-shogaol had the strongest inhibitory effect against the cell growth of HCT116. Based on the previous finding that 6-shogaol possesses its anti-cancer effect by directly targeting Akt1/2 (236), we tested the ability of ginger extract and its major components to bind with Akt. Binding assay using sepharose 4B beads showed that GE and 6-shogaol directly bound to Akt1/2 (Figure 3.3e). Interestingly, 8-gingerol was able to bind with Akt, but 6-gingerol and 10-gingerol could not bind to the protein. Overall, the previous study and this result indicate that the anti-cancer effect of GE is derived from one of its active component, 6-shogaol, and that PI3-K/Akt pathway might be the signaling targeted by GE.

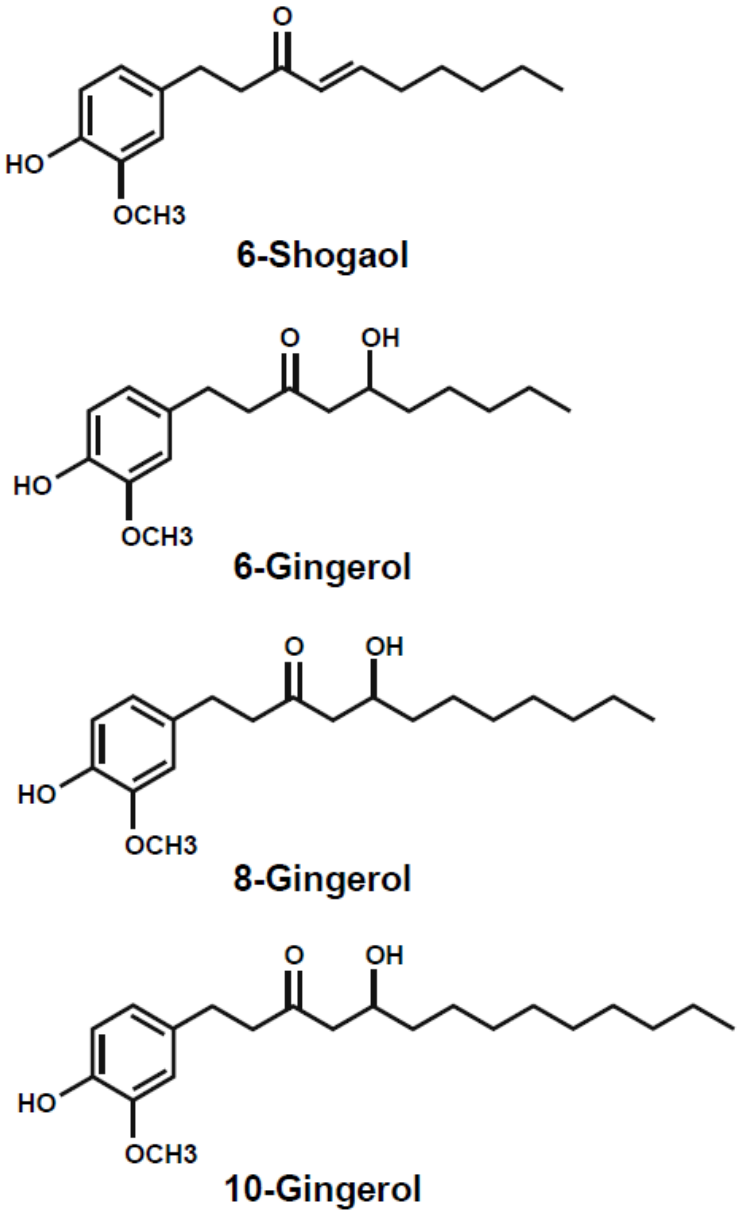

Figure 3.3a Chemical structures of four major ginger componets, 6-shogaol, 6-gingerol, 8-gingerol, and 10-gingerol.

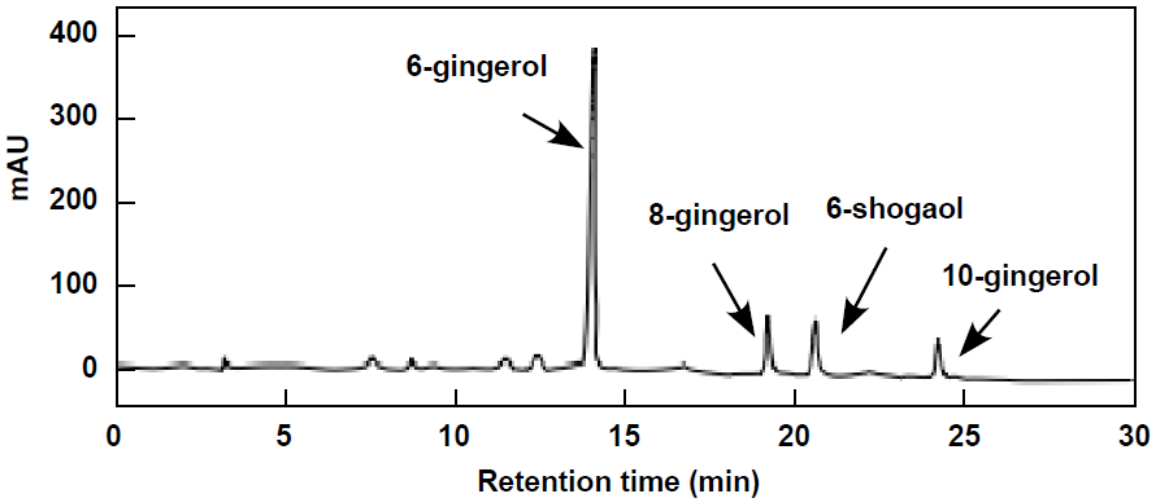

Figure 3.3b HPLC chromatograms of ginger extract. GE peaks were compared with those of 6-shogaol, 6-gingerol, 8-gingerol, and 10-gingerol (1 mM).

Table 3.1 Contents of GE. The amounts of components (μg/mg GE extract) were presented.

	6-Shogaol	6-Gingerol	8-Gingerol	10-Gingerol
μg/mg extract	107 ± 1	387 ± 1	71.7 ± 1.0	39.4 ± 0.1

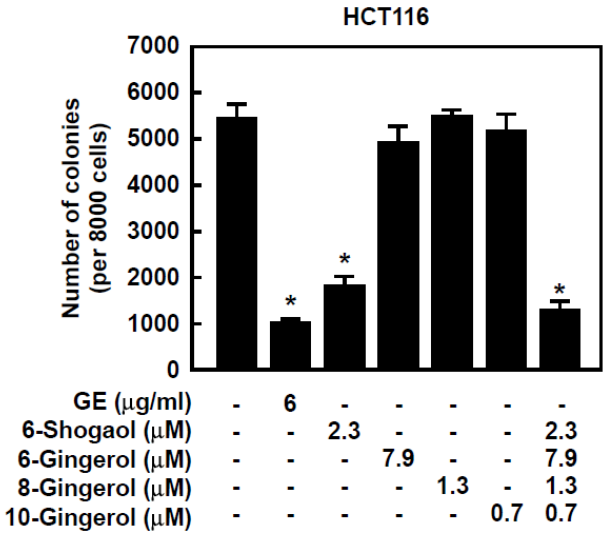

Figure 3.3c The effects of GE ingredients on anchorage-independent growth of HCT116 cells. Cells were treated with 6-shogaol, 6-, 8-, and/or 10 gingerol, or ginger extract and colonies were counted after 7 days.

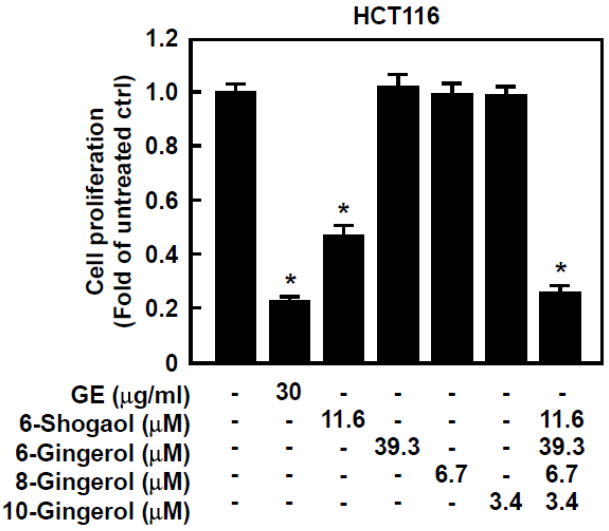

Figure 3.3d The effects of GE ingredients on HCT116 cell proliferation. Cells were treated with 6-shogaol, 6-, 8-, and/or 10 gingerol, or ginger extract and proliferation was determined at 72h by MTS assay.

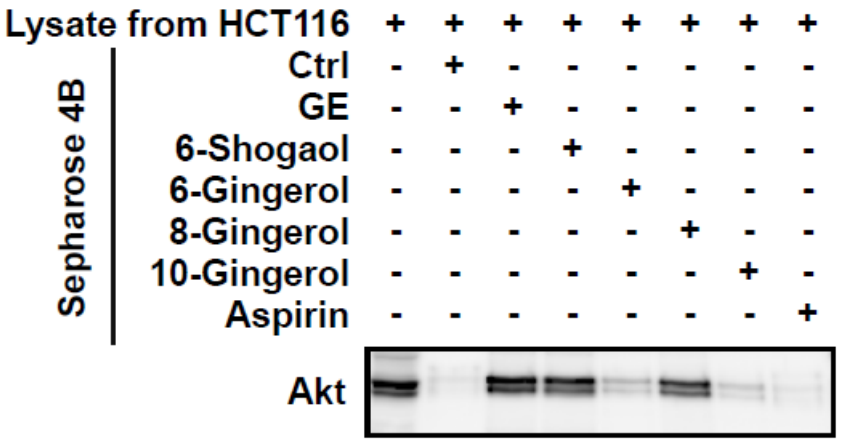

Figure 3.3e Ginger extract, 6-shogaol and 8-gingerol interact with Akt. Whole-cell lysates from HCT116 cells (500 μg) were incubated with control or chemical-conjugated Sepharose 4B beads, and then proteins bound to the beads were analyzed by western blotting.

3.3.4 Inhibition of PI3-K pathway can mimic the combination effect of ginger extract and aspirin.

Next, we sought to further confirm the combination effect of ginger extract and aspirin by mimicking the PI3-K/Akt pathway inhibition using LY294002, a PI3-K inhibitor. Co-treatment of LY294002 and aspirin also showed synergistic effects on inhibition of HCT116, DLD1 and HCT15 colon cancer cell growth (Figure 3.4). This result supports the synergistic effect of aspirin and GE, and suggests that GE can reduce aspirin dosage by inhibiting PI3-K/Akt pathway.

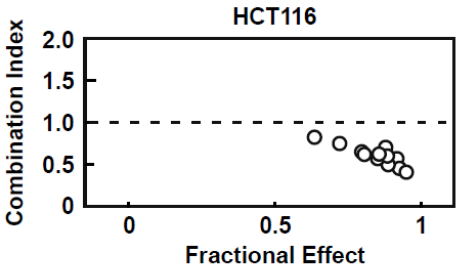

	Aspirin (mM)	LY294002 (μM)	Fa	CI
1	2	10	0.634	0.818
2	3	10	0.722	0.745
3	4	10	0.797	0.639
4	2	20	0.803	0.624
5	3	20	0.848	0.569
6	4	20	0.886	0.498
7	2	30	0.856	0.628
8	3	30	0.882	0.590
9	4	30	0.924	0.447
10	2	40	0.875	0.698
11	3	40	0.911	0.573
12	4	40	0.947	0.406

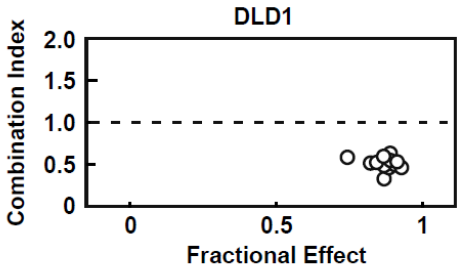

	Aspirin (mM)	LY294002 (μM)	Fa	CI
1	2	10	0.744	0.578
2	3	10	0.867	0.314
3	4	10	0.824	0.499
4	2	20	0.844	0.515
5	3	20	0.867	0.479
6	4	20	0.884	0.454
7	2	30	0.870	0.579
8	3	30	0.890	0.522
9	4	30	0.906	0.474
10	2	40	0.890	0.615
11	3	40	0.911	0.521
12	4	40	0.926	0.455

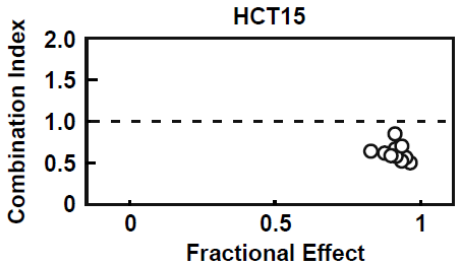

	Aspirin (mM)	LY294002 (μM)	Fa	CI
1	2	10	0.829	0.642
2	3	10	0.873	0.602
3	4	10	0.904	0.567
4	2	20	0.897	0.577
5	3	20	0.913	0.582
6	4	20	0.935	0.520
7	2	30	0.911	0.658
8	3	30	0.930	0.598
9	4	30	0.943	0.562
10	2	40	0.908	0.842
11	3	40	0.933	0.690
12	4	40	0.959	0.489

Figure 3.4 Aspirin and LY294002 combination shows synergistic effect. HCT116 cells were treated with aspirin (0-4 mM) and LY294002, a PI3K/Akt inhibitor, (0-40 μM) for 72 h and then proliferation was determined by MTS assay.

3.3.5 Ginger extract reduces aspirin dosage in tumor growth inhibition of colon cancer patient-derived xenograft (PDX) models.

Two different xenograft tumors from colon cancer patients (JG14 and JG17) were prepared subjected to aspirin and/or GE treatment. 400 mg/kg of aspirin treatment inhibited the PDX tumor volume (Figure 3.5a and b) and weight (Figure 3.5c and d). 20 mg/kg of GE treatment also showed moderate inhibitory effect against the PDX tumor growth, but the effect was weaker than that of aspirin. When treated in combination, 100 mg/kg of aspirin and ginger extract and 5 mg/kg of ginger extract exerted similar efficacy of 400 mg/kg of aspirin treatment on tumor volume and weight (Figure 3.5a-d). Of particular note, 400 mg/kg of aspirin decreased body weight of mice whereas the combination treatment did not show the adverse effect (Figure 3.5e and f). Adding 5 mg/kg of ginger extract could save 300 mg/kg of aspirin treatment while retaining the efficacy against colon cancer PDX tumor growth. Overall, this *in vivo* result shows that ginger extract can reduce the dosage of aspirin in colon cancer therapy.

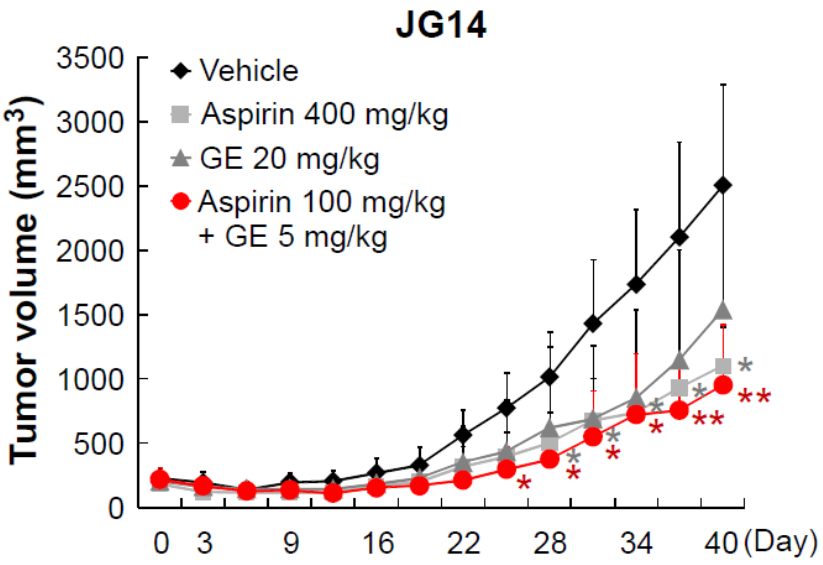

Figure 3.5a The effect of aspirin and GE against JG14 colon cancer PDX tumor volume. Aspirin and/or GE were dissolved in normal saline and administered p.o. 5 times/wk. Tumor size was measured three times a week. One-way ANOVA and Dunnett's test after log-transformation; *P < 0.05, significant difference compared to the vehicle group.

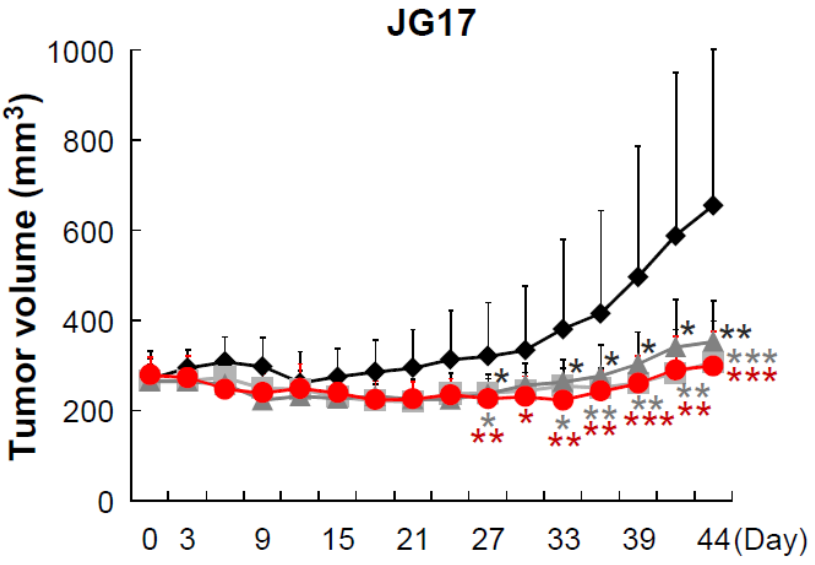

Figure 3.5b The effect of aspirin and GE against JG17 PDX tumor volume.

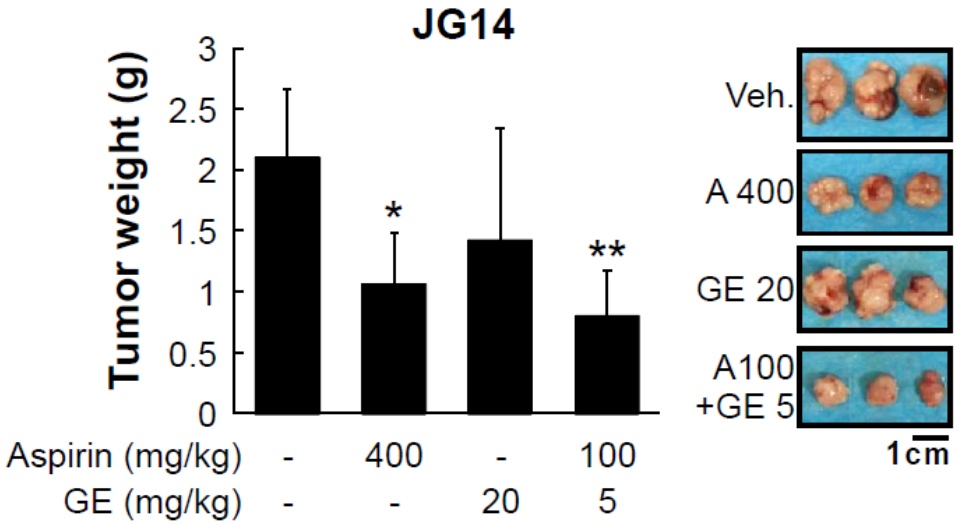

Figure 3.5c The effect of aspirin and GE against JG14 colon cancer PDX tumor weight. Aspirin and/or GE were dissolved in normal saline and administered p.o. 5 times/wk. Tumor weight was measured at the end of experiments, and representative tumor photos were taken.

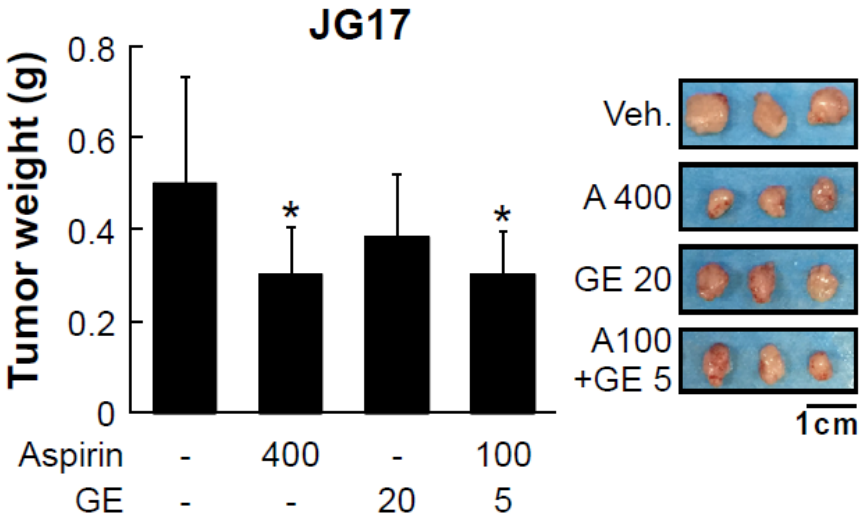

Figure 3.5d The effect of aspirin and GE against JG17 colon cancer PDX tumor weight.

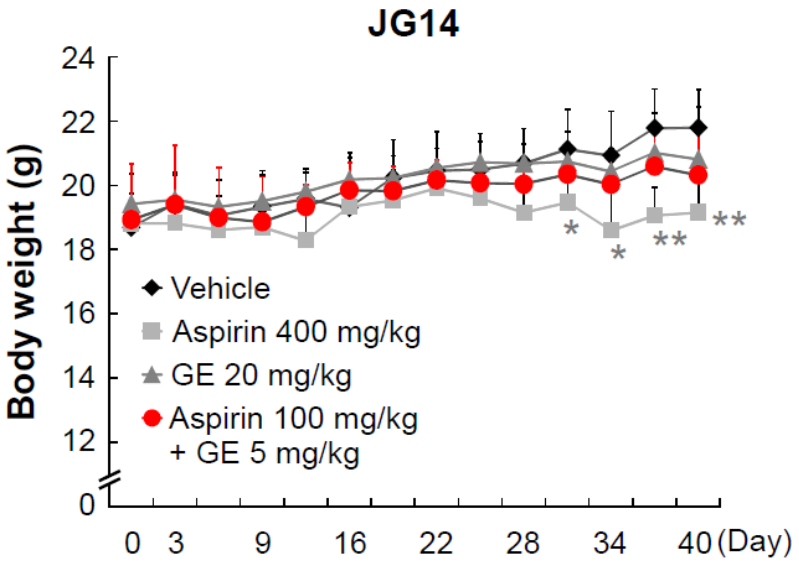

Figure 3.5e The effect of aspirin and GE against body weight of mice bearing JG14 PDX tumor. Aspirin and/or GE were dissolved in normal saline and administered p.o. 5 times/wk.

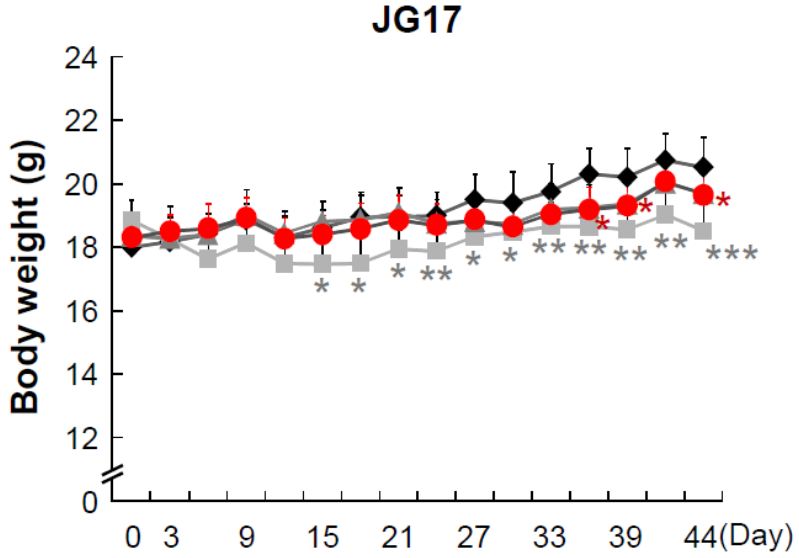

Figure 3.5f The effect of aspirin and GE against body weight of mice bearing JG17 PDX tumor.

3.4 Discussion

This study aimed to find a supplement that helps aspirin in suppressing colon cancer growth and elucidate their combination effects. Herein, we found that GE showed inhibitory effects on colon cancer cell growth, and clearly demonstrated that aspirin and GE has synergistic effect when treated together. The molecular mechanism of GE was investigated and revealed its active component, 6-shogaol, inhibited PI3-K/Akt pathway. The synergistic effect was further confirmed by aspirin-LY294002 combination that also showed synergism against colon cancer growth. The cooperative relationship of aspirin and GE was tested in colon cancer PDX models. Aspirin 100 mg/kg plus GE 5 mg/kg treatment was similarly effective as aspirin 400 mg/kg treatment. Notably, the aspirin dosage reduction by GE helped preventing weight loss that was shown at the high-dose of aspirin treatment. This work highlighted that GE, a food-derived supplement, can aid the anti-cancer effect of aspirin by inhibiting PI3-K pathway.

PI3-K pathway is one of main streams in where driver mutations are frequently found. Loss-of-function mutations in Phosphatase and Tensin Homolog (PTEN) (247) and gain-of-function mutations on PI3-K (248-249), Akt (250), and mTOR (251) facilitate carcinogenesis and tumor growth. Aspirin was selectively effective on PI3-K-activated tumor growth in mice (246) and colon cancer patients (235). Inhibition of mTORC1 signaling by aspirin also supports the underlying mechanisms of the clinical data (252-253). The synergistic effect of aspirin and GE inhibiting PI3-K pathway corresponds to Loewe additivity model that assumes two inhibitors act through a similar mechanism (254-255). When combination index was calculated following the model,

aspirin and GE showed synergism in suppressing colon cancer cell growth. The strong synergism at higher concentrations of aspirin and GE (Figure 3.2a) also support the model that targeting different levels of a single pathway can lead to synergistic effect and increase of clinical efficacy (255).

Precision medicine is becoming a new standard for cancer therapy. Prescribing the best drug for individuals increased efficacy and lowered adverse effects compared to so-called "one-size-fits-all" strategy (9). The selective effect of aspirin in colon cancer patients with *PIK3CA*-mutations but not ones without the mutations (235) reveals that aspirin will be widely used for patients with *PIK3CA*-mutated colon cancer. Our work suggests that adding GE to aspirin treatment might be helpful on reducing the dose of aspirin. PDX data showed that low dose of aspirin and GE combination is as potent as high dose of aspirin, and that the combination helps avoiding adverse effects such as weight loss (Figure 3.5). This result highlights that ginger extract might be helpful to patients who take aspirin as a therapeutic measure for PI3-K-activated colon cancer.

3.5 Materials and Methods

3.5.1 Cell culture, antibodies and reagents

HCT116 cells were cultured in McCoy's 5a Medium/10% FBS with antibiotics. DLD1 and HCT15 cells were cultured in RPMI-1640/10% FBS with antibiotics. All cell lines were purchased from American Type Culture Collection (ATCC, Manassas, VA) and cytogenetically tested and authenticated before the cells were frozen. Each vial of

frozen cells was thawed and maintained for a maximum of 8 weeks. Anti-p53 (DO-1), anti-p21 and anti-β-actin were purchased from Santa Cruz (Dallas, TX). Anti-Akt antibody is from Cell Signaling (Danvers, MA). Ginger extract (256) was obtained from Sabinsa Corporation (Piscataway, NJ). 6-Shogaol (purity > 96%) was synthesized as described earlier (236) and were analyzed and authenticated by high-performance liquid chromatography (HPLC). 6-, 8- and 10-Gingerol (purity > 95%) were purchased from Dalton Chemical Laboratories (Toronto, Canada).

3.5.2 Anchorage-independent cell growth assay

Cells (8×10^3 per well) were suspended in basal medium eagle (BME) containing 10% FBS and 0.3% agar and plated on solidified BME containing 10% FBS and 0.5% agar. After incubation for 4-10 days, the colonies were counted under a microscope using the Image-Pro Plus Software (v.6.1) program (Media Cybernetics, Rockville, MD).

3.5.3 Cell proliferation assay

Cells (3×10^3 per well) were seeded in 96-well plates and then cell proliferation was determined using the CellTiter 96 AQueous Non-Radioactive Cell Proliferation Assay kit (Promega, Madison, WI) according to the manufacturer's instructions. This kit is composed of tetrazolium compound (3-(4,5--dimethylthiazol-2-yl)-5-(3-carboxymethoxyphenyl)-2-(4-sulfophenyl)-2H-tetrazolium, inner salt; MTS) and an electron-coupling reagent (phenazine methosulfate; PMS). MTS is converted into a formazan by dehydrogenase found in metabolically active cells, and the quantity of

formazan product is directly proportional to the number of living cells.

3.5.4 Synergy assessment

Combination index (CI) was used to quantify synergism or antagonism for two drugs (231, 257), CI = $(D)_1/(Dx)_1 + (D)_2/(Dx)_2$ where CI < 1, =1, and > 1 indicate synergism, independence,

and antagonism, respectively. In the denominators, $(Dx)_1$ represents D_1 "alone" that inhibits a system *x*%, and $(Dx)_2$ is for D_2 "alone" that inhibits a system *x*%. In the numerators, $(D)_1$ and $(D)_2$ "in combination" also inhibit *x*%. CI was calculated for every dose of two drug pairs. Fraction affected (F*a*) is the fractional inhibition of a phenotype by a compound treatment(s).

F*a* of a group was calculated as F*a* = percent inhibition of cell viability/100. Fraction affected-combination index plot was drawn with every group treated with more than one compound.

3.5.5 Apoptosis assay

Cells (1×105 per well) were seeded in 6-cm dishes and then apoptosis was analyzed by a FACSCalibur flow cytometer (BD Biosciences, San Jose, CA) using the Annexin V-FITC apoptosis detection kit (MBL International Corp., Woburn, MA).

3.5.6 HPLC analysis of ginger extract

Ginger extract was dissolved in DMSO and then injected into a high performance liquid chromatography system equipped with a reverse-phase column (Luna® 5 µm C18 100 Å, LC Column 250 x 4.6 mm, Phenomenex, Torrance, CA). Ginger components were eluted at a flow rate of 1 ml/min using 65% acetonitrile in water (solvent A) and 93% methanol in water (solvent B) stepped gradient programs. Gradient elution was performed as follows: 50% B to 100% B in 5 min/100% B for 7 min/ 100% B to 50 % B in 2 min/ 50% B equilibration for 10 min. 6-Shogaol, 6-, 8-, and 10-gingerol were identified by their retention times and quantified by comparison with standards, and their levels were expressed as concentration values in µg/mg of ginger extract.

3.5.7 Binding assay

All of ginger components-conjugated Sepharose 4B beads were prepared as described previously (Cancer Res. 2010 Dec 1;70(23):9755-64). A whole cell lysate from HCT116 cells (500 mg) was incubated with resveratrol-conjugated or control beads at 4°C overnight in NP-40 lysis buffer [50 mM Tris-HCl (pH 8.0), 150 mM NaCl, 1 mM EDTA, 0.5% NP-40 and protease inhibitor]. After washing 5 times with NP-40 lysis buffer, the proteins bound to the beads were analyzed by Western blotting.

3.5.8 Western blotting

Cells were harvested and disrupted with NP-40 lysis buffer. The supernatant fraction was harvested after centrifugation at 13,000 rpm for 10 min. Protein

concentration was determined by Bio-Rad protein assay reagent (Richmond, CA). Whole cell lysates were subjected to SDS-PAGE and transferred to a polyvinylidene difluoride membrane (Millipore, Billerica, MA). After blocking with 5% non-fat dry milk in 1 x TBS containing 0.05% Tween 20 (TBS-T), the membrane was incubated with a specific primary antibody, and then protein bands were visualized with the ECL system and LAS4000 Biomolecular Imager (GE Healthcare, UK) after hybridization with a horseradish peroxidase-conjugated secondary antibody.

3.5.9 Patient-derived Xenograft (PDX)

Fresh tumor fragments were collected from colon cancer patients and transferred in RPMI 1640 medium with antibiotics at 4°C. The tumor tissues were trimmed into 3–5 mm sizes within 2 hr after surgical resection, and implanted to 6 to 8 week-old female SCID mice subcutaneously (Vital River Laboratories Co., Ltd., Beijing, China). Once mass formation reached 1,500 mm^3, mice of the first generation of PDX (named P1) were sacrificed and the tumors were segmented and expanded for 3 more generations (P2 and P3). When P4 tumors reached an average volume of 50 mm^3, mice were divided into different groups (n = 10/group) and treated with vehicle or aspirin 400 mg/kg or GE 20 mg/kg or aspirin 100 mg/kg+GE 5 mg/kg, respectively, 5 times a week by oral gavage. Aspirin and GE were dissolved in 0.9% saline. Mice were sacrificed at the end of the experiment and tumors extracted. Tumor volume was calculated using the following formula: tumor volume (mm^3) = (length × width ×height × 0.5). All studies were reviewed and approved by the Ethics Committee of Zhengzhou University. Patients

whose tumors were used in these studies were completely informed and provided consent.

3.5.10 Statistical analysis

All quantitative results are expressed as mean values ± S.D. Statistically significant differences were obtained by one-way ANOVA. ANOVA with Dunnett's test was used for multiple comparisons within experiments. A p-value of < 0.05 was considered to be statistically significant.

Chapter 4:

Multiple phytochemicals at low doses accumulatively inhibit one key protein in cancer

4.1 Summary

Fruits and vegetables are good sources of phytochemicals that possess health-promoting effects such as reducing the risk of cancer. Although the anti-cancer effects of phytochemicals are heavily investigated, there exists a limitation that a single phytochemical is not correlated with reducing risks of cancer. This is partly due to the low concentration of each phytochemical in our body. To tackle this issue, we hypothesized that many phytochemicals with similar chemical structure may have a same target protein and the natural compounds, although at low doses, can inhibit the activity of the protein to where the anti-cancerr effects are focused. From chemical similarity analysis of four known ERK inhibitors, we found six new ERK2 inhibitors with similar chemical structures. The ten phytochemicals were able to accumulatively inhibit ERK2 activity *in vitro*. ERK inhibitor mixture that each phytochemical exists at a low concentration suppressed H-ras-induced cell transformation of fibroblast, and inhibited anchorage-independent growth of cancer cells in where ERK2 is essential and highly expressed. This work will impact the cancer community by showing that many natural compounds can work together targeting ERK2, an important target in cancer.

4.2 Introduction

Fruits and vegetables are good sources of phytochemicals and believed to possess health-promoting effects such as reducing the risk of cancer (258-259). For example, a cohort study showed that high cruciferous vegetable consumption may reduce the risk of

bladder cancer (258). People are encouraged to intake more fruits and vegetables under so-called “five-a-day” campaign (260) and epidemiological data showed that a diet with higher fruit, vegetable and fiber than five-a-day diet may reduce adverse effects among breast cancer survivors (261). When it comes to molecular mechanisms, however, there exists a limitation that the health-promoting effect cannot be explained by a single phytochemical. Although many basic researches reveal anti-cancer effects of phytochemicals, especially elucidating target proteins of the small molecules (262). the physiological concentration of one phytochemical is often too low to expect any effect. An alternative model that uses low doses of phytochemicals naturally abundant might be helpful to better understand anti-cancer effects of phytochemicals.

Extracellular signal–regulated kinase 2 (ERK2) is a protein kinase receiving signals under Ras/Raf/ Mitogen-activated protein kinase kinase (MEK) pathway, and involved in carcinogenesis and cancer cell proliferation (263). ATP binding site of ERK is a concave protein surface ideal for direct interaction by small molecules (264). Recently natural small molecules that can suppress ERK activity were reported such as catechol (265), (+)-2-(1-hydroxy-4-oxocyclohexyl) ethyl caffeate (HOEC) (266), caffeic acid (267) and norathyriol (268). Catechol suppresses growth of lung cancer patient-derived xenograft (PDX) tumors by directly targeting ERK (265). HOEC, caffeic acid and norathyriol suppress solar UV-induced skin carcinogenesis in SKH-1 hairless mice by direct ERK inhibition (266-268). Therefore, targeting ERK with phytochemicals might be an effective strategy for preventing and treating cancer.

Herein, we tested our hypothesis that phytochemicals at low doses can accumulatively inhibit one protein. Chemical similarity analysis of four ERK2 inhibitors leads to determination of the crystal structure of ERK2 bound with 5,6-dihydroxychromone (5,7-DHC). Fisetin, quercetin, luteolin, 7,3',4'-THIF and cyanidin were also identified as direct ERK2 inhibitors after *in vitro*. Using the ten natural ERK2 inhibitors in mixture (Ei-mix), we prove that natural compounds at low doses can accumulatively inhibit ERK2. Ei-mix suppresses H-ras-induced cell transformation in NIH3T3 cells, and inhibits anchorage-independent growth of K562 and SK-MEL-28 cells in where ERK2 is essential and highly expressed. Signaling pathway is also analyzed to show that phosphorylation of ERK2 substrates were decreased by Ei-mix treatment.

4.3 Results

4.3.1 Chemical similarity analysis of known ERK2 inhibitors leads to determination of the crystal structure of ERK2 in complex with 5,7-dihydroxychromone.

Accumulative evidence shows that natural phytochemicals interfere oncogenic signaling pathways by directly targeting proteins (262, 269). ERK2 (extracellular signal-regulated kinase 2), for example, is one of key proteins in carcinogenesis and directly inhibited by naturally-occurring small molecules such as catechol (PDB ID: 4ZXT) (265), HOEC (266), caffeic acid (PDB ID: 4N0S) (267) and norathyriol (PDB ID: 3SA0) (268) (Figure 4.1a). We hypothesized that there will be more natural ERK2 inhibitors

with similar chemical structures. Chemical clustering of the four phytochemicals showed that catechol, HOEC and caffeic acid formed one cluster, and norathyriol composed the other cluster (Figure 4.1b). We next sought to find phytochemicals which are similar to norathyriol from SuperNatural II, a database with more than 325,000 natural compounds (270). By applying Tanimoto index, a popular method to quantify the similarity of two molecules, and threshold value of 0.9 (271-273), 14 compounds were found to be similar to norathyriol (Figure 4.1c). Twelve compounds were xanthone including norathyriol itself (1,3,6,7-tetrahydroxyxanthone), and the other two were chromone. After excluding xanthones that might be less innovative, 5,7-dihydroxychromone (5,7-DHC) was tested on co-crystallization with ERK2. We were able to resolve a crystal structure of ERK2 bound with 5,7-DHC in the ATP binding site at 1.4 Å resolution (Figure 4.1d). Superimposition of current structure with norathyriol-bound ERK2 (PDB ID: 3SA0) structure showed that 5,7-DHC and norathyriol occupy the same position in the ATP binding site (See Figure 4.1e).

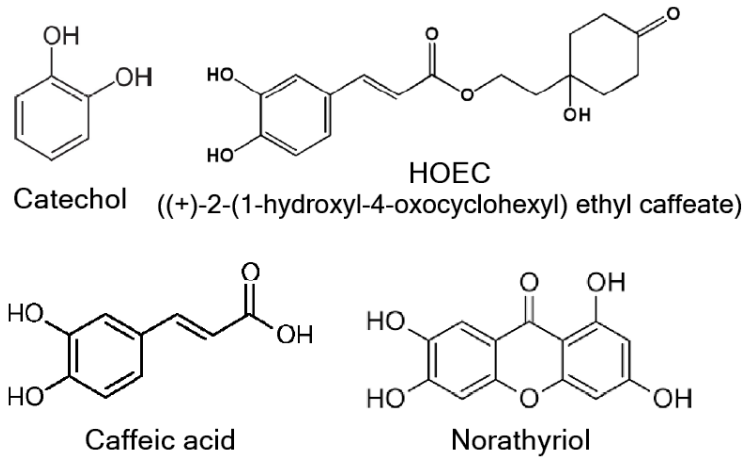

Figure 4.1a Chemical structures of previously reported ERK2 inhibitors.

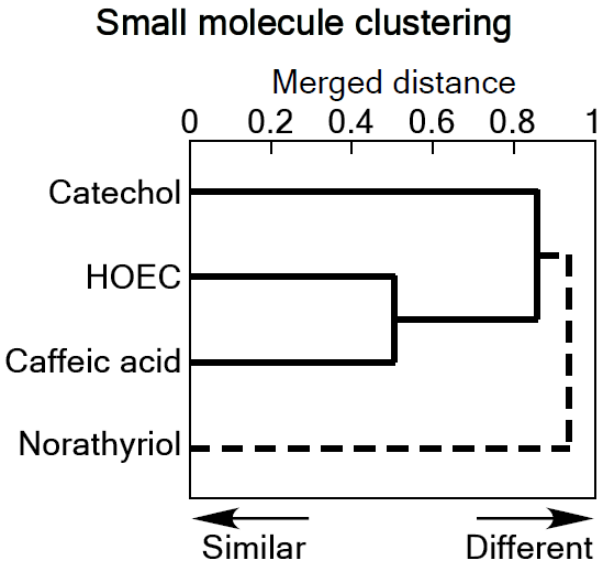

Figure 4.1b Small molecule clustering of the four ERK inhibitors. The hierarchical clustering was carried out using Canvas in from Schrödinger Suite 2016. Distance matrix was used to generate the dendrogram.

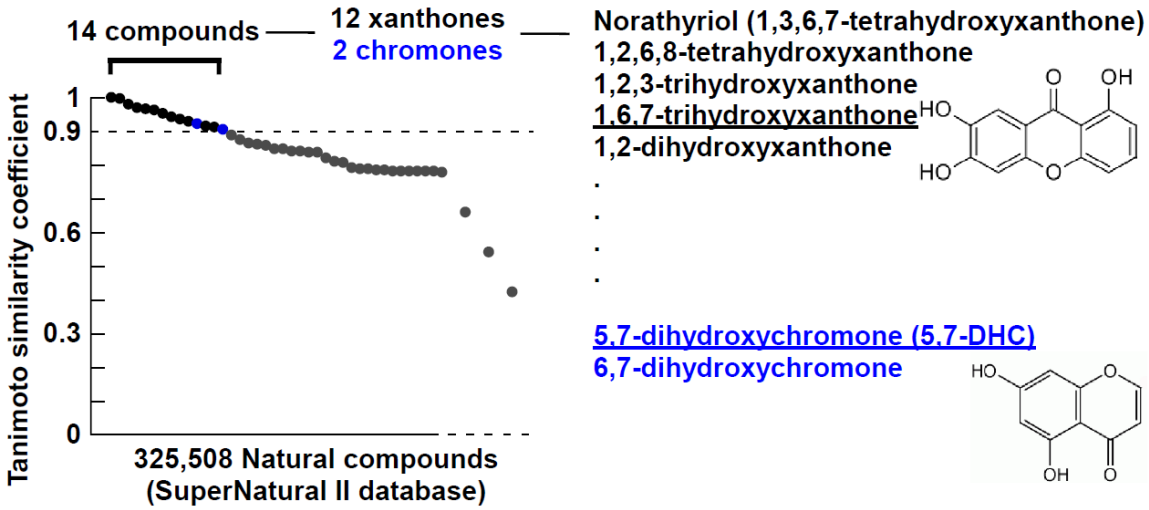

Figure 4.1c Chemical similarity analysis of norathyriol. Tanimoto similarity coefficients of natural compounds compared to norathyriol were calculated from SuperNatural II database. Tanimoto threshold 0.9 was used to determine similar chemicals.

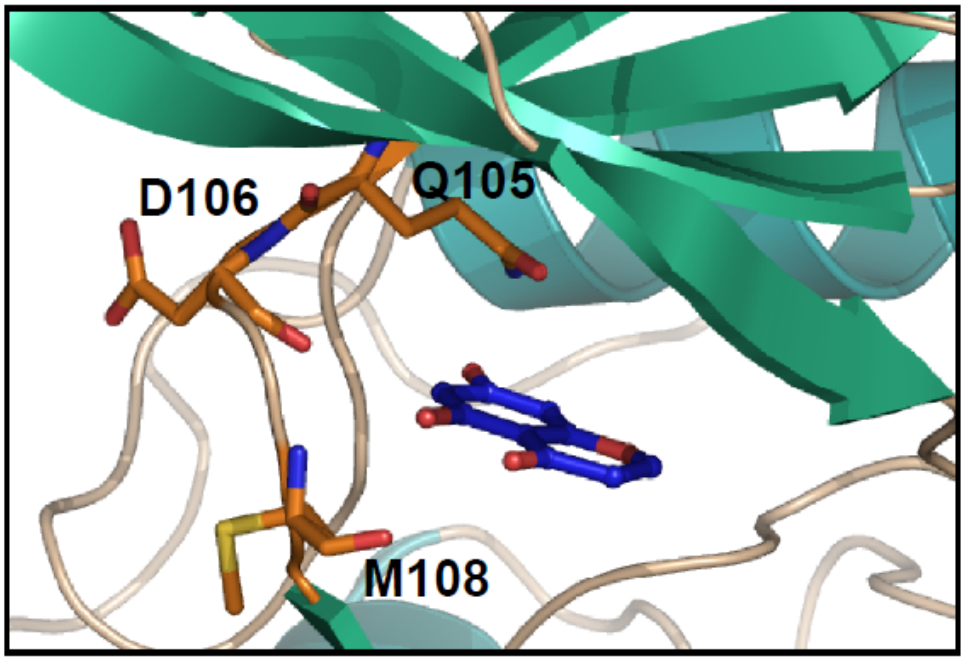

Figure 4.1d The crystal structure (1.4 Å resolution) of ERK2 bound with 5,7-DHC (blue). 5,7-DHC bound to the ATP binding site of ERK2.

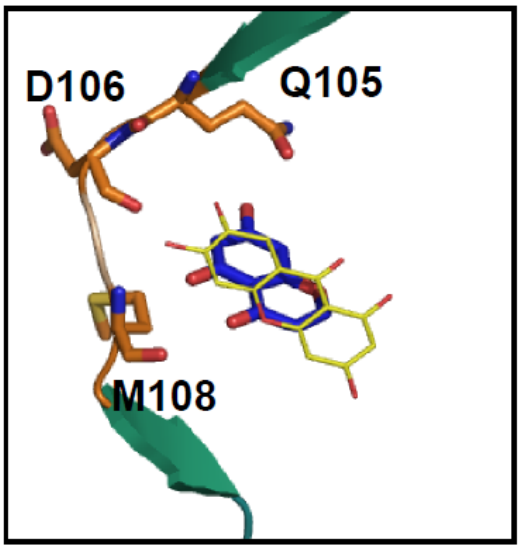

Figure 4.1e Superimposition of current structure with norathyriol-bound ERK2 (PDB ID: 3SA0) structure. Norathyriol is depicted in yellow.

4.3.2 Identification of compounds with inhibitory effects on ERK2 kinase activity.

We next focused on the identification of ERK2 inhibitors based on chemical similarity with catechol and 5,7-DHC. There were 2,720 natural compounds that have catechol moiety, and 3,978 compounds with 5,7-DHC moiety (Figure 4.2a). To increase the possibility of identifying ERK2 inhibitors, compounds with catechol moiety and 5,7-DHC (or chromone) moiety were selected and subjected to ERK2 *in vitro* kinase assay. Fisetin, quercetin, luteolin, 7,3',4'-trihydroxyisoflavone (7,3',4'-THIF) and cyanidin inhibited ERK2 kinase activity *in vitro* (Figure 4.2b and c). However, procyanidin B2, a dimer form of cyanidin, was not able to reduce ERK2 activity (Figure 4.2c). We postulated that the compound is too bulky to fit into the ATP binding site of ERK2.

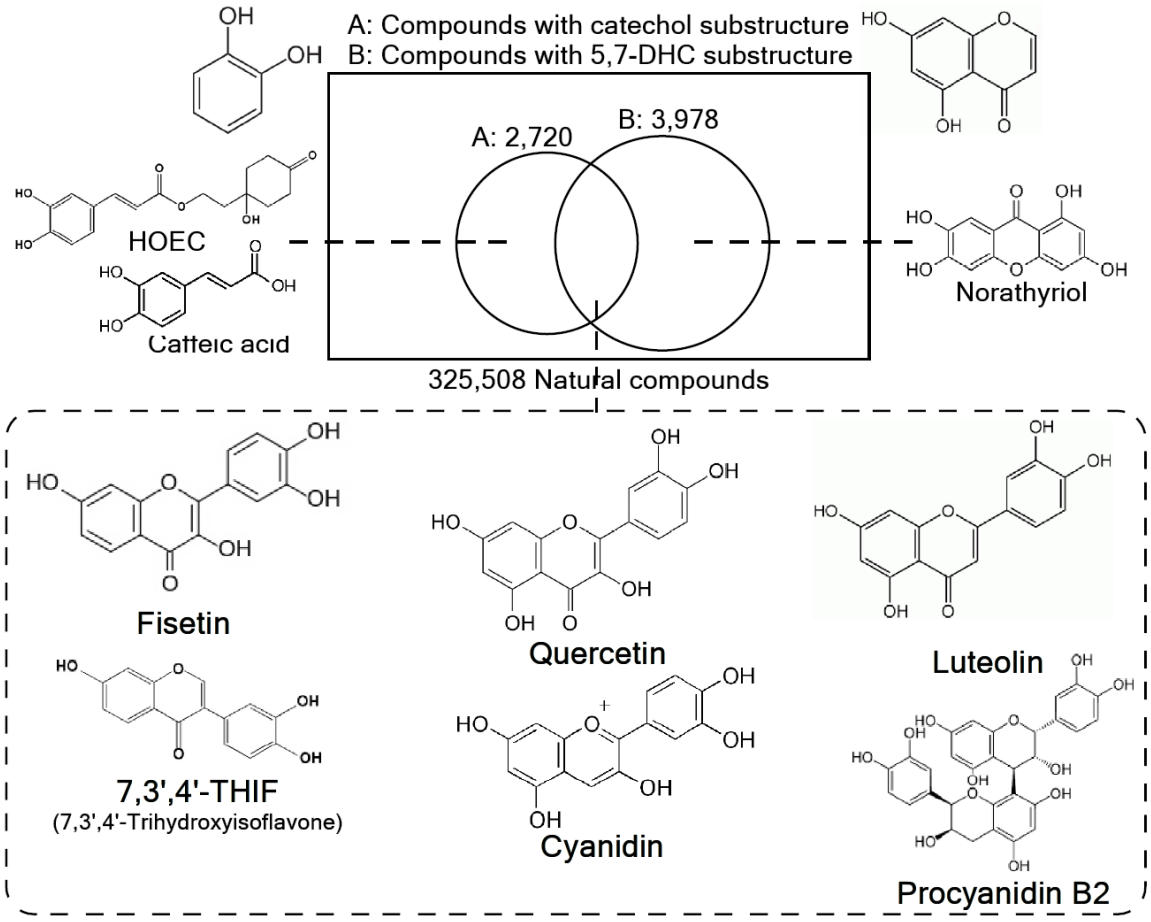

Figure 4.2a Substructure search results from SuperNatural II database. 2,720 natural compounds with catechol substructure were found. There were 3,978 compounds with 5,7-DHC substructure. To enhance the chance to find ERK2 inhibitor, compounds with catechol substructure and 5,7-DHC (or chromone) substructure were selected for in vitro ERK2 kinase screening. Fisetin, quercetin, luteolin, 7,3',4'-THIF, cyaniding and procyanidin B2 were chosen.

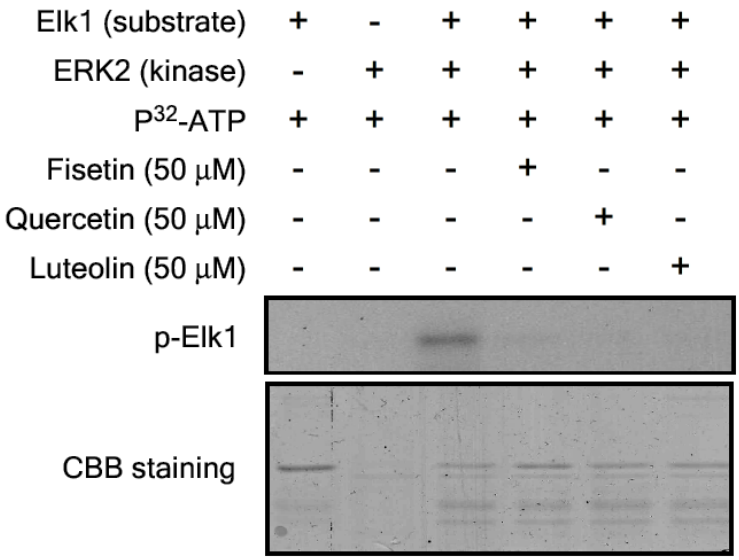

Figure 4.2b Validation assay of predicted ERK2 compounds. Elk1 fusion protein was used in an *in vitro* kinase assay with active ERK2. Results were visualized by applying p-Elk1 antibody and western blots. Coomassie brilliant blue staining served as a loading control.

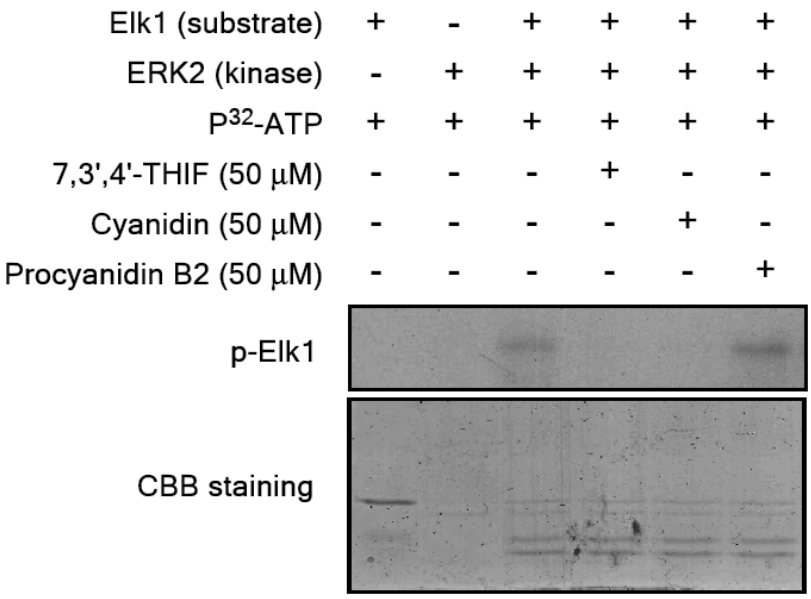

Figure 4.2c Validation assay of predicted ERK2 compounds (continued).

4.3.3 Fisetin, quercetin, luteolin, 7,3',4'-THIF and cyanidin directly bind to ERK2 and inhibit its kinase activity in a dose-dependent manner.

To further confirm the *in vitro* kinase screening, the activity of fisetin, quercetin, luteolin, 7,3',4'-THIF and cyanidin were examined at different doses. The five compounds were able to reduce ERK2 kinas activity in a dose-dependent manner (Figure 4.3a-e). Of note, the phytochemicals showed similar IC50 values (fisetin: 7.0, quercetin: 8.8, luteolin: 8.6, 7,3',4'-THIF: 12.9, cyanidin: 9.3 μM) supporting similar property principle which refers that structurally similar molecules tend to have similar properties (274). Binding assay using sepharose 4B beads showed that the five compounds directly bound to ERK2 (Figure 3f). Throughout chemical similarity analysis of four ERK2 inhibitors previously reported (catechol, HOEC, caffeic acid and norathyriol), six new phytochemicals (5,7-DHC, fisetin, quercetin, luteolin, 7,3',4'-THIF and cyanidin) were newly identified as ERK2 inhibitors.

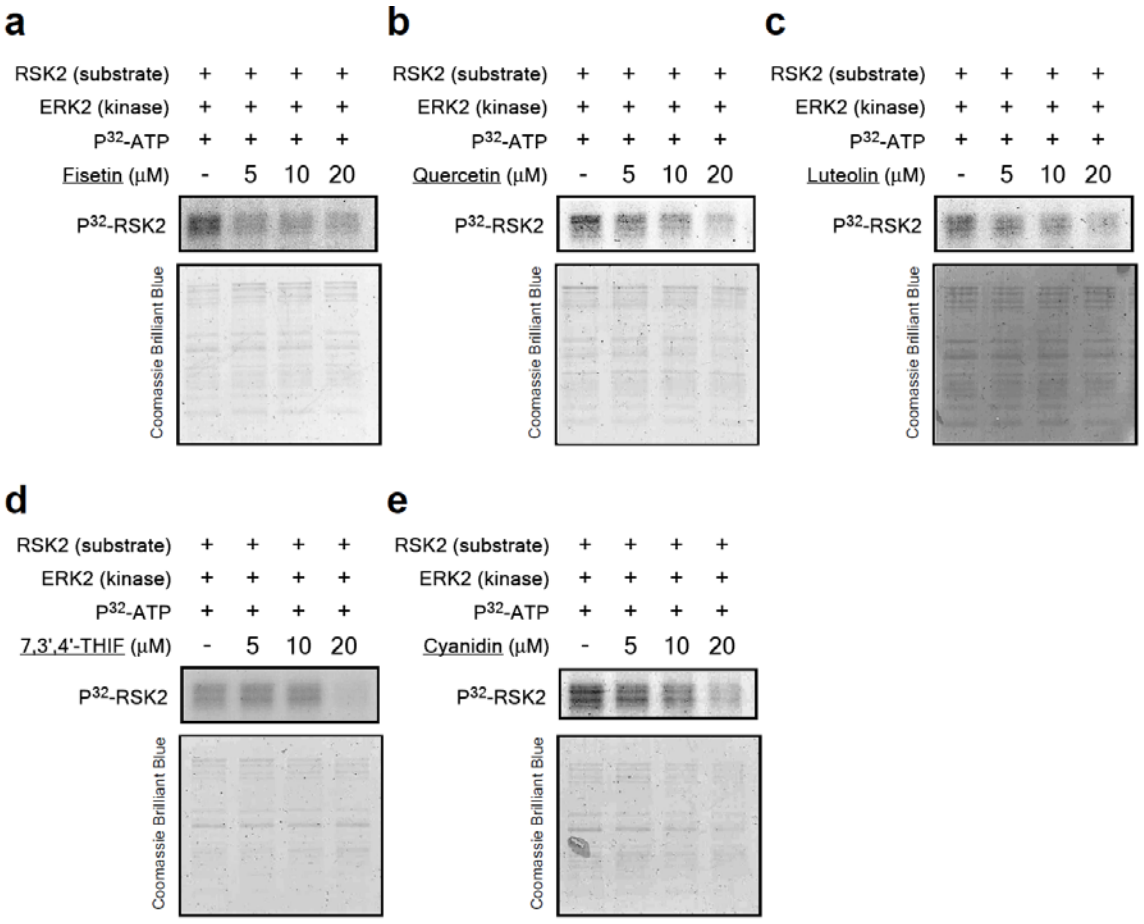

Figure 4.3a-e Newly identified natural compounds inhibit ERK2 kinase activity *in vitro*. RSK2 fusion protein was used in an *in vitro* kinase assay with active ERK2. 5-20 μM of Fisetin (a), quercetin (b), luteolin (c), 7,3',4'-THIF (d) and cyanidin (e) were tested.

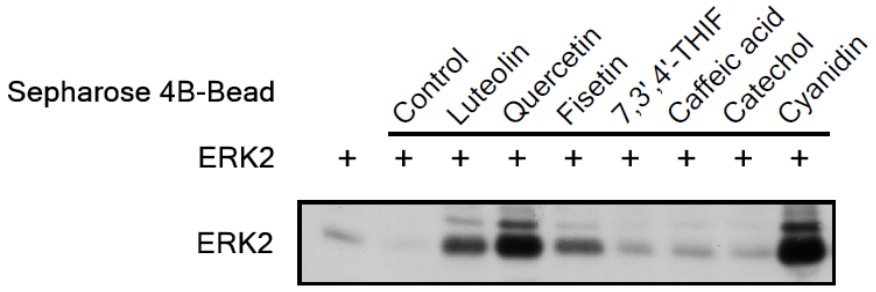

Figure 4.3f The newly identified compounds bind to ERK2 *ex vivo*. A whole cell lysate was incubated with 100 µl of phytochemical-conjugated Sepharose 4B and sepharose 4B (negative control) beads in 500 ml of reaction buffer. Pulled down proteins were detected by Western blotting. Caffeic acid and catechol served as positive controls.

4.3.4 Natural ERK2 inhibitors at low doses accumulatively inhibit ERK2 kinase activity and H-ras-induced cell transformation.

The ten phytochemicals that directly inhibit ERK2 activity were mixed to constitute ERK2 inhibitor mixture (Ei-mix) to better mimic the condition that people consume different fruits and vegetables daily. *In vitro* kinase assay showed that 20 μM of EI-mix (10 compounds, 2 μM each) inhibited the phosphorylation of RSK2, a substrate of ERK2 (Figure 4.4a). When each compound was removed one by one, the inhibitory effect was diminished. This result proved the hypothesis that phytochemicals at low doses can accumulatively inhibit one protein. Next we sought to test the effect Ei-mix on cell transformation induced by H-ras, an upstream of ERK2. As previously reported (275), constitutively-activated H-ras (G12V) induced foci formation (Figure 4.4b). Ei-mix was able to suppress H-ras-induced cell transformation of NIH3T3 cells in a dose-dependent manner (Figure 4.4c). This result highlights the possibility that phytochemicals in nature, although at low doses, can exert their anti-cancer effects if the small molecules with similar structures focus their effect on one key protein.

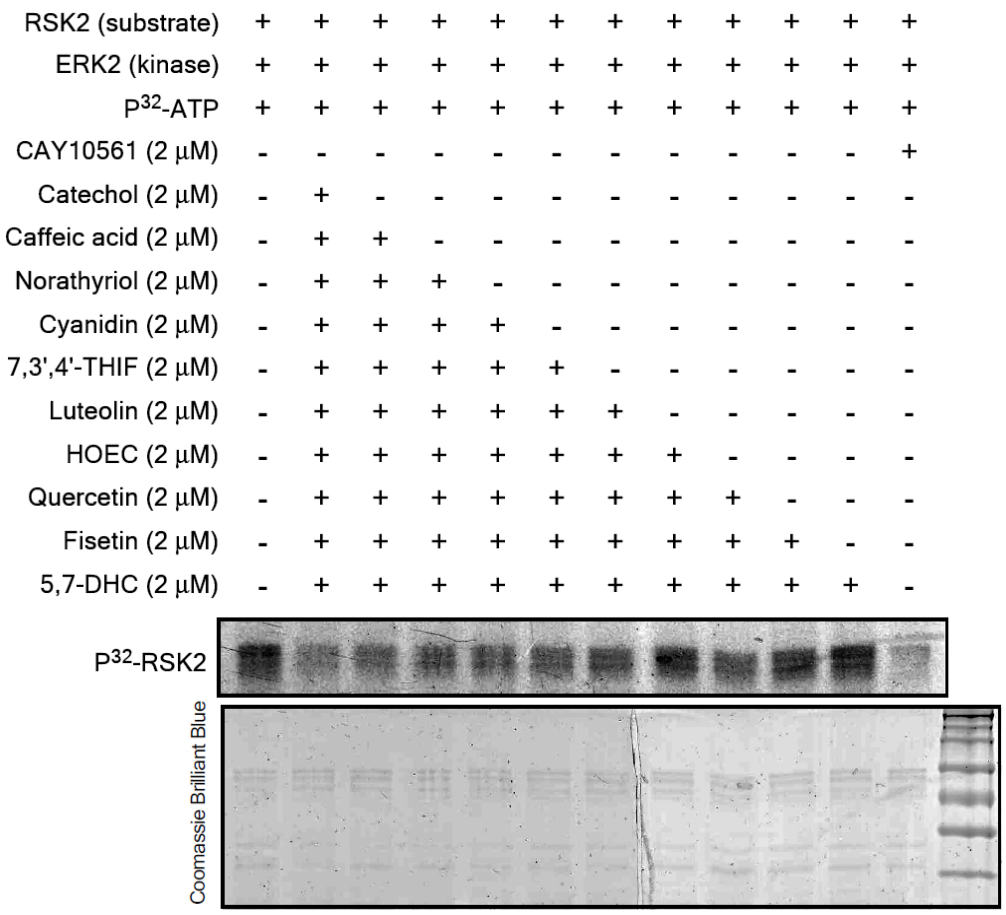

Figure 4.4a Natural ERK2 inhibitors at low doses accumulatively inhibit ERK2 kinase activity. RSK2 fusion protein was used in an *in vitro* kinase assay with active ERK2. Ten phytochemicals were at 2 μM each, to make 20 μM concentrations as Ei-mix. Each compound was replaced with DMSO one by one. Results were visualized by autoradiography. Coomassie brilliant blue staining served as a loading control. CAY10561 is a positive control.

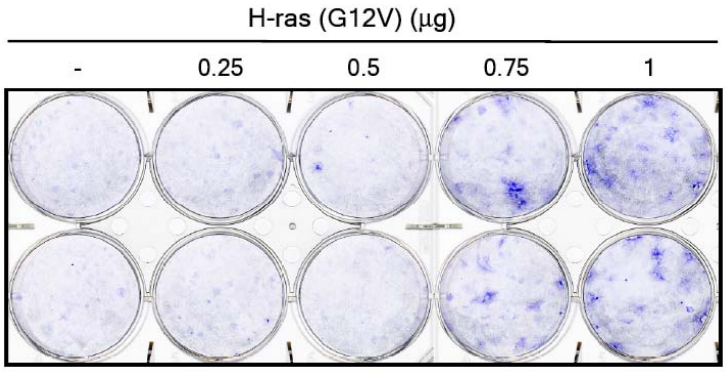

Figure 4.4b H-ras-induced foci formation assay. Foci formation assay was carried out following a protocol described in Materials and Methods. Foci were stained with 0.5% crystal violet after 2 wk-long incubation.

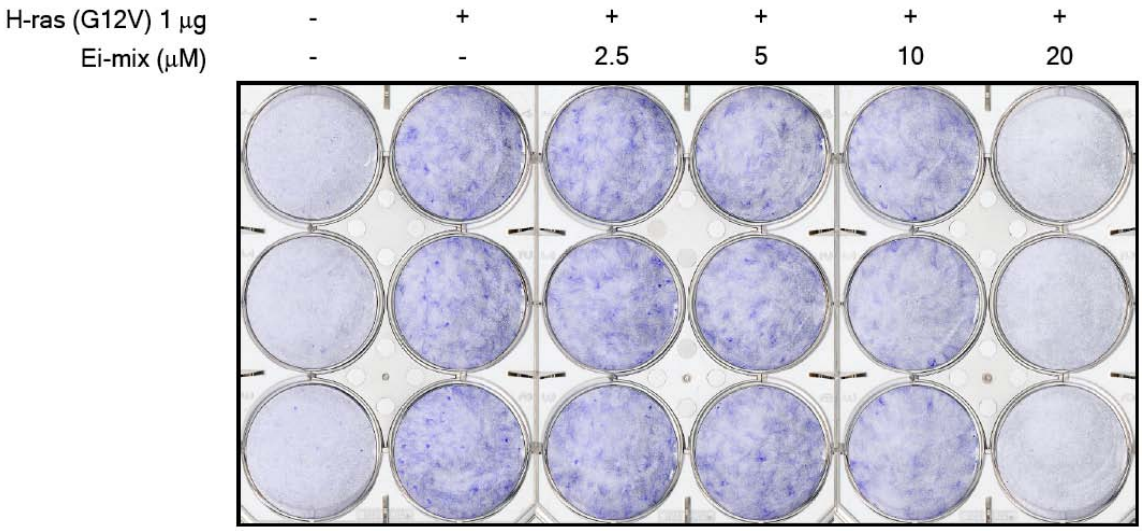

Figure 4.4c The effect of Ei-mix on H-ras-induced foci formation. Foci formation assay was carried out following a protocol described in Materials and Methods. Foci were stained with 0.5% crystal violet after 2 wk-long incubation. Media with different concentration of Ei-mix was prepared by serial dilution from 20 μM. Media was changed every other day.

4.3.5 Ei-mix inhibits the phosphorylation of ERK2 substrates and colony formation of K562 and SK-MEL-28 cell lines in where ERK2 is highly expressed and critical for growth.

Because ERK2 is an important cell signaling mediator for proliferation of cancer cells (276-277), cell lines with high expression level of ERK2 serve as a useful platform to test the efficacy of Ei-mix. Analysis of mRNA expression and copy number of ERK2 in 1,036 cancer cell lines (278) showed that K562 and SK-MEL-28 might have high-ERK2 levels whereas H1650 and SH SY5Y might have low-ERK2 levels (Figure 4.5a). Western blot analysis confirmed that the former cell lines express higher ERK2 protein levels compared to the latter ones (Figure 4.5b). K562 and SK-MEL-28 cell lines proliferated rapidly compared to H1650 and SH SY5Y cell lines in anchorage-independent conditions (Figure 4.5c). Knock-down of ERK2 inhibited anchorage-independent growth of K562 and SK-MEL-28 cells (Figure 4.5d). Treatment of Ei-mix suppressed anchorage-independent growth of K562 and SK-MEL-28 cell lines (Figure 4.5e). Subsequent western blot analysis showed that the phosphorylation levels of RSK2 and c-Myc were reduced by Ei-mix treatment in a dose-dependent manner (Figure 4.5f). Collectively, our results show that phytochemicals that have similar structure compared to known ERK2 inhibitors also possess inhibitory effects against ERK2 kinase activity. And this provides a physiologically-relevant model of phytochemicals against cancer (Figure 4.6). Naturally-occurring small molecules with similar structures can accumulatively inhibit ERK2 (Table 4.1).

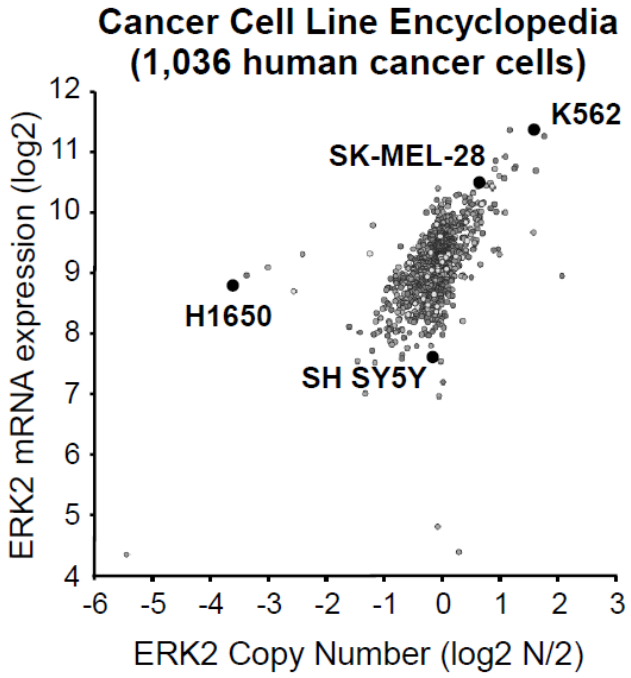

Figure 4.5a ERK2 expression analysis from cancer cell line encyclopedia (CCLE). mRNA expression and copy number of ERK2 in 1,036 cancer cell lines were downloaded from CCLE database.

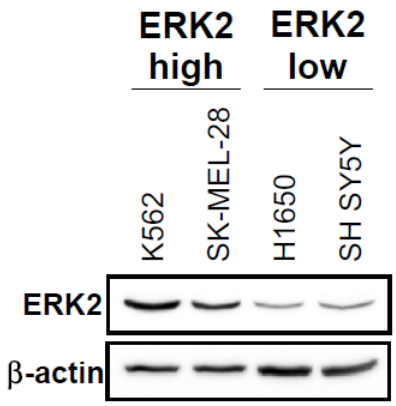

Figure 4.5b Validation of ERK2 expression levels in four cell lines. Four different cell lysates were subjected to western blots with ERK2 antibody. β-actin served as a loading control.

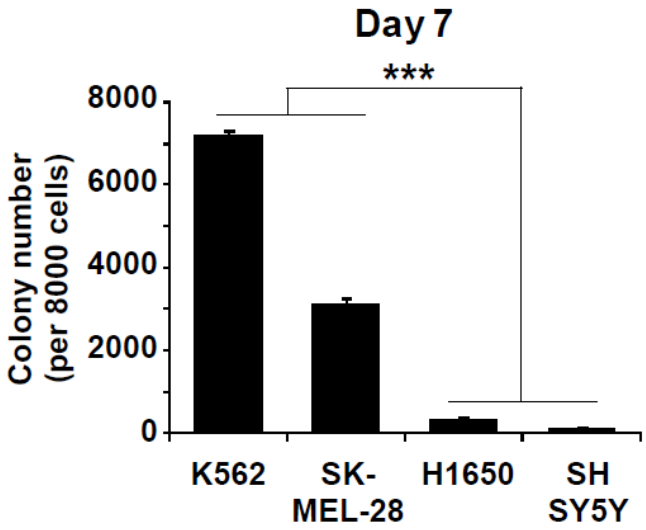

Figure 4.5c ERK2-high cell lines proliferate faster in the anchorage-independent growth condition. Same number of cells from the four different cell lines was suspended in 0.3% agar-containing media. Numbers of colonies were calculated after 7 days of incubation.

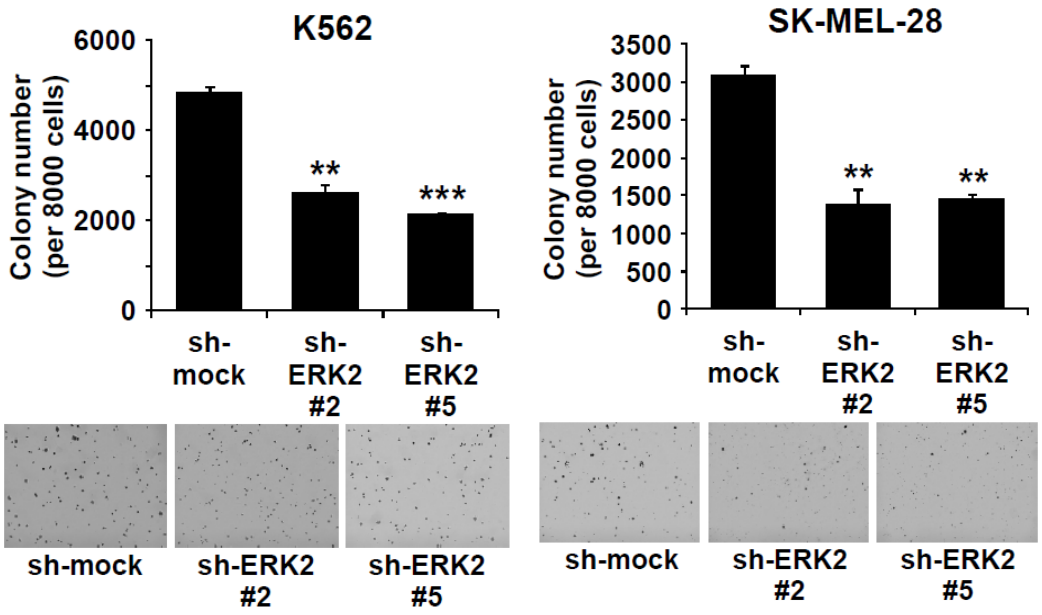

Figure 4.5d The effect of knock-down of ERK2 in K562 and SK-MEL-28 cell lines. Two different shRNA sequences targeting ERK2 were used to knock-down.

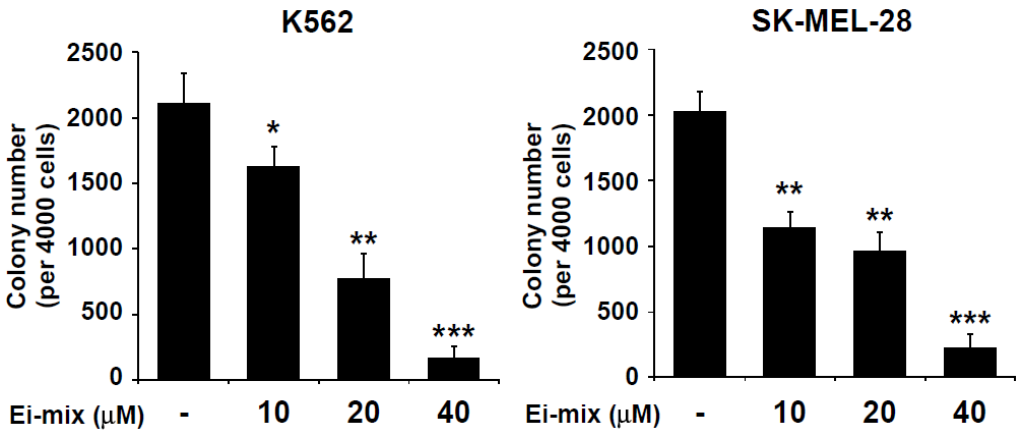

Figure 4.5e The effect of Ei-mix against anchorage-independent growth of K562 and SK-MEL-28 cell lines. Ei-mix 40 μM solution (4 μM of ten phytochemicals) was prepared and underwent serial dilution. Colony number was counted after 5 day-incubation. One-way ANOVA *P < 0.05, **P < 0.01, ***P < 0.001 significant difference compared to the control group.

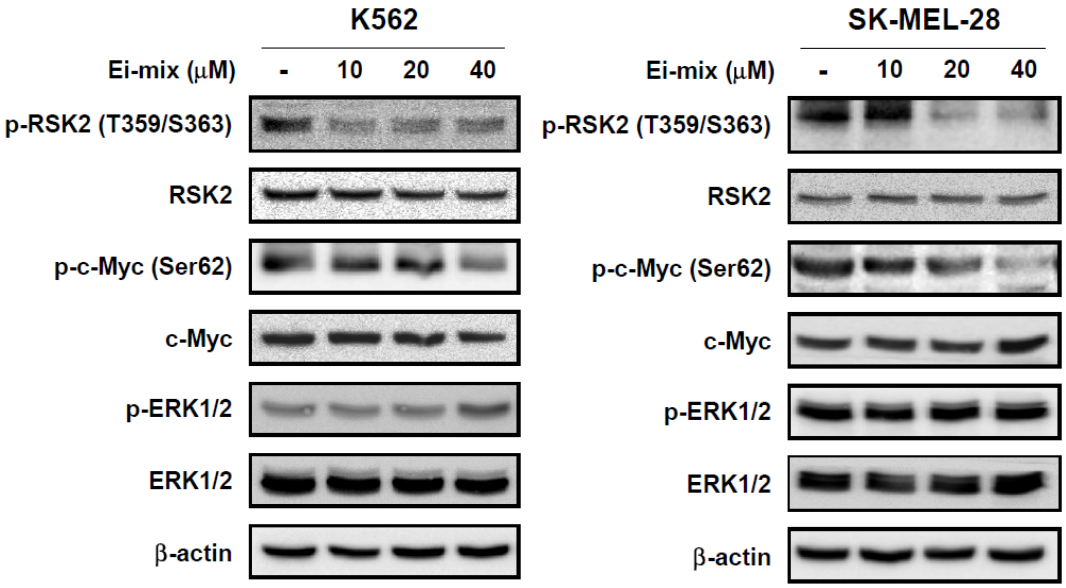

Figure 4.5f The effect of Ei-mix against ERK2 signaling pathway. Ei-mix was treated to K562 and SK-MEL-28 cell lines at different concentrations for 15 min.

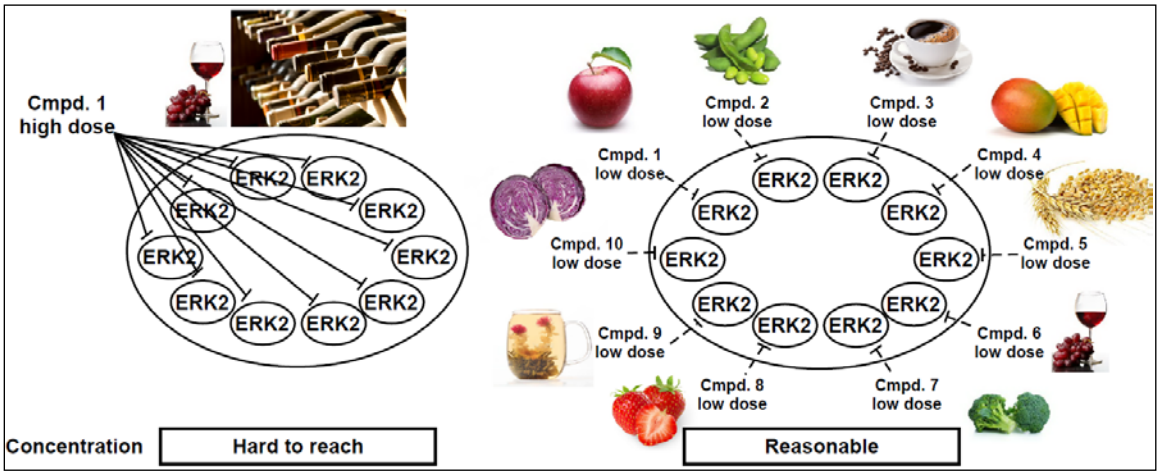

Figure 4.6 Simple depiction of a proposed mechanism of food-derived phytochemicals. A conventional anti-cancer mechanism using single phytochemical (left) was compared with the proposed mechanism where multiple phytochemicals with similar structure focus their effects on one protein (right).

Table 4.1 Food sources of the naturally-occurring ERK inhibitors that constitute Ei-mix.

Natural compound	Food sources
Catechol	Apple, onion, Banana, olive oil
HOEC	*Incarvillea mairei* (Flower, seed)
Caffeic acid	Coffee, cinnamon, sun flower
Norathyriol	Mango
5,7-DHC	Barley
Fisetin	Grape, strawberry, persimmon
Quercetin	Red wine, apple, tomato
Luteolin	Broccoli, celery, carrot, oregano
7,3',4'-THIF	Soybean (metabolite)
Cyanidin	Blueberry, plum, red cabbage

4.4 Discussion

This work aimed to find a physiologically-relevant model that explains anti-cancer effects of phytochemicals. Herein, we found that chemical similarity analysis of known ERK2 inhibitors led to determination of the crystal structure of ERK2 in complex with 5,7-DHC. Fisetin, quercetin, luteolin, 7,3',4'-THIF and cyanidin were also identified as direct ERK2 inhibitors *in vitro*. Using 10 phytochemicals in mixture (Ei-mix), we proved that natural compounds at low doses can accumulatively inhibit ERK2. Ei-mix suppressed H-ras-induced cell transformation in NIH3T3 cells, and inhibited anchorage-independent growth of K562 and SK-MEL-28 cells in where ERK2 is essential and highly expressed. Notably, western blots showed that phosphorylation of ERK2 substrates were decreased by Ei-mix treatment.

Fruits and vegetables are good sources of phytochemicals with health-promoting effects such as reducing cancer risks (258-259). Many basic researches revealing anti-cancer effects of phytochemicals, especially ones elucidating target proteins of the small molecules, enhanced our understanding on molecular mechanisms (262). However, a limitation is that the health-promoting effect cannot be explained by a single phytochemical. In many cases, the physiological concentration of one phytochemical is too low to expect any effect, and this is a huge gap between basic research of phytochemicals and cohort studies. To tackle this issue, we hypothesized that similar phytochemicals may have a same target protein and the small molecules, although at low concentrations, can inhibit the target to where the effect is focused. Under *in vitro* condition, 10 different phytochemicals were able to accumulatively suppress ERK2

activity (Figure 4.4a). The Ei-mix worked as an ERK inhibitor by reducing phosphorylation of ERK2 substrates in cancer cells (Figure 4.5f). This new model (depicted in Figure 4.6) opens up possibilities that even phytochemicals with moderate or relatively weak activities can be used when combined with other molecules which have same target protein.

Precision medicine refers to matching the right treatments with the individuals (4). Setting up prevention and treatment strategies often involves inhibition of genes and proteins that promote disease (4, 9). This new model using phytochemicals can be beneficial to who needs to inhibit Ras/Raf/MEK (mitogen-activated protein kinase kinase) pathway because ERK is their downstream protein. By increasing the consumption of food sources of Ei-mix (Table 4.1), one could boost up the concentration and thus degree of ERK inhibition. Although this new model still needs further evaluations, it will impact the cancer community by showing that many natural compounds can work together targeting ERK2, an important target in cancer.

4.5 Experimental Procedures

4.5.1 Cell culture, antibodies and reagents

All cell lines were purchased from American Type Culture Collection (ATCC, Manassas, VA) and cytogenetically tested and authenticated before the cells were frozen. Cells are cultured in 10% FBS and antibiotic-containing RPMI (K562 and H1650), MEM (SK-MEL-28), MEM/F-12 (SH SY5Y). NIH3T3 was cultured in DMDM containing 10%

CS and antibiotics. Each vial of frozen cells was thawed and maintained for a maximum of 8 weeks (NIH3T3: 4 weeks). All antibodies were commercially available, including RSK2 and β-actin from Santa Cruz (Dallas, TX), pElk1 (S383), ERK2, pRSK (T359/S363), c-Myc, pERK1/2 (T202/Y204) and ERK1/2 from Cell Signaling Technology (Beverly, MA), p-c-Myc (S62) from Abcam (Cambridge, UK). Catechol, caffeic acid, fisetin, quercetin, luteolin and procyanidin B2 were purchased from Sigma-Aldrich (St. Louis, MO). 5,7-DHC and cyanidin were purchased from ApexBio (Houston, TX). 7,3',4'-THIF and CAY10561 were purchased from Cayman (Ann Arbor, MI). HOEC (266) and norathyriol (268) were synthesized as described earlier and were analyzed and authenticated by HPLC.

4.5.2 ERK2/5,7-dihydroxychromone structure determination

His-tagged recombinant human ERK2 was purified as described previously (ref). The crystals were produced by co-crystallization. Protein at 7.5 mg/ml was mixed with 5,7-DHC 100mM stock solution in DMSO to achieve 1.5 mM of 5,7-DHC concentration and 1:9 protein/compound molar ratio. One or two microliters of protein:compound mixture were mixed with equal volume of precipitant comprised of 1.4M-1.5M ammonium sulfate, 2% PEG550, 0.1M HEPES, pH 7.5. The crystals grew slowly and were packed and tested after 1 month. The cryoprotectant solution comprised of 1.8M ammonium sulfate, 2% PEG550, 0.1M HEPES, pH 7.5 and 20% xylitol.

4.5.3 *In vitro* kinase assay

The kinase assay was performed according to the instructions provided by Millipore. Briefly, ERK2 active kinase (100 ng) was incubated with compounds for 30 min at 30°C. Then each reaction mixture was mixed with a relevantly respective substrate, isotope-unlabeled ATP and/or 10 μCi [γ-^{32}P] ATP with each compound in 10 μL of reaction buffer containing 20 mM HEPES (pH 7.4), 10 mM $MgCl_2$, 10 mM $MnCl_2$, and 1 mM dithiothreitol (DTT). After incubation at 30°C for 30 min, the reaction was stopped by adding 4 μL protein loading buffer and the mixture was separated by SDS-PAGE. The ^{32}P-labeled substrate was visualized by autoradiography. For the isotope-unlabeled ATP kinase assay, p-Elk1 antibodies were visualized by Western blotting.

4.5.4 Anchorage-independent cell growth assay

Cells (8×10^3 per well) were suspended in basal medium eagle (BME) containing 10% FBS and 0.3% agar and plated on solidified BME containing 10% FBS and 0.5% agar. After incubation for 5-10 days, the colonies were counted under a microscope using the Image-Pro Plus Software (v.6.1) program (Media Cybernetics, Rockville, MD).

4.5.5 Foci formation assay

Transformation of NIH3T3 cells was performing following standard protocols. Cells were transiently transfected with different concentrations of pcDNA3-H-RasG12V and pcDNA3-mock (as compensation to achieve equal amounts of DNA) plasmids and incubated overnight. Then the cells were cultured in 5% CS-DMEM with or without Ei-

mix for 2 wk. The media were changed every other day. Foci were fixed and stained with 0.5% crystal violet (220).

4.5.6 Binding assay

Compound-conjugated Sepharose 4B beads were prepared as described previously (265-266). A whole cell lysate was incubated with resveratrol-conjugated or control beads at 4°C overnight in NP-40 lysis buffer [50 mM Tris-HCl (pH 8.0), 150 mM NaCl, 1 mM EDTA, 0.5% NP-40 and protease inhibitor]. After washing 5 times with NP-40 lysis buffer, the proteins bound to the beads were analyzed by Western blotting.

4.5.7 Western blotting

Cells were harvested and disrupted with NP-40 lysis buffer. The supernatant fraction was harvested after centrifugation at 13,000 rpm for 10 min. Protein concentration was determined by Bio-Rad protein assay reagent (Richmond, CA). Whole cell lysates were subjected to SDS-PAGE and transferred to a polyvinylidene difluoride membrane (Millipore, Billerica, MA). After blocking with 5% non-fat dry milk in 1 x TBS containing 0.05% Tween 20 (TBS-T), the membrane was incubated with a specific primary antibody, and then protein bands were visualized with the ECL system and LAS4000 Biomolecular Imager (GE Healthcare, UK) after hybridization with a horseradish peroxidase-conjugated secondary antibody.

4.5.8 Statistical analysis

All quantitative results are expressed as mean values ± S.D. Statistically significant differences were obtained by one-way ANOVA. A *p*-value of < 0.05 was considered to be statistically significant.

Chapter 5:

Recapitulation

In Chapter 1, the work flow of precision oncology was categorized into two segments, precision diagnosis and precision therapy. We provided milestones and important aspects characterizing each segment. By reviewing targeted therapies clinically approved against breast cancer, lung cancer and melanoma, we revealed the current status and exposed possible challenges in precision oncology. Two of the most effective state-of-the-art tools for the success of precision oncology were described.

Throughout the next three chapters (Chapters 2, 3 and 4), we presented three examples of utilizing drugs and/or natural compounds for precision oncology: new drug candidate, drug-natural compound combination, and multiple compounds mixed at low doses. Newly synthesized small molecules can be developed as a direct inhibitor of important proteins (Chapter 2). Extracts from plants and their active compounds can reinforce the therapeutic effects of drugs (Chapter 3). Natural compounds from various food source can be mixed to suppress carcinogenesis (Chapter 4).

Colorectal cancer is associated with aberrant activation of the Wnt pathway. β-Catenin plays essential roles in the Wnt pathway by interacting with T-cell factor 4 (TCF4) to transcribe oncogenes. We synthesized a small molecule, referred to as HI-B1, and evaluated signaling changes and biological consequences induced by the compound (Chapter 2). HI-B1 inhibited β-catenin/TCF4 luciferase activity and preferentially caused apoptosis of cancer cells which the survival is dependent on β-catenin. The formation of the β-catenin/TCF4 complex was disrupted by HI-B1 due to the direct interaction of HI-B1 with β-catenin. Colon cancer patient-derived xenograft (PDX) studies showed that a tumor with higher levels of β-catenin expression was more sensitive to HI-B1 treatment

compared to a tumor with lower expression levels of β-catenin. The different sensitivities of PDX tumors to HI-B1 were dependent on the β-catenin expression level and potentially could be further exploited for biomarker development and therapeutic applications against colon cancer.

Aspirin has received a considerable attention due to its anti-cancer effects on colon cancer patients with *PIK3CA* mutations. Ginger extract (GE) has protective effect against aspirin-induced hemorrhagic ulcer, and active components of GE possess anti-colon cancer effects. This led us to investigate on the effects and mechanisms of aspirin and GE combination (Chapter 3). Co-treatment of aspirin and GE resulted in synergistic cytotoxicity in HCT116, DLD1 and HCT15 colon cancer cell lines. The combination treatment caused apoptosis by enhancing p53 and p21 protein expressions. 6-Shogaol was identified as an active component of GE showing inhibition of anchorage-independent growth and direct binding with Akt1/2. In colon cancer patient-derived xenograft (PDX) models, co-treatment of aspirin 100 mg/kg plus GE 5 mg/kg significantly suppressed tumor growth. Of note, tumor-suppressive effects were similar between the combination group and aspirin 400 mg/kg group, but weight loss was shown only in aspirin-only group. The combination of aspirin and GE could be further exploited for therapeutic applications against colon cancer.

Fruits and vegetables are good sources of phytochemicals that possess health-promoting effects such as reducing the risk of cancer. Although the anti-cancer effects of phytochemicals are heavily investigated, there exists a limitation that a single phytochemical is not correlated with reducing risks of cancer. This is partly due to the

low concentration of each phytochemical in our body. To tackle this issue, we hypothesized that many phytochemicals with similar chemical structure may have a same target protein and the natural compounds, although at low doses, can inhibit the activity of the protein to where the anti-cancerr effects are focused (Chapter 4). From chemical similarity analysis of four known ERK inhibitors, we found six new ERK2 inhibitors with similar chemical structures. The ten phytochemicals were able to accumulatively inhibit ERK2 activity *in vitro*. ERK inhibitor mixture that each phytochemical exists at a low concentration suppressed H-ras-induced cell transformation of fibroblast, and inhibited anchorage-independent growth of cancer cells in where ERK2 is essential and highly expressed. This work will impact the cancer community by showing that many natural compounds can work together targeting ERK2, an important target in cancer.

Bibliography

1. Fox AL. The Relationship between Chemical Constitution and Taste. Proc Natl Acad Sci U S A. 1932;18:115-20.

2. Dance A. Medical histories. Nature. 2016;537:S52-3.

3. Hamburg MA, Collins FS. The path to personalized medicine. N Engl J Med. 2010;363:301-4.

4. Collins FS, Varmus H. A new initiative on precision medicine. N Engl J Med. 2015;372:793-5.

5. Aelion CM, Airhihenbuwa CO, Alemagno S, Amler RW, Arnett DK, Balas A, et al. The US Cancer Moonshot initiative. Lancet Oncol. 2016;17:e178-80.

6. Janda M, Soyer P. Greater Precision in Melanoma Prevention. JAMA Dermatol. 2016.

7. Scott AR. Technology: Read the instructions. Nature. 2016;537:S54-6.

8. Bode AM, Dong Z. Precision oncology- the future of personalized cancer medicine? Npj Precision Oncology. 2017;1:1-2.

9. Shin SH, Bode AM, Dong Z. Precision medicine: the foundation of future cancer therapeutics. npj Precision Oncology. 2017;1:12.

10. Miki Y, Swensen J, Shattuck-Eidens D, Futreal PA, Harshman K, Tavtigian S, et al. A strong candidate for the breast and ovarian cancer susceptibility gene BRCA1. Science. 1994;266:66-71.

11. Wooster R, Bignell G, Lancaster J, Swift S, Seal S, Mangion J, et al. Identification of the breast cancer susceptibility gene BRCA2. Nature. 1995;378:789-92.

12. Friedman AA, Letai A, Fisher DE, Flaherty KT. Precision medicine for cancer with next-generation functional diagnostics. Nat Rev Cancer. 2015;15:747-56.

13. Borrebaeck CA. Precision diagnostics: moving towards protein biomarker signatures of clinical utility in cancer. Nat Rev Cancer. 2017;17:199-204.

14. Dienstmann R, Vermeulen L, Guinney J, Kopetz S, Tejpar S, Tabernero J. Consensus molecular subtypes and the evolution of precision medicine in colorectal cancer. Nat Rev Cancer. 2017;17:79-92.

15. Couch FJ, Nathanson KL, Offit K. Two decades after BRCA: setting paradigms in personalized cancer care and prevention. Science. 2014;343:1466-70.

16. Michailidou K, Hall P, Gonzalez-Neira A, Ghoussaini M, Dennis J, Milne RL, et al. Large-scale genotyping identifies 41 new loci associated with breast cancer risk. Nat Genet. 2013;45:353-61, 61e1-2.

17. Bahcall OG. iCOGS collection provides a collaborative model. Foreword. Nat Genet. 2013;45:343.

18. Peto J, Collins N, Barfoot R, Seal S, Warren W, Rahman N, et al. Prevalence of BRCA1 and BRCA2 gene mutations in patients with early-onset breast cancer. J Natl Cancer Inst. 1999;91:943-9.

19. Osin PP, Lakhani SR. The pathology of familial breast cancer: Immunohistochemistry and molecular analysis. Breast Cancer Res. 1999;1:36-40.

20. Moelans CB, Kibbelaar RE, van den Heuvel MC, Castigliego D, de Weger RA, van Diest PJ. Validation of a fully automated HER2 staining kit in breast cancer. Cell Oncol. 2010;32:149-55.

21. Rangachari D, VanderLaan PA, Shea M, Le X, Huberman MS, Kobayashi SS, et al. Correlation between Classic Driver Oncogene Mutations in EGFR, ALK, or ROS1 and 22C3-PD-L1 >/=50% Expression in Lung Adenocarcinoma. J Thorac Oncol. 2017;12:878-83.

22. Paik S, Shak S, Tang G, Kim C, Baker J, Cronin M, et al. A multigene assay to predict recurrence of tamoxifen-treated, node-negative breast cancer. N Engl J Med. 2004;351:2817-26.

23. van de Vijver MJ, He YD, van't Veer LJ, Dai H, Hart AA, Voskuil DW, et al. A gene-expression signature as a predictor of survival in breast cancer. N Engl J Med. 2002;347:1999-2009.

24. Sorlie T, Tibshirani R, Parker J, Hastie T, Marron JS, Nobel A, et al. Repeated observation of breast tumor subtypes in independent gene expression data sets. Proc Natl Acad Sci U S A. 2003;100:8418-23.

25. Andre F, Bachelot T, Commo F, Campone M, Arnedos M, Dieras V, et al. Comparative genomic hybridisation array and DNA sequencing to direct treatment of metastatic breast cancer: a multicentre, prospective trial (SAFIR01/UNICANCER). Lancet Oncol. 2014;15:267-74.

26. Glas AM, Floore A, Delahaye LJ, Witteveen AT, Pover RC, Bakx N, et al. Converting a breast cancer microarray signature into a high-throughput diagnostic test. BMC Genomics. 2006;7:278.

27. Blumencranz P, Whitworth PW, Deck K, Rosenberg A, Reintgen D, Beitsch P, et al. Scientific Impact Recognition Award. Sentinel node staging for breast cancer:

intraoperative molecular pathology overcomes conventional histologic sampling errors. Am J Surg. 2007;194:426-32.

28. Foged NT, Brugmann A, Jorgensen JT. The HER2 CISH pharmDx() Kit in the assessment of breast cancer patients for anti-HER2 treatment. Expert Rev Mol Diagn. 2013;13:233-42.

29. Lim SJ, Cantillep A, Carpenter PM. Validation and workflow optimization of human epidermal growth factor receptor 2 testing using INFORM HER2 dual-color in situ hybridization. Hum Pathol. 2013;44:2590-6.

30. Nielsen T, Wallden B, Schaper C, Ferree S, Liu S, Gao D, et al. Analytical validation of the PAM50-based Prosigna Breast Cancer Prognostic Gene Signature Assay and nCounter Analysis System using formalin-fixed paraffin-embedded breast tumor specimens. BMC Cancer. 2014;14:177.

31. Cobleigh MA, Tabesh B, Bitterman P, Baker J, Cronin M, Liu ML, et al. Tumor gene expression and prognosis in breast cancer patients with 10 or more positive lymph nodes. Clin Cancer Res. 2005;11:8623-31.

32. Filipits M, Rudas M, Jakesz R, Dubsky P, Fitzal F, Singer CF, et al. A new molecular predictor of distant recurrence in ER-positive, HER2-negative breast cancer adds independent information to conventional clinical risk factors. Clin Cancer Res. 2011;17:6012-20.

33. Zhang Y, Schnabel CA, Schroeder BE, Jerevall PL, Jankowitz RC, Fornander T, et al. Breast cancer index identifies early-stage estrogen receptor-positive breast cancer patients at risk for early- and late-distant recurrence. Clin Cancer Res. 2013;19:4196-205.

34. Harms W, Malter W, Kramer S, Drebber U, Drzezga A, Schmidt M. Clinical significance of urokinase-type plasminogen activator (uPA) and its type-1 inhibitor (PAI-1) for metastatic sentinel lymph node involvement in breast cancer. Anticancer Res. 2014;34:4457-62.

35. Kimura H, Ohira T, Uchida O, Matsubayashi J, Shimizu S, Nagao T, et al. Analytical performance of the cobas EGFR mutation assay for Japanese non-small-cell lung cancer. Lung Cancer. 2014;83:329-33.

36. Malik SM, Maher VE, Bijwaard KE, Becker RL, Zhang L, Tang SW, et al. U.S. Food and Drug Administration approval: crizotinib for treatment of advanced or metastatic non-small cell lung cancer that is anaplastic lymphoma kinase positive. Clin Cancer Res. 2014;20:2029-34.

37. Vallee A, Le Loupp AG, Denis MG. Efficiency of the Therascreen(R) RGQ PCR kit for the detection of EGFR mutations in non-small cell lung carcinomas. Clin Chim Acta. 2014;429:8-11.

38. Conde E, Hernandez S, Prieto M, Martinez R, Lopez-Rios F. Profile of Ventana ALK (D5F3) companion diagnostic assay for non-small-cell lung carcinomas. Expert Rev Mol Diagn. 2016;16:707-13.

39. Sanders H, Qu K, Li H, Ma L, Barlan C, Zhang X, et al. Mutation Yield of a 34-Gene Solid Tumor Panel in Community-Based Tumor Samples. Mol Diagn Ther. 2016;20:241-53.

40. Abel HJ, Al-Kateb H, Cottrell CE, Bredemeyer AJ, Pritchard CC, Grossmann AH, et al. Detection of gene rearrangements in targeted clinical next-generation sequencing. J Mol Diagn. 2014;16:405-17.

41. Di Cristofaro J, Silvy M, Chiaroni J, Bailly P. Single PCR multiplex SNaPshot reaction for detection of eleven blood group nucleotide polymorphisms: optimization, validation, and one year of routine clinical use. J Mol Diagn. 2010;12:453-60.

42. Halait H, Demartin K, Shah S, Soviero S, Langland R, Cheng S, et al. Analytical performance of a real-time PCR-based assay for V600 mutations in the BRAF gene, used as the companion diagnostic test for the novel BRAF inhibitor vemurafenib in metastatic melanoma. Diagn Mol Pathol. 2012;21:1-8.

43. Marchant J, Mange A, Larrieux M, Costes V, Solassol J. Comparative evaluation of the new FDA approved THxID-BRAF test with High Resolution Melting and Sanger sequencing. BMC Cancer. 2014;14:519.

44. Sivendran S, Chang R, Pham L, Phelps RG, Harcharik ST, Hall LD, et al. Dissection of immune gene networks in primary melanoma tumors critical for antitumor surveillance of patients with stage II-III resectable disease. J Invest Dermatol. 2014;134:2202-11.

45. Minca EC, Al-Rohil RN, Wang M, Harms PW, Ko JS, Collie AM, et al. Comparison between melanoma gene expression score and fluorescence in situ hybridization for the classification of melanocytic lesions. Mod Pathol. 2016;29:832-43.

46. Chan M, Lee CW, Wu M. Integrating next-generation sequencing into clinical cancer diagnostics. Expert Rev Mol Diagn. 2013;13:647-50.

47. Cardoso F, van't Veer LJ, Bogaerts J, Slaets L, Viale G, Delaloge S, et al. 70-Gene Signature as an Aid to Treatment Decisions in Early-Stage Breast Cancer. N Engl J Med. 2016;375:717-29.

48. McVeigh TP, Kerin MJ. Clinical use of the Oncotype DX genomic test to guide treatment decisions for patients with invasive breast cancer. Breast Cancer (Dove Med Press). 2017;9:393-400.

49. Cronin M, Sangli C, Liu ML, Pho M, Dutta D, Nguyen A, et al. Analytical validation of the Oncotype DX genomic diagnostic test for recurrence prognosis and therapeutic response prediction in node-negative, estrogen receptor-positive breast cancer. Clin Chem. 2007;53:1084-91.

50. Sparano JA, Paik S. Development of the 21-gene assay and its application in clinical practice and clinical trials. J Clin Oncol. 2008;26:721-8.

51. Arnedos M, Vicier C, Loi S, Lefebvre C, Michiels S, Bonnefoi H, et al. Precision medicine for metastatic breast cancer--limitations and solutions. Nat Rev Clin Oncol. 2015;12:693-704.

52. Smith IE, Dowsett M. Aromatase inhibitors in breast cancer. N Engl J Med. 2003;348:2431-42.

53. Desta Z, Ward BA, Soukhova NV, Flockhart DA. Comprehensive evaluation of tamoxifen sequential biotransformation by the human cytochrome P450 system in vitro: prominent roles for CYP3A and CYP2D6. J Pharmacol Exp Ther. 2004;310:1062-75.

54. Mates M, Fletcher GG, Freedman OC, Eisen A, Gandhi S, Trudeau ME, et al. Systemic targeted therapy for her2-positive early female breast cancer: a systematic

review of the evidence for the 2014 Cancer Care Ontario systemic therapy guideline. Curr Oncol. 2015;22:S114-22.

55. Cobleigh MA, Vogel CL, Tripathy D, Robert NJ, Scholl S, Fehrenbacher L, et al. Multinational study of the efficacy and safety of humanized anti-HER2 monoclonal antibody in women who have HER2-overexpressing metastatic breast cancer that has progressed after chemotherapy for metastatic disease. J Clin Oncol. 1999;17:2639-48.

56. Citri A, Yarden Y. EGF-ERBB signalling: towards the systems level. Nat Rev Mol Cell Biol. 2006;7:505-16.

57. Slamon DJ, Leyland-Jones B, Shak S, Fuchs H, Paton V, Bajamonde A, et al. Use of chemotherapy plus a monoclonal antibody against HER2 for metastatic breast cancer that overexpresses HER2. N Engl J Med. 2001;344:783-92.

58. Swain SM, Baselga J, Kim SB, Ro J, Semiglazov V, Campone M, et al. Pertuzumab, trastuzumab, and docetaxel in HER2-positive metastatic breast cancer. N Engl J Med. 2015;372:724-34.

59. Verma S, Miles D, Gianni L, Krop IE, Welslau M, Baselga J, et al. Trastuzumab emtansine for HER2-positive advanced breast cancer. N Engl J Med. 2012;367:1783-91.

60. Stephens PJ, Tarpey PS, Davies H, Van Loo P, Greenman C, Wedge DC, et al. The landscape of cancer genes and mutational processes in breast cancer. Nature. 2012;486:400-4.

61. TheCancerGenomeAtlasNetwork. Comprehensive molecular portraits of human breast tumours. Nature. 2012;490:61-70.

62. Loi S, Michiels S, Baselga J, Bartlett JM, Singhal SK, Sabine VS, et al. PIK3CA genotype and a PIK3CA mutation-related gene signature and response to everolimus and letrozole in estrogen receptor positive breast cancer. PLoS One. 2013;8:e53292.

63. Richards S, Aziz N, Bale S, Bick D, Das S, Gastier-Foster J, et al. Standards and guidelines for the interpretation of sequence variants: a joint consensus recommendation of the American College of Medical Genetics and Genomics and the Association for Molecular Pathology. Genet Med. 2015;17:405-24.

64. Spurdle AB, Healey S, Devereau A, Hogervorst FB, Monteiro AN, Nathanson KL, et al. ENIGMA--evidence-based network for the interpretation of germline mutant alleles: an international initiative to evaluate risk and clinical significance associated with sequence variation in BRCA1 and BRCA2 genes. Hum Mutat. 2012;33:2-7.

65. Tavtigian SV, Greenblatt MS, Lesueur F, Byrnes GB. In silico analysis of missense substitutions using sequence-alignment based methods. Hum Mutat. 2008;29:1327-36.

66. Lindor NM, Guidugli L, Wang X, Vallee MP, Monteiro AN, Tavtigian S, et al. A review of a multifactorial probability-based model for classification of BRCA1 and BRCA2 variants of uncertain significance (VUS). Hum Mutat. 2012;33:8-21.

67. Collett K, Stefansson IM, Eide J, Braaten A, Wang H, Eide GE, et al. A basal epithelial phenotype is more frequent in interval breast cancers compared with screen detected tumors. Cancer Epidemiol Biomarkers Prev. 2005;14:1108-12.

68. Stockmans G, Deraedt K, Wildiers H, Moerman P, Paridaens R. Triple-negative breast cancer. Curr Opin Oncol. 2008;20:614-20.

69. Amir E, Miller N, Geddie W, Freedman O, Kassam F, Simmons C, et al. Prospective study evaluating the impact of tissue confirmation of metastatic disease in patients with breast cancer. J Clin Oncol. 2012;30:587-92.

70. Niikura N, Liu J, Hayashi N, Mittendorf EA, Gong Y, Palla SL, et al. Loss of human epidermal growth factor receptor 2 (HER2) expression in metastatic sites of HER2-overexpressing primary breast tumors. J Clin Oncol. 2012;30:593-9.

71. Nakai K, Hung MC, Yamaguchi H. A perspective on anti-EGFR therapies targeting triple-negative breast cancer. Am J Cancer Res. 2016;6:1609-23.

72. Reis-Filho JS, Tutt AN. Triple negative tumours: a critical review. Histopathology. 2008;52:108-18.

73. Bianchini G, Balko JM, Mayer IA, Sanders ME, Gianni L. Triple-negative breast cancer: challenges and opportunities of a heterogeneous disease. Nat Rev Clin Oncol. 2016;13:674-90.

74. Ciardiello F, Tortora G. A novel approach in the treatment of cancer: targeting the epidermal growth factor receptor. Clin Cancer Res. 2001;7:2958-70.

75. Maemondo M, Inoue A, Kobayashi K, Sugawara S, Oizumi S, Isobe H, et al. Gefitinib or chemotherapy for non-small-cell lung cancer with mutated EGFR. N Engl J Med. 2010;362:2380-8.

76. Mitsudomi T, Morita S, Yatabe Y, Negoro S, Okamoto I, Tsurutani J, et al. Gefitinib versus cisplatin plus docetaxel in patients with non-small-cell lung cancer harbouring mutations of the epidermal growth factor receptor (WJTOG3405): an open label, randomised phase 3 trial. Lancet Oncol. 2010;11:121-8.

77. Zhou C, Wu YL, Chen G, Feng J, Liu XQ, Wang C, et al. Erlotinib versus chemotherapy as first-line treatment for patients with advanced EGFR mutation-positive non-small-cell lung cancer (OPTIMAL, CTONG-0802): a multicentre, open-label, randomised, phase 3 study. Lancet Oncol. 2011;12:735-42.

78. Rosell R, Carcereny E, Gervais R, Vergnenegre A, Massuti B, Felip E, et al. Erlotinib versus standard chemotherapy as first-line treatment for European patients with advanced EGFR mutation-positive non-small-cell lung cancer (EURTAC): a multicentre, open-label, randomised phase 3 trial. Lancet Oncol. 2012;13:239-46.

79. Wu YL, Lee JS, Thongprasert S, Yu CJ, Zhang L, Ladrera G, et al. Intercalated combination of chemotherapy and erlotinib for patients with advanced stage non-small-cell lung cancer (FASTACT-2): a randomised, double-blind trial. Lancet Oncol. 2013;14:777-86.

80. Seto T, Kato T, Nishio M, Goto K, Atagi S, Hosomi Y, et al. Erlotinib alone or with bevacizumab as first-line therapy in patients with advanced non-squamous non-small-cell lung cancer harbouring EGFR mutations (JO25567): an open-label, randomised, multicentre, phase 2 study. Lancet Oncol. 2014;15:1236-44.

81. Kobayashi S, Boggon TJ, Dayaram T, Janne PA, Kocher O, Meyerson M, et al. EGFR mutation and resistance of non-small-cell lung cancer to gefitinib. N Engl J Med. 2005;352:786-92.

82. Yu HA, Arcila ME, Rekhtman N, Sima CS, Zakowski MF, Pao W, et al. Analysis of tumor specimens at the time of acquired resistance to EGFR-TKI therapy in 155 patients with EGFR-mutant lung cancers. Clin Cancer Res. 2013;19:2240-7.

83. Sequist LV, Yang JC, Yamamoto N, O'Byrne K, Hirsh V, Mok T, et al. Phase III study of afatinib or cisplatin plus pemetrexed in patients with metastatic lung adenocarcinoma with EGFR mutations. J Clin Oncol. 2013;31:3327-34.

84. Wu YL, Zhou C, Hu CP, Feng J, Lu S, Huang Y, et al. Afatinib versus cisplatin plus gemcitabine for first-line treatment of Asian patients with advanced non-small-cell lung cancer harbouring EGFR mutations (LUX-Lung 6): an open-label, randomised phase 3 trial. Lancet Oncol. 2014;15:213-22.

85. Janne PA, Yang JC, Kim DW, Planchard D, Ohe Y, Ramalingam SS, et al. AZD9291 in EGFR inhibitor-resistant non-small-cell lung cancer. N Engl J Med. 2015;372:1689-99.

86. Sequist LV, Rolfe L, Allen AR. Rociletinib in EGFR-Mutated Non-Small-Cell Lung Cancer. N Engl J Med. 2015;373:578-9.

87. Greig SL. Osimertinib: First Global Approval. Drugs. 2016;76:263-73.

88. Hallberg B, Palmer RH. Mechanistic insight into ALK receptor tyrosine kinase in human cancer biology. Nat Rev Cancer. 2013;13:685-700.

89. Soda M, Choi YL, Enomoto M, Takada S, Yamashita Y, Ishikawa S, et al. Identification of the transforming EML4-ALK fusion gene in non-small-cell lung cancer. Nature. 2007;448:561-6.

90. Rikova K, Guo A, Zeng Q, Possemato A, Yu J, Haack H, et al. Global survey of phosphotyrosine signaling identifies oncogenic kinases in lung cancer. Cell. 2007;131:1190-203.

91. Takeuchi K, Choi YL, Togashi Y, Soda M, Hatano S, Inamura K, et al. KIF5B-ALK, a novel fusion oncokinase identified by an immunohistochemistry-based diagnostic system for ALK-positive lung cancer. Clin Cancer Res. 2009;15:3143-9.

92. Heuckmann JM, Balke-Want H, Malchers F, Peifer M, Sos ML, Koker M, et al. Differential protein stability and ALK inhibitor sensitivity of EML4-ALK fusion variants. Clin Cancer Res. 2012;18:4682-90.

93. Togashi Y, Soda M, Sakata S, Sugawara E, Hatano S, Asaka R, et al. KLC1-ALK: a novel fusion in lung cancer identified using a formalin-fixed paraffin-embedded tissue only. PLoS One. 2012;7:e31323.

94. Kim HR, Shim HS, Chung JH, Lee YJ, Hong YK, Rha SY, et al. Distinct clinical features and outcomes in never-smokers with nonsmall cell lung cancer who harbor EGFR or KRAS mutations or ALK rearrangement. Cancer. 2012;118:729-39.

95. Davies KD, Doebele RC. Molecular pathways: ROS1 fusion proteins in cancer. Clin Cancer Res. 2013;19:4040-5.

96. Michels S, Wolf J. Stratified Treatment in Lung Cancer. Oncol Res Treat. 2016;39:760-6.

97. Shaw AT, Kim DW, Nakagawa K, Seto T, Crino L, Ahn MJ, et al. Crizotinib versus chemotherapy in advanced ALK-positive lung cancer. N Engl J Med. 2013;368:2385-94.

98. Solomon BJ, Mok T, Kim DW, Wu YL, Nakagawa K, Mekhail T, et al. First-line crizotinib versus chemotherapy in ALK-positive lung cancer. N Engl J Med. 2014;371:2167-77.

99. Shaw AT, Ou SH, Bang YJ, Camidge DR, Solomon BJ, Salgia R, et al. Crizotinib in ROS1-rearranged non-small-cell lung cancer. N Engl J Med. 2014;371:1963-71.

100. Paik PK, Drilon A, Fan PD, Yu H, Rekhtman N, Ginsberg MS, et al. Response to MET inhibitors in patients with stage IV lung adenocarcinomas harboring MET mutations causing exon 14 skipping. Cancer Discov. 2015;5:842-9.

101. Shaw AT, Kim DW, Mehra R, Tan DS, Felip E, Chow LQ, et al. Ceritinib in ALK-rearranged non-small-cell lung cancer. N Engl J Med. 2014;370:1189-97.

102. Sakamoto H, Tsukaguchi T, Hiroshima S, Kodama T, Kobayashi T, Fukami TA, et al. CH5424802, a selective ALK inhibitor capable of blocking the resistant gatekeeper mutant. Cancer Cell. 2011;19:679-90.

103. Hyman DM, Puzanov I, Subbiah V, Faris JE, Chau I, Blay JY, et al. Vemurafenib in Multiple Nonmelanoma Cancers with BRAF V600 Mutations. N Engl J Med. 2015;373:726-36.

104. Planchard D, Besse B, Groen HJ, Souquet PJ, Quoix E, Baik CS, et al. Dabrafenib plus trametinib in patients with previously treated BRAF(V600E)-mutant metastatic non-small cell lung cancer: an open-label, multicentre phase 2 trial. Lancet Oncol. 2016;17:984-93.

105. Lee L, Gupta M, Sahasranaman S. Immune Checkpoint inhibitors: An introduction to the next-generation cancer immunotherapy. J Clin Pharmacol. 2016;56:157-69.

106. Chen YM. Immune checkpoint inhibitors for nonsmall cell lung cancer treatment. J Chin Med Assoc. 2017;80:7-14.

107. Rizvi NA, Mazieres J, Planchard D, Stinchcombe TE, Dy GK, Antonia SJ, et al. Activity and safety of nivolumab, an anti-PD-1 immune checkpoint inhibitor, for patients with advanced, refractory squamous non-small-cell lung cancer (CheckMate 063): a phase 2, single-arm trial. Lancet Oncol. 2015;16:257-65.

108. Gettinger SN, Horn L, Gandhi L, Spigel DR, Antonia SJ, Rizvi NA, et al. Overall Survival and Long-Term Safety of Nivolumab (Anti-Programmed Death 1 Antibody, BMS-936558, ONO-4538) in Patients With Previously Treated Advanced Non-Small-Cell Lung Cancer. J Clin Oncol. 2015;33:2004-12.

109. Brahmer J, Reckamp KL, Baas P, Crino L, Eberhardt WE, Poddubskaya E, et al. Nivolumab versus Docetaxel in Advanced Squamous-Cell Non-Small-Cell Lung Cancer. N Engl J Med. 2015;373:123-35.

110. Borghaei H, Paz-Ares L, Horn L, Spigel DR, Steins M, Ready NE, et al. Nivolumab versus Docetaxel in Advanced Nonsquamous Non-Small-Cell Lung Cancer. N Engl J Med. 2015;373:1627-39.

111. Garon EB, Rizvi NA, Hui R, Leighl N, Balmanoukian AS, Eder JP, et al. Pembrolizumab for the treatment of non-small-cell lung cancer. N Engl J Med. 2015;372:2018-28.

112. Hirsch FR, Scagliotti GV, Mulshine JL, Kwon R, Curran WJ, Jr., Wu YL, et al. Lung cancer: current therapies and new targeted treatments. Lancet. 2017;389:299-311.

113. Greaves M, Maley CC. Clonal evolution in cancer. Nature. 2012;481:306-13.

114. Nowell PC. The clonal evolution of tumor cell populations. Science. 1976;194:23-8.

115. Lipinski KA, Barber LJ, Davies MN, Ashenden M, Sottoriva A, Gerlinger M. Cancer Evolution and the Limits of Predictability in Precision Cancer Medicine. Trends Cancer. 2016;2:49-63.

116. Piotrowska Z, Niederst MJ, Karlovich CA, Wakelee HA, Neal JW, Mino-Kenudson M, et al. Heterogeneity Underlies the Emergence of EGFRT790 Wild-Type Clones Following Treatment of T790M-Positive Cancers with a Third-Generation EGFR Inhibitor. Cancer Discov. 2015;5:713-22.

117. Sequist LV, Soria JC, Goldman JW, Wakelee HA, Gadgeel SM, Varga A, et al. Rociletinib in EGFR-mutated non-small-cell lung cancer. N Engl J Med. 2015;372:1700-9.

118. Niederst MJ, Hu H, Mulvey HE, Lockerman EL, Garcia AR, Piotrowska Z, et al. The Allelic Context of the C797S Mutation Acquired upon Treatment with Third-Generation EGFR Inhibitors Impacts Sensitivity to Subsequent Treatment Strategies. Clin Cancer Res. 2015;21:3924-33.

119. Davies H, Bignell GR, Cox C, Stephens P, Edkins S, Clegg S, et al. Mutations of the BRAF gene in human cancer. Nature. 2002;417:949-54.

120. Menzies AM, Haydu LE, Visintin L, Carlino MS, Howle JR, Thompson JF, et al. Distinguishing clinicopathologic features of patients with V600E and V600K BRAF-mutant metastatic melanoma. Clin Cancer Res. 2012;18:3242-9.

121. Chapman PB, Hauschild A, Robert C, Haanen JB, Ascierto P, Larkin J, et al. Improved survival with vemurafenib in melanoma with BRAF V600E mutation. N Engl J Med. 2011;364:2507-16.

122. Hauschild A, Grob JJ, Demidov LV, Jouary T, Gutzmer R, Millward M, et al. Dabrafenib in BRAF-mutated metastatic melanoma: a multicentre, open-label, phase 3 randomised controlled trial. Lancet. 2012;380:358-65.

123. Lovly CM, Shaw AT. Molecular pathways: resistance to kinase inhibitors and implications for therapeutic strategies. Clin Cancer Res. 2014;20:2249-56.

124. Nazarian R, Shi H, Wang Q, Kong X, Koya RC, Lee H, et al. Melanomas acquire resistance to B-RAF(V600E) inhibition by RTK or N-RAS upregulation. Nature. 2010;468:973-7.

125. Flaherty KT, Robert C, Hersey P, Nathan P, Garbe C, Milhem M, et al. Improved survival with MEK inhibition in BRAF-mutated melanoma. N Engl J Med. 2012;367:107-14.

126. Johannessen CM, Boehm JS, Kim SY, Thomas SR, Wardwell L, Johnson LA, et al. COT drives resistance to RAF inhibition through MAP kinase pathway reactivation. Nature. 2010;468:968-72.

127. Flaherty KT, Infante JR, Daud A, Gonzalez R, Kefford RF, Sosman J, et al. Combined BRAF and MEK inhibition in melanoma with BRAF V600 mutations. N Engl J Med. 2012;367:1694-703.

128. Ascierto PA, McArthur GA, Dreno B, Atkinson V, Liszkay G, Di Giacomo AM, et al. Cobimetinib combined with vemurafenib in advanced BRAF(V600)-mutant melanoma (coBRIM): updated efficacy results from a randomised, double-blind, phase 3 trial. Lancet Oncol. 2016;17:1248-60.

129. Chapon M, Randriamampita C, Maubec E, Badoual C, Fouquet S, Wang SF, et al. Progressive upregulation of PD-1 in primary and metastatic melanomas associated with blunted TCR signaling in infiltrating T lymphocytes. J Invest Dermatol. 2011;131:1300-7.

130. Hodi FS, O'Day SJ, McDermott DF, Weber RW, Sosman JA, Haanen JB, et al. Improved survival with ipilimumab in patients with metastatic melanoma. N Engl J Med. 2010;363:711-23.

131. O'Day SJ, Maio M, Chiarion-Sileni V, Gajewski TF, Pehamberger H, Bondarenko IN, et al. Efficacy and safety of ipilimumab monotherapy in patients with pretreated advanced melanoma: a multicenter single-arm phase II study. Ann Oncol. 2010;21:1712-7.

132. Topalian SL, Hodi FS, Brahmer JR, Gettinger SN, Smith DC, McDermott DF, et al. Safety, activity, and immune correlates of anti-PD-1 antibody in cancer. N Engl J Med. 2012;366:2443-54.

133. Topalian SL, Sznol M, McDermott DF, Kluger HM, Carvajal RD, Sharfman WH, et al. Survival, durable tumor remission, and long-term safety in patients with advanced melanoma receiving nivolumab. J Clin Oncol. 2014;32:1020-30.

134. Robert C, Long GV, Brady B, Dutriaux C, Maio M, Mortier L, et al. Nivolumab in previously untreated melanoma without BRAF mutation. N Engl J Med. 2015;372:320-30.

135. Robert C, Schachter J, Long GV, Arance A, Grob JJ, Mortier L, et al. Pembrolizumab versus Ipilimumab in Advanced Melanoma. N Engl J Med. 2015;372:2521-32.

136. Larkin J, Chiarion-Sileni V, Gonzalez R, Grob JJ, Cowey CL, Lao CD, et al. Combined Nivolumab and Ipilimumab or Monotherapy in Untreated Melanoma. N Engl J Med. 2015;373:23-34.

137. Zaretsky JM, Garcia-Diaz A, Shin DS, Escuin-Ordinas H, Hugo W, Hu-Lieskovan S, et al. Mutations Associated with Acquired Resistance to PD-1 Blockade in Melanoma. N Engl J Med. 2016;375:819-29.

138. Shin DS, Zaretsky JM, Escuin-Ordinas H, Garcia-Diaz A, Hu-Lieskovan S, Kalbasi A, et al. Primary Resistance to PD-1 Blockade Mediated by JAK1/2 Mutations. Cancer Discov. 2017;7:188-201.

139. Allard WJ, Matera J, Miller MC, Repollet M, Connelly MC, Rao C, et al. Tumor cells circulate in the peripheral blood of all major carcinomas but not in healthy subjects or patients with nonmalignant diseases. Clin Cancer Res. 2004;10:6897-904.

140. Jiang P, Chan CW, Chan KC, Cheng SH, Wong J, Wong VW, et al. Lengthening and shortening of plasma DNA in hepatocellular carcinoma patients. Proc Natl Acad Sci U S A. 2015;112:E1317-25.

141. Schwarzenbach H, Hoon DS, Pantel K. Cell-free nucleic acids as biomarkers in cancer patients. Nat Rev Cancer. 2011;11:426-37.

142. Alix-Panabieres C, Pantel K. Clinical Applications of Circulating Tumor Cells and Circulating Tumor DNA as Liquid Biopsy. Cancer Discov. 2016;6:479-91.

143. Mavroudis D. Circulating cancer cells. Ann Oncol. 2010;21 Suppl 7:vii95-100.

144. Miller MC, Doyle GV, Terstappen LW. Significance of Circulating Tumor Cells Detected by the CellSearch System in Patients with Metastatic Breast Colorectal and Prostate Cancer. J Oncol. 2010;2010:617421.

145. Alix-Panabieres C, Pantel K. Circulating tumor cells: liquid biopsy of cancer. Clin Chem. 2013;59:110-8.

146. Scher HI, Heller G, Molina A, Attard G, Danila DC, Jia X, et al. Circulating tumor cell biomarker panel as an individual-level surrogate for survival in metastatic castration-resistant prostate cancer. J Clin Oncol. 2015;33:1348-55.

147. Smerage JB, Barlow WE, Hortobagyi GN, Winer EP, Leyland-Jones B, Srkalovic G, et al. Circulating tumor cells and response to chemotherapy in metastatic breast cancer: SWOG S0500. J Clin Oncol. 2014;32:3483-9.

148. Diehl F, Li M, Dressman D, He Y, Shen D, Szabo S, et al. Detection and quantification of mutations in the plasma of patients with colorectal tumors. Proc Natl Acad Sci U S A. 2005;102:16368-73.

149. Bettegowda C, Sausen M, Leary RJ, Kinde I, Wang Y, Agrawal N, et al. Detection of circulating tumor DNA in early- and late-stage human malignancies. Sci Transl Med. 2014;6:224ra24.

150. Siravegna G, Mussolin B, Buscarino M, Corti G, Cassingena A, Crisafulli G, et al. Clonal evolution and resistance to EGFR blockade in the blood of colorectal cancer patients. Nat Med. 2015;21:827.

151. Hidalgo M, Amant F, Biankin AV, Budinska E, Byrne AT, Caldas C, et al. Patient-derived xenograft models: an emerging platform for translational cancer research. Cancer Discov. 2014;4:998-1013.

152. Aparicio S, Hidalgo M, Kung AL. Examining the utility of patient-derived xenograft mouse models. Nat Rev Cancer. 2015;15:311-6.

153. Fiebig HH, Neumann HA, Henss H, Koch H, Kaiser D, Arnold H. Development of three human small cell lung cancer models in nude mice. Recent Results Cancer Res. 1985;97:77-86.

154. Bruna A, Rueda OM, Greenwood W, Batra AS, Callari M, Batra RN, et al. A Biobank of Breast Cancer Explants with Preserved Intra-tumor Heterogeneity to Screen Anticancer Compounds. Cell. 2016;167:260-74 e22.

155. Morton JJ, Bird G, Refaeli Y, Jimeno A. Humanized Mouse Xenograft Models: Narrowing the Tumor-Microenvironment Gap. Cancer Res. 2016;76:6153-8.

156. Gao H, Korn JM, Ferretti S, Monahan JE, Wang Y, Singh M, et al. High-throughput screening using patient-derived tumor xenografts to predict clinical trial drug response. Nat Med. 2015;21:1318-25.

157. Ledford H. US cancer institute to overhaul tumour cell lines. Nature. 2016;530:391.

158. Townsend EC, Murakami MA, Christodoulou A, Christie AL, Koster J, DeSouza TA, et al. The Public Repository of Xenografts Enables Discovery and Randomized Phase II-like Trials in Mice. Cancer Cell. 2016;29:574-86.

159. Byrne AT, Alferez DG, Amant F, Annibali D, Arribas J, Biankin AV, et al. Interrogating open issues in cancer precision medicine with patient-derived xenografts. Nat Rev Cancer. 2017;17:254-68.

160. Prasad V. Perspective: The precision-oncology illusion. Nature. 2016;537:S63.

161. Prasad V, Fojo T, Brada M. Precision oncology: origins, optimism, and potential. Lancet Oncol. 2016;17:e81-6.

162. Le Tourneau C, Delord JP, Goncalves A, Gavoille C, Dubot C, Isambert N, et al. Molecularly targeted therapy based on tumour molecular profiling versus conventional therapy for advanced cancer (SHIVA): a multicentre, open-label, proof-of-concept, randomised, controlled phase 2 trial. Lancet Oncol. 2015;16:1324-34.

163. Tannock IF, Hickman JA. Limits to Personalized Cancer Medicine. N Engl J Med. 2016;375:1289-94.

164. Gerlinger M, Rowan AJ, Horswell S, Larkin J, Endesfelder D, Gronroos E, et al. Intratumor heterogeneity and branched evolution revealed by multiregion sequencing. N Engl J Med. 2012;366:883-92.

165. Mullard A. NCI-MATCH trial pushes cancer umbrella trial paradigm. Nat Rev Drug Discov. 2015;14:513-5.

166. Brower V. NCI-MATCH pairs tumor mutations with matching drugs. Nat Biotechnol. 2015;33:790-1.

167. Coyne GO, Takebe N, Chen AP. Defining precision: The precision medicine initiative trials NCI-MPACT and NCI-MATCH. Curr Probl Cancer. 2017;41:182-93.

168. Shin SH, Bode AM, Dong Z. Precision medicine: the foundation of future cancer therapeutics. npj Precision Oncology 2017 [cited 1 12]; 1-3].

169. O'Brien SG, Guilhot F, Larson RA, Gathmann I, Baccarani M, Cervantes F, et al. Imatinib compared with interferon and low-dose cytarabine for newly diagnosed chronic-phase chronic myeloid leukemia. N Engl J Med. 2003;348:994-1004.

170. Barone A, Hazarika M, Theoret MR, Mishra-Kalyani P, Chen H, He K, et al. FDA Approval Summary: Pembrolizumab for the Treatment of Patients with Unresectable or Metastatic Melanoma. Clin Cancer Res. 2017.

171. Sul J, Blumenthal GM, Jiang X, He K, Keegan P, Pazdur R. FDA Approval Summary: Pembrolizumab for the Treatment of Patients With Metastatic Non-Small Cell Lung Cancer Whose Tumors Express Programmed Death-Ligand 1. Oncologist. 2016;21:643-50.

172. Pembrolizumab Approved for Hodgkin Lymphoma. Cancer Discov. 2017;7:OF1.

173. Larkins E, Blumenthal GM, Yuan W, He K, Sridhara R, Subramaniam S, et al. U.S. Food and Drug Administration Approval Summary: Pembrolizumab for the Treatment of Recurrent or Metastatic Head and Neck Squamous Cell Carcinoma with Disease Progression on or After Platinum-Containing Chemotherapy. Oncologist. 2017.

174. Nogova L, Sequist LV, Perez Garcia JM, Andre F, Delord JP, Hidalgo M, et al. Evaluation of BGJ398, a Fibroblast Growth Factor Receptor 1-3 Kinase Inhibitor, in Patients With Advanced Solid Tumors Harboring Genetic Alterations in Fibroblast Growth Factor Receptors: Results of a Global Phase I, Dose-Escalation and Dose-Expansion Study. J Clin Oncol. 2017;35:157-65.

175. Wenk MR. The emerging field of lipidomics. Nat Rev Drug Discov. 2005;4:594-610.

176. Hall Z, Ament Z, Wilson CH, Burkhart DL, Ashmore T, Koulman A, et al. Myc Expression Drives Aberrant Lipid Metabolism in Lung Cancer. Cancer Res. 2016;76:4608-18.

177. Nickell S, Kofler C, Leis AP, Baumeister W. A visual approach to proteomics. Nat Rev Mol Cell Biol. 2006;7:225-30.

178. Taylor NMI, Manolaridis I, Jackson SM, Kowal J, Stahlberg H, Locher KP. Structure of the human multidrug transporter ABCG2. Nature. 2017;546:504-9.

179. Koppel N, Maini Rekdal V, Balskus EP. Chemical transformation of xenobiotics by the human gut microbiota. Science. 2017;356.

180. Wallace BD, Wang H, Lane KT, Scott JE, Orans J, Koo JS, et al. Alleviating cancer drug toxicity by inhibiting a bacterial enzyme. Science. 2010;330:831-5.

181. Siegel RL, Miller KD, Jemal A. Cancer statistics, 2016. CA Cancer J Clin. 2016;66:7-30.

182. Bokemeyer C, Bondarenko I, Makhson A, Hartmann JT, Aparicio J, de Braud F, et al. Fluorouracil, leucovorin, and oxaliplatin with and without cetuximab in the first-line treatment of metastatic colorectal cancer. J Clin Oncol. 2009;27:663-71.

183. Douillard JY, Siena S, Cassidy J, Tabernero J, Burkes R, Barugel M, et al. Randomized, phase III trial of panitumumab with infusional fluorouracil, leucovorin, and oxaliplatin (FOLFOX4) versus FOLFOX4 alone as first-line treatment in patients with

previously untreated metastatic colorectal cancer: the PRIME study. J Clin Oncol. 2010;28:4697-705.

184. Polakis P. Drugging Wnt signalling in cancer. EMBO J. 2012;31:2737-46.

185. Clevers H, Nusse R. Wnt/beta-catenin signaling and disease. Cell. 2012;149:1192-205.

186. Kahn M. Can we safely target the WNT pathway? Nat Rev Drug Discov. 2014;13:513-32.

187. Gumbiner BM. Carcinogenesis: a balance between beta-catenin and APC. Curr Biol. 1997;7:R443-6.

188. Leung JY, Kolligs FT, Wu R, Zhai Y, Kuick R, Hanash S, et al. Activation of AXIN2 expression by beta-catenin-T cell factor. A feedback repressor pathway regulating Wnt signaling. J Biol Chem. 2002;277:21657-65.

189. Shtutman M, Zhurinsky J, Simcha I, Albanese C, D'Amico M, Pestell R, et al. The cyclin D1 gene is a target of the beta-catenin/LEF-1 pathway. Proc Natl Acad Sci U S A. 1999;96:5522-7.

190. He TC, Sparks AB, Rago C, Hermeking H, Zawel L, da Costa LT, et al. Identification of c-MYC as a target of the APC pathway. Science. 1998;281:1509-12.

191. Anastas JN, Moon RT. WNT signalling pathways as therapeutic targets in cancer. Nat Rev Cancer. 2013;13:11-26.

192. Chen B, Dodge ME, Tang W, Lu J, Ma Z, Fan CW, et al. Small molecule-mediated disruption of Wnt-dependent signaling in tissue regeneration and cancer. Nat Chem Biol. 2009;5:100-7.

193. Huang SM, Mishina YM, Liu S, Cheung A, Stegmeier F, Michaud GA, et al. Tankyrase inhibition stabilizes axin and antagonizes Wnt signalling. Nature. 2009;461:614-20.

194. Thorne CA, Hanson AJ, Schneider J, Tahinci E, Orton D, Cselenyi CS, et al. Small-molecule inhibition of Wnt signaling through activation of casein kinase 1alpha. Nat Chem Biol. 2010;6:829-36.

195. Sukhdeo K, Mani M, Zhang Y, Dutta J, Yasui H, Rooney MD, et al. Targeting the beta-catenin/TCF transcriptional complex in the treatment of multiple myeloma. Proc Natl Acad Sci U S A. 2007;104:7516-21.

196. Lepourcelet M, Chen YN, France DS, Wang H, Crews P, Petersen F, et al. Small-molecule antagonists of the oncogenic Tcf/beta-catenin protein complex. Cancer Cell. 2004;5:91-102.

197. Hwang SY, Deng X, Byun S, Lee C, Lee SJ, Suh H, et al. Direct Targeting of beta-Catenin by a Small Molecule Stimulates Proteasomal Degradation and Suppresses Oncogenic Wnt/beta-Catenin Signaling. Cell Rep. 2016;16:28-36.

198. Cho SY, Kang W, Han JY, Min S, Kang J, Lee A, et al. An Integrative Approach to Precision Cancer Medicine Using Patient-Derived Xenografts. Mol Cells. 2016;39:77-86.

199. Bertotti A, Migliardi G, Galimi F, Sassi F, Torti D, Isella C, et al. A molecularly annotated platform of patient-derived xenografts ("xenopatients") identifies HER2 as an effective therapeutic target in cetuximab-resistant colorectal cancer. Cancer Discov. 2011;1:508-23.

200. Cunningham D, Humblet Y, Siena S, Khayat D, Bleiberg H, Santoro A, et al. Cetuximab monotherapy and cetuximab plus irinotecan in irinotecan-refractory metastatic colorectal cancer. N Engl J Med. 2004;351:337-45.

201. Bardelli A, Corso S, Bertotti A, Hobor S, Valtorta E, Siravegna G, et al. Amplification of the MET receptor drives resistance to anti-EGFR therapies in colorectal cancer. Cancer Discov. 2013;3:658-73.

202. Kawazoe A, Shitara K, Fukuoka S, Kuboki Y, Bando H, Okamoto W, et al. A retrospective observational study of clinicopathological features of KRAS, NRAS, BRAF and PIK3CA mutations in Japanese patients with metastatic colorectal cancer. BMC Cancer. 2015;15:258.

203. Grossmann TN, Yeh JT, Bowman BR, Chu Q, Moellering RE, Verdine GL. Inhibition of oncogenic Wnt signaling through direct targeting of beta-catenin. Proc Natl Acad Sci U S A. 2012;109:17942-7.

204. Hao J, Ao A, Zhou L, Murphy CK, Frist AY, Keel JJ, et al. Selective small molecule targeting beta-catenin function discovered by in vivo chemical genetic screen. Cell Rep. 2013;4:898-904.

205. Li X, Pu J, Jiang S, Su J, Kong L, Mao B, et al. Henryin, an ent-kaurane diterpenoid, inhibits Wnt signaling through interference with beta-catenin/TCF4 interaction in colorectal cancer cells. PLoS One. 2013;8:e68525.

206. Fang L, Zhu Q, Neuenschwander M, Specker E, Wulf-Goldenberg A, Weis WI, et al. A Small-Molecule Antagonist of the beta-Catenin/TCF4 Interaction Blocks the Self-

Renewal of Cancer Stem Cells and Suppresses Tumorigenesis. Cancer Res. 2016;76:891-901.

207. Jang GB, Hong IS, Kim RJ, Lee SY, Park SJ, Lee ES, et al. Wnt/beta-Catenin Small-Molecule Inhibitor CWP232228 Preferentially Inhibits the Growth of Breast Cancer Stem-like Cells. Cancer Res. 2015;75:1691-702.

208. Licchesi JD, Westra WH, Hooker CM, Machida EO, Baylin SB, Herman JG. Epigenetic alteration of Wnt pathway antagonists in progressive glandular neoplasia of the lung. Carcinogenesis. 2008;29:895-904.

209. Kolligs FT, Bommer G, Goke B. Wnt/beta-catenin/tcf signaling: a critical pathway in gastrointestinal tumorigenesis. Digestion. 2002;66:131-44.

210. Espada J, Galaz S, Sanz-Rodriguez F, Blazquez-Castro A, Stockert JC, Bagazgoitia L, et al. Oncogenic H-Ras and PI3K signaling can inhibit E-cadherin-dependent apoptosis and promote cell survival after photodynamic therapy in mouse keratinocytes. J Cell Physiol. 2009;219:84-93.

211. Damalas A, Kahan S, Shtutman M, Ben-Ze'ev A, Oren M. Deregulated beta-catenin induces a p53- and ARF-dependent growth arrest and cooperates with Ras in transformation. EMBO J. 2001;20:4912-22.

212. Jamieson C, Sharma M, Henderson BR. Targeting the beta-catenin nuclear transport pathway in cancer. Semin Cancer Biol. 2014;27:20-9.

213. Segditsas S, Tomlinson I. Colorectal cancer and genetic alterations in the Wnt pathway. Oncogene. 2006;25:7531-7.

214. Korinek V, Barker N, Morin PJ, van Wichen D, de Weger R, Kinzler KW, et al. Constitutive transcriptional activation by a beta-catenin-Tcf complex in APC-/- colon carcinoma. Science. 1997;275:1784-7.

215. Arteaga CL, Sliwkowski MX, Osborne CK, Perez EA, Puglisi F, Gianni L. Treatment of HER2-positive breast cancer: current status and future perspectives. Nat Rev Clin Oncol. 2011;9:16-32.

216. Almeida JL, Cole KD, Plant AL. Standards for Cell Line Authentication and Beyond. PLoS Biol. 2016;14:e1002476.

217. Chen TR. In situ detection of mycoplasma contamination in cell cultures by fluorescent Hoechst 33258 stain. Exp Cell Res. 1977;104:255-62.

218. Marx V. Cell-line authentication demystified. Nat Methods. 2014;11:483-8.

219. Sun C, Hobor S, Bertotti A, Zecchin D, Huang S, Galimi F, et al. Intrinsic resistance to MEK inhibition in KRAS mutant lung and colon cancer through transcriptional induction of ERBB3. Cell Rep. 2014;7:86-93.

220. Clark GJ, Cox AD, Graham SM, Der CJ. Biological assays for Ras transformation. Methods Enzymol. 1995;255:395-412.

221. Li H, Zhu F, Boardman LA, Wang L, Oi N, Liu K, et al. Aspirin Prevents Colorectal Cancer by Normalizing EGFR Expression. EBioMedicine. 2015;2:447-55.

222. Langley RE, Burdett S, Tierney JF, Cafferty F, Parmar MK, Venning G. Aspirin and cancer: has aspirin been overlooked as an adjuvant therapy? Br J Cancer. 2011;105:1107-13.

223. Sandler RS, Halabi S, Baron JA, Budinger S, Paskett E, Keresztes R, et al. A randomized trial of aspirin to prevent colorectal adenomas in patients with previous colorectal cancer. N Engl J Med. 2003;348:883-90.

224. Chan AT, Ogino S, Fuchs CS. Aspirin use and survival after diagnosis of colorectal cancer. JAMA. 2009;302:649-58.

225. Din FV, Theodoratou E, Farrington SM, Tenesa A, Barnetson RA, Cetnarskyj R, et al. Effect of aspirin and NSAIDs on risk and survival from colorectal cancer. Gut. 2010;59:1670-9.

226. Siegel RL, Miller KD, Jemal A. Cancer Statistics, 2017. CA Cancer J Clin. 2017;67:7-30.

227. Kim KM, Song JJ, An JY, Kwon YT, Lee YJ. Pretreatment of acetylsalicylic acid promotes tumor necrosis factor-related apoptosis-inducing ligand-induced apoptosis by down-regulating BCL-2 gene expression. J Biol Chem. 2005;280:41047-56.

228. Din FV, Stark LA, Dunlop MG. Aspirin-induced nuclear translocation of NFkappaB and apoptosis in colorectal cancer is independent of p53 status and DNA mismatch repair proficiency. Br J Cancer. 2005;92:1137-43.

229. Din FV, Dunlop MG, Stark LA. Evidence for colorectal cancer cell specificity of aspirin effects on NF kappa B signalling and apoptosis. Br J Cancer. 2004;91:381-8.

230. McQuaid KR, Laine L. Systematic review and meta-analysis of adverse events of low-dose aspirin and clopidogrel in randomized controlled trials. Am J Med. 2006;119:624-38.

231. Chou TC. Theoretical basis, experimental design, and computerized simulation of synergism and antagonism in drug combination studies. Pharmacol Rev. 2006;58:621-81.

232. Johnson SM, Gulhati P, Rampy BA, Han Y, Rychahou PG, Doan HQ, et al. Novel expression patterns of PI3K/Akt/mTOR signaling pathway components in colorectal cancer. J Am Coll Surg. 2010;210:767-76, 76-8.

233. Zheng L, Ren JQ, Li H, Kong ZL, Zhu HG. Downregulation of wild-type p53 protein by HER-2/neu mediated PI3K pathway activation in human breast cancer cells: its effect on cell proliferation and implication for therapy. Cell Res. 2004;14:497-506.

234. Zhou BP, Liao Y, Xia W, Zou Y, Spohn B, Hung MC. HER-2/neu induces p53 ubiquitination via Akt-mediated MDM2 phosphorylation. Nat Cell Biol. 2001;3:973-82.

235. Liao X, Lochhead P, Nishihara R, Morikawa T, Kuchiba A, Yamauchi M, et al. Aspirin use, tumor PIK3CA mutation, and colorectal-cancer survival. N Engl J Med. 2012;367:1596-606.

236. Kim MO, Lee MH, Oi N, Kim SH, Bae KB, Huang Z, et al. [6]-shogaol inhibits growth and induces apoptosis of non-small cell lung cancer cells by directly regulating Akt1/2. Carcinogenesis. 2014;35:683-91.

237. Bode AM, Dong Z. The Amazing and Mighty Ginger. 2011.

238. Surh YJ. Anti-tumor promoting potential of selected spice ingredients with antioxidative and anti-inflammatory activities: a short review. Food Chem Toxicol. 2002;40:1091-7.

239. Wang Z, Hasegawa J, Wang X, Matsuda A, Tokuda T, Miura N, et al. Protective Effects of Ginger against Aspirin-Induced Gastric Ulcers in Rats. Yonago Acta Med. 2011;54:11-9.

240. Tahir AA, Sani NF, Murad NA, Makpol S, Ngah WZ, Yusof YA. Combined ginger extract & Gelam honey modulate Ras/ERK and PI3K/AKT pathway genes in colon cancer HT29 cells. Nutr J. 2015;14:31.

241. Jeong CH, Bode AM, Pugliese A, Cho YY, Kim HG, Shim JH, et al. [6]-Gingerol suppresses colon cancer growth by targeting leukotriene A4 hydrolase. Cancer Res. 2009;69:5584-91.

242. Tan BS, Kang O, Mai CW, Tiong KH, Khoo AS, Pichika MR, et al. 6-Shogaol inhibits breast and colon cancer cell proliferation through activation of peroxisomal proliferator activated receptor gamma (PPARgamma). Cancer Lett. 2013;336:127-39.

243. Samuels Y, Diaz LA, Jr., Schmidt-Kittler O, Cummins JM, Delong L, Cheong I, et al. Mutant PIK3CA promotes cell growth and invasion of human cancer cells. Cancer Cell. 2005;7:561-73.

244. Vasudevan KM, Barbie DA, Davies MA, Rabinovsky R, McNear CJ, Kim JJ, et al. AKT-independent signaling downstream of oncogenic PIK3CA mutations in human cancer. Cancer Cell. 2009;16:21-32.

245. Goel A, Chang DK, Ricciardiello L, Gasche C, Boland CR. A novel mechanism for aspirin-mediated growth inhibition of human colon cancer cells. Clin Cancer Res. 2003;9:383-90.

246. Zumwalt TJ, Wodarz D, Komarova NL, Toden S, Turner J, Cardenas J, et al. Aspirin-Induced Chemoprevention and Response Kinetics Are Enhanced by PIK3CA Mutations in Colorectal Cancer Cells. Cancer Prev Res (Phila). 2017;10:208-18.

247. Costa HA, Leitner MG, Sos ML, Mavrantoni A, Rychkova A, Johnson JR, et al. Discovery and functional characterization of a neomorphic PTEN mutation. Proc Natl Acad Sci U S A. 2015;112:13976-81.

248. McGranahan N, Favero F, de Bruin EC, Birkbak NJ, Szallasi Z, Swanton C. Clonal status of actionable driver events and the timing of mutational processes in cancer evolution. Sci Transl Med. 2015;7:283ra54.

249. Cheung LW, Hennessy BT, Li J, Yu S, Myers AP, Djordjevic B, et al. High frequency of PIK3R1 and PIK3R2 mutations in endometrial cancer elucidates a novel mechanism for regulation of PTEN protein stability. Cancer Discov. 2011;1:170-85.

250. Yi KH, Axtmayer J, Gustin JP, Rajpurohit A, Lauring J. Functional analysis of non-hotspot AKT1 mutants found in human breast cancers identifies novel driver mutations: implications for personalized medicine. Oncotarget. 2013;4:29-34.

251. Wu TJ, Wang X, Zhang Y, Meng L, Kerrigan JE, Burley SK, et al. Identification of a Non-Gatekeeper Hot Spot for Drug-Resistant Mutations in mTOR Kinase. Cell Rep. 2015;11:446-59.

252. Henry WS, Laszewski T, Tsang T, Beca F, Beck AH, McAllister SS, et al. Aspirin Suppresses Growth in PI3K-Mutant Breast Cancer by Activating AMPK and Inhibiting mTORC1 Signaling. Cancer Res. 2017;77:790-801.

253. Sun D, Dai X, Yan J, Wei R, Shen A, Huang M, et al. Aspirin disrupts the mTOR-Raptor complex and potentiates the anti-cancer activities of sorafenib via mTORC1 inhibition. Cancer Lett. 2017.

254. Loewe S. The problem of synergism and antagonism of combined drugs. Arzneimittelforschung. 1953;3:285-90.

255. Fitzgerald JB, Schoeberl B, Nielsen UB, Sorger PK. Systems biology and combination therapy in the quest for clinical efficacy. Nat Chem Biol. 2006;2:458-66.

256. Sang S, Hong J, Wu H, Liu J, Yang CS, Pan MH, et al. Increased growth inhibitory effects on human cancer cells and anti-inflammatory potency of shogaols from Zingiber officinale relative to gingerols. J Agric Food Chem. 2009;57:10645-50.

257. Byun S, Lim S, Mun JY, Kim KH, Ramadhar TR, Farrand L, et al. Identification of a Dual Inhibitor of Janus Kinase 2 (JAK2) and p70 Ribosomal S6 Kinase1 (S6K1) Pathways. J Biol Chem. 2015;290:23553-62.

258. Michaud DS, Spiegelman D, Clinton SK, Rimm EB, Willett WC, Giovannucci EL. Fruit and vegetable intake and incidence of bladder cancer in a male prospective cohort. J Natl Cancer Inst. 1999;91:605-13.

259. Surh YJ. Cancer chemoprevention with dietary phytochemicals. Nat Rev Cancer. 2003;3:768-80.

260. Subar AF, Heimendinger J, Patterson BH, Krebs-Smith SM, Pivonka E, Kessler R. Fruit and vegetable intake in the United States: the baseline survey of the Five A Day for Better Health Program. Am J Health Promot. 1995;9:352-60.

261. Gold EB, Pierce JP, Natarajan L, Stefanick ML, Laughlin GA, Caan BJ, et al. Dietary pattern influences breast cancer prognosis in women without hot flashes: the women's healthy eating and living trial. J Clin Oncol. 2009;27:352-9.

262. Lee KW, Bode AM, Dong Z. Molecular targets of phytochemicals for cancer prevention. Nat Rev Cancer. 2011;11:211-8.

263. Roberts PJ, Der CJ. Targeting the Raf-MEK-ERK mitogen-activated protein kinase cascade for the treatment of cancer. Oncogene. 2007;26:3291-310.

264. Cobb MH, Goldsmith EJ. How MAP kinases are regulated. J Biol Chem. 1995;270:14843-6.

265. Lim do Y, Shin SH, Lee MH, Malakhova M, Kurinov I, Wu Q, et al. A natural small molecule, catechol, induces c-Myc degradation by directly targeting ERK2 in lung cancer. Oncotarget. 2016;7:35001-14.

266. Lim DY, Lee MH, Shin SH, Chen H, Ryu J, Shan L, et al. (+)-2-(1-Hydroxyl-4-oxocyclohexyl) ethyl caffeate suppresses solar UV-induced skin carcinogenesis by targeting PI3K, ERK1/2, and p38. Cancer Prev Res (Phila). 2014;7:856-65.

267. Yang G, Fu Y, Malakhova M, Kurinov I, Zhu F, Yao K, et al. Caffeic acid directly targets ERK1/2 to attenuate solar UV-induced skin carcinogenesis. Cancer Prev Res (Phila). 2014;7:1056-66.

268. Li J, Malakhova M, Mottamal M, Reddy K, Kurinov I, Carper A, et al. Norathyriol suppresses skin cancers induced by solar ultraviolet radiation by targeting ERK kinases. Cancer Res. 2012;72:260-70.

269. Kang NJ, Shin SH, Lee HJ, Lee KW. Polyphenols as small molecular inhibitors of signaling cascades in carcinogenesis. Pharmacol Ther. 2011;130:310-24.

270. Banerjee P, Erehman J, Gohlke BO, Wilhelm T, Preissner R, Dunkel M. Super Natural II--a database of natural products. Nucleic Acids Res. 2015;43:D935-9.

271. Holliday JD, Hu CY, Willett P. Grouping of coefficients for the calculation of inter-molecular similarity and dissimilarity using 2D fragment bit-strings. Comb Chem High Throughput Screen. 2002;5:155-66.

272. Bajusz D, Racz A, Heberger K. Why is Tanimoto index an appropriate choice for fingerprint-based similarity calculations? J Cheminform. 2015;7:20.

273. Chen X, Reynolds CH. Performance of similarity measures in 2D fragment-based similarity searching: comparison of structural descriptors and similarity coefficients. J Chem Inf Comput Sci. 2002;42:1407-14.

274. Johnson MA, Maggiora GM. Concepts and Applications of Molecular Similarity: Wiley; 1990.

275. White MA, Nicolette C, Minden A, Polverino A, Van Aelst L, Karin M, et al. Multiple Ras functions can contribute to mammalian cell transformation. Cell. 1995;80:533-41.

276. Meloche S, Pouyssegur J. The ERK1/2 mitogen-activated protein kinase pathway as a master regulator of the G1- to S-phase transition. Oncogene. 2007;26:3227-39.

277. Kim EK, Choi EJ. Pathological roles of MAPK signaling pathways in human diseases. Biochim Biophys Acta. 2010;1802:396-405.

278. Barretina J, Caponigro G, Stransky N, Venkatesan K, Margolin AA, Kim S, et al. The Cancer Cell Line Encyclopedia enables predictive modelling of anticancer drug sensitivity. Nature. 2012;483:603-7.

279. Wells C. Ancient Egyptian Pathology. The Journal of Laryngology & Otology. 1963;77:261-5.

280. David AR, Zimmerman MR. Cancer: an old disease, a new disease or something in between? Nat Rev Cancer. 2010;10:728-33.

281. Kampen KR. The discovery and early understanding of leukemia. Leuk Res. 2012;36:6-13.

282. Alizadeh AA, Aranda V, Bardelli A, Blanpain C, Bock C, Borowski C, et al. Toward understanding and exploiting tumor heterogeneity. Nat Med. 2015;21:846-53.

283. Aisner D, Sholl LM, Berry LD, Haura EB, Ramalingam SS, Glisson BS, et al. Effect of expanded genomic testing in lung adenocarcinoma (LUCA) on survival benefit: The Lung Cancer Mutation Consortium II (LCMC II) experience. J Clin Oncol. 2016;34:abstr 11510.

284. Bedard PL, Oza A, Clarke B, Tsao M-S, Leighl NB, Chen EX, et al. Abstract PR03: Molecular profiling of advanced solid tumors at Princess Margaret Cancer Centre and patient outcomes with genotype-matched clinical trials. Clin Can Res. 2016;22:Supplement.

285. Lawler M, Kaplan R, Wilson RH, Maughan T, Consortium SC. Changing the Paradigm-Multistage Multiarm Randomized Trials and Stratified Cancer Medicine. Oncologist. 2015;20:849-51.

286. Meric-Bernstam F, Brusco L, Shaw K, Horombe C, Kopetz S, Davies MA, et al. Feasibility of Large-Scale Genomic Testing to Facilitate Enrollment Onto Genomically Matched Clinical Trials. J Clin Oncol. 2015;33:2753-62.

287. Le Tourneau C, Delord JP, Goncalves A, Gavoille C, Dubot C, Isambert N, et al. Molecularly targeted therapy based on tumour molecular profiling versus conventional therapy for advanced cancer (SHIVA): a multicentre, open-label, proof-of-concept, randomised, controlled phase 2 trial. Lancet Oncol. 2015;16:1324-34.

288. Kuntz TM, Gilbert JA. Introducing the Microbiome into Precision Medicine. Trends Pharmacol Sci. 2017;38:81-91.

289. A framework for human microbiome research. Nature. 2012;486:215-21.

290. Saussele S, Krauss MP, Hehlmann R, Lauseker M, Proetel U, Kalmanti L, et al. Impact of comorbidities on overall survival in patients with chronic myeloid leukemia: results of the randomized CML study IV. Blood. 2015;126:42-9.

291. Geyer CE, Forster J, Lindquist D, Chan S, Romieu CG, Pienkowski T, et al. Lapatinib plus capecitabine for HER2-positive advanced breast cancer. N Engl J Med. 2006;355:2733-43.

292. Kaelin WG, Jr. The concept of synthetic lethality in the context of anticancer therapy. Nat Rev Cancer. 2005;5:689-98.

293. Chan DA, Giaccia AJ. Harnessing synthetic lethal interactions in anticancer drug discovery. Nat Rev Drug Discov. 2011;10:351-64.

294. Bryant HE, Schultz N, Thomas HD, Parker KM, Flower D, Lopez E, et al. Specific killing of BRCA2-deficient tumours with inhibitors of poly(ADP-ribose) polymerase. Nature. 2005;434:913-7.

295. Farmer H, McCabe N, Lord CJ, Tutt AN, Johnson DA, Richardson TB, et al. Targeting the DNA repair defect in BRCA mutant cells as a therapeutic strategy. Nature. 2005;434:917-21.

296. Fong PC, Boss DS, Yap TA, Tutt A, Wu P, Mergui-Roelvink M, et al. Inhibition of poly(ADP-ribose) polymerase in tumors from BRCA mutation carriers. N Engl J Med. 2009;361:123-34.

297. Audeh MW, Carmichael J, Penson RT, Friedlander M, Powell B, Bell-McGuinn KM, et al. Oral poly(ADP-ribose) polymerase inhibitor olaparib in patients with BRCA1 or BRCA2 mutations and recurrent ovarian cancer: a proof-of-concept trial. Lancet. 2010;376:245-51.

298. Kaye SB, Lubinski J, Matulonis U, Ang JE, Gourley C, Karlan BY, et al. Phase II, open-label, randomized, multicenter study comparing the efficacy and safety of olaparib, a poly (ADP-ribose) polymerase inhibitor, and pegylated liposomal doxorubicin in patients with BRCA1 or BRCA2 mutations and recurrent ovarian cancer. J Clin Oncol. 2012;30:372-9.

299. Ledermann J, Harter P, Gourley C, Friedlander M, Vergote I, Rustin G, et al. Olaparib maintenance therapy in patients with platinum-sensitive relapsed serous ovarian cancer: a preplanned retrospective analysis of outcomes by BRCA status in a randomised phase 2 trial. Lancet Oncol. 2014;15:852-61.

300. Goga A, Yang D, Tward AD, Morgan DO, Bishop JM. Inhibition of CDK1 as a potential therapy for tumors over-expressing MYC. Nat Med. 2007;13:820-7.

301. Yang D, Liu H, Goga A, Kim S, Yuneva M, Bishop JM. Therapeutic potential of a synthetic lethal interaction between the MYC proto-oncogene and inhibition of aurora-B kinase. Proc Natl Acad Sci U S A. 2010;107:13836-41.

302. Zuber J, Shi J, Wang E, Rappaport AR, Herrmann H, Sison EA, et al. RNAi screen identifies Brd4 as a therapeutic target in acute myeloid leukaemia. Nature. 2011;478:524-8.

303. Mertz JA, Conery AR, Bryant BM, Sandy P, Balasubramanian S, Mele DA, et al. Targeting MYC dependence in cancer by inhibiting BET bromodomains. Proc Natl Acad Sci U S A. 2011;108:16669-74.

304. Delmore JE, Issa GC, Lemieux ME, Rahl PB, Shi J, Jacobs HM, et al. BET bromodomain inhibition as a therapeutic strategy to target c-Myc. Cell. 2011;146:904-17.

305. Fece de la Cruz F, Gapp BV, Nijman SM. Synthetic lethal vulnerabilities of cancer. Annu Rev Pharmacol Toxicol. 2015;55:513-31.

306. Berthon C, Raffoux E, Thomas X, Vey N, Gomez-Roca C, Yee K, et al. Bromodomain inhibitor OTX015 in patients with acute leukaemia: a dose-escalation, phase 1 study. Lancet Haematol. 2016;3:e186-95.

307. Do K, O'Sullivan Coyne G, Chen AP. An overview of the NCI precision medicine trials-NCI MATCH and MPACT. Chin Clin Oncol. 2015;4:31.

308. Wang H, Yang H, Shivalila CS, Dawlaty MM, Cheng AW, Zhang F, et al. One-step generation of mice carrying mutations in multiple genes by CRISPR/Cas-mediated genome engineering. Cell. 2013;153:910-8.

309. Cyranoski D. CRISPR gene-editing tested in a person for the first time. Nature. 2016;539:479.

310. Kuhlbrandt W. Cryo-EM enters a new era. Elife. 2014;3:e03678.

311. Banerjee S, Bartesaghi A, Merk A, Rao P, Bulfer SL, Yan Y, et al. 2.3 A resolution cryo-EM structure of human p97 and mechanism of allosteric inhibition. Science. 2016;351:871-5.

Appendix

Precision medicine: the foundation of future cancer therapeutics

(This commentary is published in *npj* Precision Oncology, (2017) 1:12; doi:10.1038/s41698-017-0016-z)

Based on early evidence of fossilized bone tumors that were found in ancient Egyptian mummies, cancer is an ancient disease (279). The term “carcinoma” to refer to cancer was first used around 400 BC by Hippocrates (280). The understanding of cancer mechanisms began when John Bennett and Rudolf Virchow observed the abnormal accumulation of white blood cells in patients in 1845, which was one of the first cancers detected by microscopy (281). In contrast to the long history of the disease, diagnosis and treatment of cancer at a cellular or molecular level is a relatively new strategy. Although the field of oncology has developed and expanded dramatically, a single drug has not yet been discovered that can cure all patients, even those with similar cancer types. We now know that cancer is an extremely heterogeneous disease, which explains differences not only between cancer cells from different patients, but also differences between cancer cells within a single patient (282). Clearly, more effective strategies are critically needed to defeat the long-standing enemy known as cancer.

The concept and practice of precision medicine is a methodical and systematic movement aimed at defeating diseases such as cancer (4). Cancer is a major focus of the precision medicine initiative and developments in precise and effective treatments could benefit many other chronic diseases. Precision oncology or precision medicine of cancer

focuses on matching the most accurate and effective treatment to each individual cancer patient based on the genetic profile of the cancer and the individual. Because every single cancer patient exhibits a different genetic profile and the profile can change over time, more patients will benefit if therapeutic options can be tailored to that individual, thus avoiding the idea that “one-size-fits-all” in terms of cancer treatment.

Results of one randomized clinical trial and a small number of feasibility and/or tumor response studies (25, 283-286) focusing on the concept of precision medicine have had limited success(287). Naturally, opponents of precision medicine have criticized the strategy based on the results of the small number of clinical studies (160, 163). However, concluding that precision medicine will not work is premature because the precision medicine approach has not yet been fully tested in a sufficient number of trials. In addition, the suggestion has been made that having inadequate access to specific therapeutic agents and an insufficient number of tumor samples may have contributed to the limited success (163). Because cancer is a highly heterogeneous disease both between patients and within the same patient, the ability to cope with changes in the clinical trial setting is extremely challenging. Many creative and bold ideas of precision medicine have not yet made the transition from the lab bench to the clinic and need to be more fully evaluated in small clinical studies. For example, the microbiota is now recognized as a key player in health (288). The microbiota influences endocrinology and disease status and alters drug response and resistance, and this could hold true for cancer and the efficiency of cancer treatments. Sequencing the human microbiome and modulating the

host-microbiota interactions in individual patients may be one approach to improve therapeutic outcomes (288-289).

Questions that must be addressed include whether precision oncology is just a theory or whether it realistically assures a better future and if truly promising, how can the application of precision oncology be improved and effectively implemented into the clinic? Several lines of evidence strongly support the idea that precision oncology could likely benefit more patients compared to traditional chemotherapies. First, some patients' lives have already been substantially improved by target-based therapies compared to conventional cytotoxic therapies. One of the most notable examples is the discovery of the *Bcr-Abl* gene fusion in chronic myeloid leukemia (CML). Uncovering this genetic driver of CML lead to the development of a selective inhibitor of BCR-ABL, imatinib, which exhibited broader treatment coverage because, unlike other gene mutations, the *Bcr-Abl* gene fusion occurs in almost all CML patients. This compound improved the overall survival rates of CML patients to 90% over 5 years and 88% over 8 years (290). Another example includes the effectiveness of drugs like trastuzumab, lapatinib, pertuzumab or ado-trastuzumab emtansine against human epidermal growth factor receptor 2 (HER2)-positive breast cancer. Compared to chemotherapy alone, the addition of trastuzumab to chemotherapy significantly slowed the disease progression (i.e., median, 4.6 vs. 7.4 months), increased the objective response rate (i.e., 32 vs. 50%), prolonged survival time (i.e., median, 20.3 vs. 25.1 months) and reduced the risk of death by 20% (57). Lapatinib plus chemotherapy (i.e., capecitabine) achieved a longer median time to disease progression compared to chemotherapy alone (i.e., 8.4 vs. 4.4 months)

(291). A combination of pertuzumab, trastuzumab, and chemotherapy (i.e., docetaxel) further improved the median overall survival time to 56.5 months compared with a combination of only trastuzumab and chemotherapy (i.e., 40.8 months) (58). Treatment with ado-trastuzumab emtansine, a conjugate of a HER2 monoclonal antibody and a cytoxic drug, significantly improved the length of progression-free survival and overall survival with lower adverse effects when compared with lapatinib and chemotherapy (i.e., capecitabine) (59). These two excamples demonstrate how the identification of key mutations like the *Bcr-Abl* fusion or HER2 can clearly benefit a larger number of select cancer patients.

Second, many strategies are now available to identify important molecular targets for therapeutic intervention. Synthetic lethality is one unique strategy directed toward identifying cancer vulnerabilities (292). This strategy is based on the discovery that cell death is caused by a combination of deficiencies in the expression of two or more genes, whereas deficiency in only one of these genes can increase viability (292-293). In 2005, the *BRCA* and *poly ADP ribose polymerase (PARP*) genes were found to have a synthetic lethal relationship (294-295). In 2014, the FDA (Food and Drug Administration) authorized accelerated approval of olaparib, a PARP inhibitor, to treat *BRCA*-mutant ovarian cancer patients (296-299). Progression free survival of *BRCA*-mutant ovarian cancer patients was significantly prolonged by olaparib compared to the placebo treatment (i.e., median, 11.2 vs. 4.3 months) (299). Likewise, several candidate proteins were identified to treat cancers that over-express Myc, a transcription factor for which small-molecule inhibitors are currently unavailable (300-304). Within just a 5-year

timespan, researchers found that Myc-amplified tumors were sensitive to CDK1, aurora kinase B, and BRD4 inhibition (300-301). Although many of these inhibitors have yet to translate into clinical successes, Phase I trials of three BRD4 inhibitors are ongoing (CPI-0610 and TEN-010) or have just finished (OTX015) (305-306). These findings suggest that changes in *gene A* in cancer does not necessarily mean that *gene A* is the best target but instead, targeting its synthetic lethal partner might be a more effective strategy.

Third, clinical trial design is constantly evolving to overtake tumor heterogeneity from patient to patient. The Molecular Analysis for Therapy Choice (NCI-MATCH) is a clinical trial selecting treatments based on genetic features of patients, not traditional tumor histology (165). The cancer patients will be assigned to 1 of 25 different treatment arms based on their genetic mutation profile. The overall response rate will be the endpoint to measure success. However, no control arms will be included, which could dramatically affect the interpretation of the final results. Even though a number of questions have been raised, the investigators are very optimistic that the results will further the efforts to implement precision oncology treatments. The Molecular Profiling-based Assignment of Cancer Therapy (NCI-MPACT) is another innovative clinical trial to test the hypothesis that targeting an oncogenic driver mutation is more efficacious than not targeting it. NCI-MPACT will recruit advanced cancer patients who have been unresponsive to standard therapeutic options and possess mutations in one of three genetic pathways that include DNA repair, PI3-K/mTOR (phosphoinositide-3 kinase/mammalian target of rapamycin) and Ras/Raf/MEK (mitogen-activated protein kinase kinase). Patients without a driver mutation will not be eligible for further treatment

(307). Although this trial is similar to the NCI-MATCH in that patients will undergo tumor biopsies when enrolled, patients in the NCI-MPACT study will be assigned to one of two arms: treatment with drug(s) designed to target the mutation or treatment with drug(s) not prospectively identified to target the mutation. By evaluating gene targets across the histologic subtypes with NCI-MATCH and addressing the importance of driver mutations with NCI-MPACT trials, the efficacy of diagnosis and therapies could be significantly enhanced.

Finally, the influence of new technologies such as the CRISPR/Cas system and cryo-electron microscopy (cryo-EM) will broaden and sharpen our ability to identify novel therapeutic targets for precision oncology. CRISPR/Cas technology enables controlled exchange, insertion and deletion of DNA sequences unlike spontaneous mutation and can easily generate animal models that mimic mutations status of patients (308). Recently, a gene therapy trial to treat myeloma, melanoma and sarcoma with CRISPR/Cas has been approved by the National Institute of Health (NIH) and is awaiting approval from the FDA (309). In addition to CRISPR/Cas, cryo-EM is a promising tool for precision oncology. Cryo-EM is a type of transmission EM in which samples are examined at cryogenic temperatures (310). Because the samples (e.g., proteins and viruses) are frozen in their native states, researchers can study biological events accurately at the subatomic or atomic level. For an instance, a 2.3 Å resolution cryo-EM structure of p97 showed a large corkscrew-like hexameric form, revealed its interactions with an allosteric inhibitor and displayed conformational changes induced by adenosine tri-phosphate (ATP) (311). Visualization of intact proteins and anti-cancer drugs at

subatomic or atomic levels will assist researchers in understanding the consequences of genetic alterations on drug response and resistance.

In spite of some early setbacks, precision oncology still has a great deal of promise and should not be abandoned hastily. The challenge of tumor heterogeneity should not discourage or intimidate efforts to overcome cancer but should push the field forward. As practice makes perfect, precision mends patients.